CAIT-UTC-NC4

Satellite Assessment and Monitoring for Pavement Management

Final Report
November 2015

Ardeshir Fagrhi, Ph.D.
Professor

Mingxin Li, Ph.D.
Research Associate II

Abdulkadir Ozden
Graduate Research Assistant

Department of Civil and Environmental Engineering
Delaware Center for Transportation
University of Delaware
Newark, DE 19716

External Project Manager
Kaz Tabrizi, Ph.D., P.E.
Executive Vice President
Advanced Infrastructure Design, Inc.

In cooperation with
Rutgers, The State University of New Jersey
And
State of Delaware
Department of Transportation
And
U.S. Department of Transportation
Federal Highway Administration

Disclaimer Statement

TECHNICAL REPORT STANDARD TITLE PAGE

1. Report No.	2. Government Accession No.	3. Recipient's Catalog No.
CAIT-UTC-NC4		

4. Title and Subtitle	5. Report Date
Satellite Assessment and Monitoring for Pavement Management	November 2015
	6. Performing Organization Code CAIT/Delaware

7. Author(s)	8. Performing Organization Report No.
Ardeshir Fagrhi, Ph.D., Mingxin Li, Ph.D., Abdulkadir Ozden, Ph.D. Candidate	CAIT-UTC-NC4

9. Performing Organization, Name and Address	10. Work Unit No.
Department of Civil and Environmental Engineering Delaware Center for Transportation Newark, DE 19716	11. Contract or Grant No. DTRT13-G-UTC28

12. Sponsoring Agency Name and Address	13. Type of Report and Period Covered
Center for Advanced Infrastructure and Transportation Rutgers, The State University of New Jersey 100 Brett Road Piscataway, NJ 08854	Final Report 9/1/14 - 8/31/2015
	14. Sponsoring Agency Code

15. Supplementary Notes

U.S Department of Transportation/Research and Innovative Technology Administration
1200 New Jersey Avenue, SE
Washington, DC 20590-0001

16. Abstract

To minimize the obstruction to the traffic, this project aims to carry out investigation of the capability of remote sensing satellite data, including Synthetic Aperture Radar (SAR) satellite data for use in advanced infrastructure monitoring, which is a tangible breakthrough in remote sensing technology allowing to assess the pavement deformations with millimetric accuracy on single specific points. Recent developments in remote sensing satellite systems and availability of high-resolution Synthetic Aperture Radar (SAR) products have created an opportunity for SAR-based monitoring in pavement and infrastructure management. SAR Interferometry (InSAR) and developed advanced methods such as PSInSAR and SqueeSAR are able to measure even small deformations and determine the deformation velocities over a set of images. Additionally, high-resolution SAR images may significantly increase the quality and level of detail in end products. Therefore, this newly emerging SAR-based monitoring has become valuable for monitoring and rehabilitating the nation's deteriorating roadway infrastructure elements such as bridge settlements and displacements, roadway surface deformations, geohazards and sinkhole detection, historical analysis of problematic sites, etc. In this research study, the feasibility, accuracy, and effectiveness of use of satellite remote sensing technology, specifically SAR for pavement and infrastructure monitoring, were evaluated. A cost benefit analysis for a possible SAR-based monitoring system was performed. It was found that SAR-based methods are useful as a complementary tool rather than a replacement for current technologies and practices, specifically in a state of good repair.

17. Key Words	18 Distributional Statement
Sythetic Aperture Radar (SAR), InSAR, Remote Sensing Satellite Data, Pavement Survey, Pavement Management	

19. Security Classification	20. Security Classification (of this page)	21. No. of Pages	22. Price
Unclassified	Unclassified	95	

Form DOT F 1700.7 (8-69)

ACKNOWLEDGEMENTS

The support of the Center for Advanced Infrastructure and Transportation University Transportation Center (CAIT-UTC) for this research is greatly appreciated. Dr. Kaz Tabrizi, Executive Vice President of Advanced Infrastructure Design, Inc. served as the external project manager and added valuable comments during the research. We thank him for his support and advice.

Ardeshir Faghri, Mingxin Li, and Abdulkadir Ozden

TABLE OF CONTENTS

LIST OF TABLES

LIST OF FIGURES

LIST OF ABBREVIATIONS

AASHTO	American Association of State Highway and Transportation Officials
AOI	Area of Interest
ASF	Alaska Satellite Facility
ASTER	Advanced Spaceborne Thermal Emission and Reflection Radiometer
AVIRIS	Airborne Visible / Infrared Imaging Spectrometer
CBA	Cost–Benefit Analysis
DEM	Digital Elevation Model
DInSAR	Differential Interferometric SAR
DN	Digital Numbers
DORIS	Delft Object-oriented Radar Interferometry Software
DS	Distributed Scatterer(s)
EA	Effective Area
EOSDIS	Earth Observing Systems Data and Information Systems
ERS	Earth Resources Satellite
ESA	European Space Agency
FHWA	Federal Highway Administration
GCP	Ground Control Point
GIS	Geographic Information System
GMT	Ground Mapping Tool
GPR	Ground Penetrating Radar
GPS	Global Positioning System
GRASS	Geographic Resources Analysis Support System
HPMS	Highway Performance Monitoring System
IRI	International Roughness Index
InSAR	Interferometric SAR
JPL	Jet Propulsion Laboratory
LIDAR	Light Detection Radar
LOS	Line of Sight
NASA	National Aeronautics and Space Administration
OFGT	Open Foris Geospatial Toolkit
PMS	Pavement Monitoring System
PS	Permanent Scatterer(s)
PSInSAR™	Permanent Scatterers SAR Interferometry
PSR	Present Serviceability Rating
ROI-PAC	Repeat Orbit Interferometry Package
SAGA	System for Automated Geoscientific Analysis
SLC	Single Look Complex
SAR	Synthetic Aperture Radar
SqueeSAR™	Advanced InSAR algorithm
TDI	Time Delayed Integrated
TS	Time Series (Permanent Scatterer Displacement)
WINSAR	Western North America Interferometric Synthetic Aperture Radar

1 DESCRIPTION OF THE PROBLEM

1.1 BACKGROUND

Transportation systems ensure mobility of people and goods, and are key for well-functioning economic activities. As a vital part of the system, adequate infrastructure is an essential precondition for complex and dynamic transportation systems. FHWA and states collect variety of measures of transportation infrastructure and pavement condition. However, there are many different approaches regarding the degree of coverage, method and frequency of data collection, and consistency of measures, etc. *(1)*. In fact, fast growing technological developments have brought new opportunities for data collection and monitoring of transportation infrastructure, however they have increased the uncertainty of which existing methods and measures best represents the current state of the assets *(2)*.

Traditional pavement inspection techniques, e.g., manual distress surveys, semi- or automated condition surveys using specially equipped vehicles, offer a method of determining pavement condition through observing and recording, which causes this pavement survey work to be cumbersome and inefficient. In fact, some of these periodic inspection-based monitoring efforts are redundant and some of them cause late-detection of the problems. This effort consequently increases the cost of monitoring and management of transportation infrastructure systems and cause money and energy loss.

Aging transportation infrastructures in the U.S. require more attention for cost-effective management and treatment for providing continuous mobility of people and goods *(3)*. Therefore, preserving the existing assets and maintaining the transportation system in sustainable level is critical. Budget limitations increased the importance of maintaining and improving the transportation infrastructure with well-planned, cost-effective monitoring and maintenance programs, which answers the questions of “what”, “where” and “when” the maintenance and rehabilitation is necessary" *(4)*.

Recent developments in remote sensing satellite systems and availability of high-resolution Synthetic Aperture Radar (SAR) products have taken the attention of researchers for possibility of using satellite remote sensing technology for pavement and infrastructure management. SAR Interferometry (InSAR) and developed advanced deformation detection techniques upon InSAR (such as DInSAR, PSInSAR^{TM} and SqueeSAR^{TM}) are able to measure the millimetric surface deformation over an area *(5, 6)*, and high-resolution satellite images can significantly increase the number of detected points *(7, 8)*. Therefore, satellite based monitoring could be possible for deteriorating roadway infrastructure such as bridge settlements and displacements, large-scale

deformations in roadway infrastructure and sinkhole detection *(2, 9, 10)* or detailed analysis of targeted areas that are already known problematic by previous studies *(11)*. The promising satellite remote sensing technology is expected to play a crucial role for reducing the cost of network-scale pavement and infrastructure monitoring for state and federal agencies in near future as the high-resolution satellite imaging become more available and less costly, and analysis methods and algorithms become more mature *(2, 8)*.

1.2 PROBLEM STATEMENT

One of the biggest challenges in pavement and infrastructure management is timely detection of problems for applying preventive measures and early rehabilitation. Many studies and experiences of agencies have shown that early detection of problems treated with preventive measures increase the service life and reduce the total maintenance cost. Therefore, there is a need for network-scale monitoring tools that facilitate the detection of the problems, reduce the unnecessary vehicle-based inspection trips to the sites, enable detection of slow-moving settlements on and around the transportation infrastructure, and help building more robust infrastructure data systems to increase the effectiveness of the monitoring programs. Such tools will benefit state and federal agencies to prioritize their investment strategies that will yield economic and other benefits.

The challenges and opportunities associated with the evaluation of traffic and environmental impact on pavements necessitate USDOT adopting new technologies to determine the presence of specific types and severities of distresses or defects in the pavement surface. For example, the location, size and depth of the pothole acquired from SAR data can determine the priority for DOT crews to repair them. Therefore, this study directly addresses the US Department of Transportation (US DOT) Strategic Goal of "State of Good Repair" and "Economic competitiveness", and at the same time touches upon the goals of "Safety", "Environmental Sustainability", "Livable Communities", and more.

1.3 PROJECT OBJECTIVES AND SCOPE

In the light of current infrastructure and pavement monitoring practices, this study aims to investigate the capability of remote sensing satellite technologies, specifically SAR satellite data for use in advance infrastructure monitoring, which is tangible breakthrough in sensing technology allowing to assess deformation with millimetric accuracy.

Scope of this research is limited to the evaluation of the possibility of using SAR-based systems for pavement and infrastructure monitoring in general and does not include the effectiveness of such systems for detecting different type and severity of pavement

surface distresses and infrastructure problems. However, all recent efforts on SAR-based pavement and infrastructure monitoring are briefly included in the literature review section.

The report documented the research steps undertaken for this project. Section 2 includes the approach used in this research. Section 3 documents the extensive literature on pavement and infrastructure monitoring, satellite remote sensing, specifically SAR and InSAR methods as well as applications in transportation field. It is followed by two case studies to demonstrate the use of SAR based monitoring. The next section discusses the cost-benefit analysis of the satellite remote sensing systems. Then, the report is finalized with summary, conclusions and recommendations.

2 APPROACH

In order to evaluate and implement satellite based remote sensing, it is extremely important to understand the two main components of this interdisciplinary system. Briefly described below and extensively presented in the next section, these two main components are:

SAR image acquisition and processing: The first step includes the understanding the available remote sensing data products to select the appropriate data and tools to perform the analysis. Previous and currently operating satellites carry different type of sensors in different band, polarization, repeat cycle, etc., and used for variety of application from monitoring atmospheric particulars to millimetric ground deformations. Therefore, it is critically important to select proper satellite remote sensing data to further the analysis. After the image acquisition, some necessary data processing steps should be performed based on project objectives and needs such as removal of atmospheric and topographic effects, classification of detected ground objects, co-registration of images, calculation of deformations and their velocities, etc. This step, requires expertise in the field and generally falls into the interests of electrical and computer engineers. Based on project objectives, customer needs and budget, this step is sometimes conducted by third party professionals or contractors.

SAR integration with current database: The second main step includes the integration of SAR data processing outputs, mostly geo-referenced data such as GIS files, with current databases in the agency such as roadway and infrastructure network, geological features of the area, maintenance operations and operation history, etc. to create layers of information for further evaluation. This step will enhance the information database in the agency and could be used for variety of applications in many divisions.

It is important to note two constraints that shaped the approach in this research: complexity of SAR image acquisition and processing, and difficulty of finding freely available InSAR stacks.

The first constrain includes a very complex system that requires a high-level expertise in the field of satellite SAR image processing that is mostly driven by electrical and computer engineering or remote sensing data analysts in different fields. Next section presents an extensive literature on the components of this complex system and some used methods and algorithms. Although some agencies might prefer outsourcing the image acquisition and processing, long-term use of satellite remote sensing technology significantly affects the budget spending on this component. This step is thus especially important for such agencies. In this regard, possible freely available SAR data sources and data analysis software are presented in the next section.

The second constraint affected the possibility of conducting a case study analysis in the area of interest along with the first constraint. Besides all difficulties in data processing and image analysis, all freely available resources are archived medium-resolution SAR images covering late 1990s and 2000s. The costs of high-resolution SAR images provided by currently operating satellites are high ($2,000+) and InSAR processing requires image acquisition from a stack of images (20+). Thus, excessive image acquisition cost, over $50,000, limits researchers' ability to conduct a case study with high-resolution and recently acquired SAR images. Therefore, the research team was able to use limited available medium- and high resolution SAR imagery to demonstrate the possible use of SAR-based monitoring with two free software for InSAR processing. The research team aimed at identifying suitable SAR image resources and processing tools that might be used to help transportation agencies in their decision making process. Furthermore, cost-benefit analysis was conducted for a possible SAR-based pavement and infrastructure monitoring to inform researchers and practitioners about the economic viability of various image acquisition and processing options.

3 METHODOLOGY

Performance of a transportation system mainly depends on the physical condition of the asset it comprises. Therefore, preserving the existing assets and maintaining the transportation system in sustainable level is critical. Researches indicate that 65% of the roadways are rated as “less than good condition” and 25% of bridges require “significant repair” in the U.S. *(3)*. The Federal Highway Administration (FHWA) has estimated the necessary annual investment of $77 billion for federal-aid highway system compared to federal highway receipts of $34 billion as of 2014 *(12)*. Budget limitations and decreased revenues have made extremely difficult for many states to maintain state of good repair on our roadways *(12)*.

Lately, technological developments such as real time data collection and processing capabilities, remote sensing and imaging technologies are also contributing to the monitoring and management of transportation infrastructure systems. Many states replaced their manual data collection methods with automated and remote sensing systems in the last decade *(2)* and gradually improving and adapting as the new technologies become available. Although these improvements facilitated the data collection process, dealing with enormous amount of data and adaptation of fast changing technologies require well-planned decision-making process. There are great amount of literature on available/potential technologies and methodologies for pavement and infrastructure management and assessment for further review *(2, 13)*.

In the last two decades, SAR technology and InSAR applications have been widely investigated by the research community for large-scale monitoring studies. Ouchi *(14)* summarized the mature fields for SAR-based applications in his study, presented in Table 1. Recently, availability of high-resolution SAR images and developed advance processing methodologies has taken the attention of transportation and infrastructure research community. With the high-resolution SAR images, extracting information about the identity and quantity of the targeted scene became possible for relatively small areas, such as <100 ft^2, which makes the technique useful for pavement and infrastructure studies.

Table 1: Selected fields of SAR application examples *(14)*

Fields	***Objects***
Geology	Topography, DEM & DSM production, crust movement, faults, GIS, soil structure, lithology, underground resources
Agriculture	Crop classification, plantation acreage, growth, harvest & disaster, soil moisture
Forestry	Tree biomass, height, species, plantation & deforestation, forest fire monitoring
Hydrology	Soil moisture, wetland, drainage pattern, river flow, water equivalent snow & ice water cycle, water resources in desert
Urban	Urban structure & density, change detection, subsidence, urbanization, skyscraper height estimation, traffic monitoring
Disaster	Prediction, lifeline search, monitoring of damage & recovery, tsunami & high tide landslide & subsidence by earthquake, volcano & groundwater extraction
Oceanography	Ocean waves, internal waves, wind, ship detection, identification & navigation, currents, front, circulation, oil slick, offshore oil field, bottom topography
Cryosphere	Classification, distribution & changes of ice & snow on land, sea & lake, ice age, equivalent water, glacier flow, iceberg tracking, ship navigation in sea ice
Archeology	Exploration of aboveground and underground remains, survey, management

Source: *(14)*

3.1 LITERATURE REVIEW

3.1.1 Pavement Management System

Pavement management involves all activities related to pavement. The FHWA defines a Pavement Management System (PMS) as "set of tools or methods that can assist decision makers in finding cost-effective strategies for providing, evaluating, and maintaining pavements in a serviceable condition." This definition clearly highlights two key concepts: "cost-effective" and "in a serviceable condition". Both concepts are rely on an effective pavement monitoring system, which answers the questions of "what", "where" and "when" the maintenance and rehabilitation is necessary" *(4)*.

Pavement Monitoring System (PMS) has been in place since late 1970s and had a major breakthrough with automated pavement condition surveying units in early 1990s *(15)*. Then, many different technologies and methods developed such as line and area scanners, ground penetrating radars, acoustic sensors, thermal infrared imagery, optical imagery, light detection and ranging, etc. Each of these automated techniques has its own strong and weak sides in addition to limitations on processing speed, accuracy and

implementation cost *(2)*. Later in 2000s, development of Geographic Information Systems (GIS) and Global Positioning Systems (GPS) increased the accuracy and efficiency of PMS *(15)*.

Pavement condition surveys provide an indication of physical condition of the pavements and consist of data collection, pavement condition rating and quality management elements *(16)*. Both manual and automated data collection techniques are widely used based on agencies' priorities, available resources and limitations. The condition ratings are then used for managing the rehabilitation and maintenance works, estimating the level of repair and rehabilitation, providing uniform rating systems within state, long-term economic planning and historical pavement performance records *(16, 17)*.

Pavement condition data has been collected in variety forms due to states' consideration of different factors for evaluating the pavements. However, most common data types could be categorized as distress data, structural capacity data, ride quality data and skid resistance data as suggested by Attoh-Okine et al *(16)*. Distress data are used to describe the type, severity and extend of the pavement surface distress, and could be collected by manual observations or image/video processing techniques. Ride quality data refer to the comfort level of roadways and commonly represented by International Roughness Index (IRI) or Present Serviceability Rating (PSR) *(16-19)*. These two categories found relevant for considering the potential contribution of SAR based monitoring.

One of the biggest challenges in pavement management is timely detection of pavement and infrastructure problems for the application of preventive measures *(4)*. This is very critical for the pavement's performance and its life cycle cost. Many studies and experiences of agencies show that early detection of problems treated with preventive measures increase the service life of the assets and reduce the total maintenance cost while maintaining the safety and quality *(20)*. AASHTO estimates that "every dollar spent on road maintenance avoids $6 to $14 needed later to rebuild a road that has irreparably deteriorated" *(20)*. As illustrated in Figure 1, the right treatment at the right time will have a significant impact on service life and associated life cycle cost of pavements. Therefore, efficient and cost-effective methods and approaches that improve the pavement and infrastructure monitoring systems are needed. Any contribution towards improving the monitoring and management of pavement and infrastructure systems is highly valuable for responsible agencies.

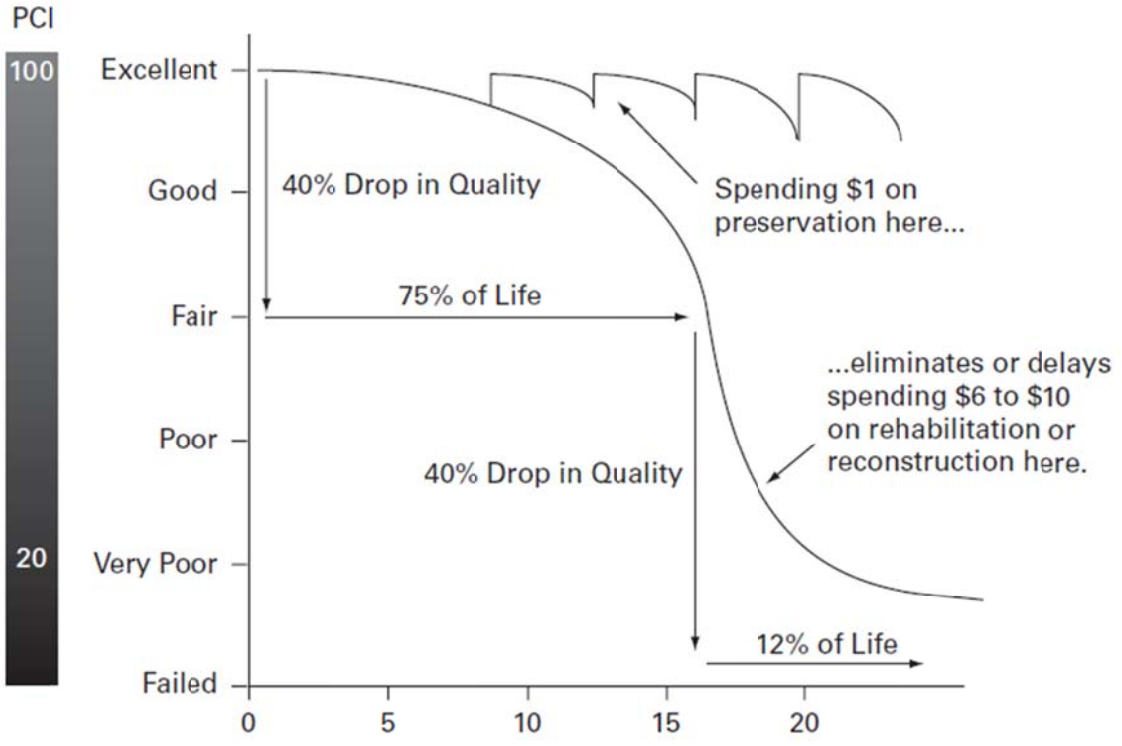

Figure 1. Typical pavement deterioration curve
Source: ***(21)***

On the other hand, the frequency of pavement condition data collection is highly important on predicting pavement performance and PMS decisions. Haider et al. *(22)* stated that "longer monitoring intervals may underpredict the expected roughness and overpredict the expected life on the basis of roughness" and emphasized the importance of early detection of problems, specifically cracks in their study, for the prediction of propagation. In the same study *(22)*, it is reported that monitoring intervals could highly affect the evaluation of network-level pavement conditions and might overestimate and/or underestimate the associated cost. From this perspective, a satellite-based routine monitoring system might help building more robust pavement and infrastructure monitoring system and reduces routine vehicle-based inspection trips and associated monitoring cost. Monitoring pavement and infrastructure elements with monthly satellite imagery can at least prioritize inspection trips for deteriorating elements for early treatment and reduce unnecessary trips to the site. Considering most agencies perform routine inspections for pavement and infrastructure elements in different cycles (for instance, every year some high priority roads, every 2-3 years for low density rural roads), monthly monitoring with satellite imagery is expected to contribute routine monitoring efforts by providing more frequent data in network-level.

3.1.2 Pavement/Infrastructure Monitoring Technologies and Methods

There are many methods and technologies used for pavement and infrastructure monitoring. Federal and state requirements, geographical constrains, budget limitations, data needs, and many other factors affect the decision of which technologies and methods should be used, and if the selected technology should be owned or data collection effort could be partially/fully contracted. Here, some well-known and emerging technologies and methods for pavement and infrastructure monitoring are highlighted.

Since the early applications of pavement monitoring, manual surveys based on human observations are still applied in small scale. However, this method is highly labor-intensive, prone to errors and considerable hazard to the field personnel *(23)*. Manual pavement condition surveys require the operation of a vehicle with at least two personnel (one driver, one data collector) on a regular basis and increase the overall cost of data collection. Additionally, inconsistency occurs due to the effect of human judgments in the data collection process. Acoustic technology has also been used for detection of surface crack by collecting the slapping sound against the crack while a data collection vehicle is traveling at high speed. Reliability issues and course texture problems are reported as the main limitations of this method *(18)*.

Another remote sensing application, LIDAR, illuminates the targeted scene with a laser and analyses the reflected light to generate a surface model. The system can be installed on either ground-based or airborne vehicles. As shown in Figure 2, the point-cloud LIDAR is successfully used for determination of grades and cross-slopes of roadways *(15)*, bridge deck surface monitoring, concrete and steel section loss on bridges *(13)*, monitoring surrounding roadway assets, etc. LIDAR-based Digital Elevation Models (DEM) can also be used to increase the accuracy of data received by optical imagery *(24)*. One of the major limitations of LIDAR is that the technology is sensitive to weather conditions *(24)*.

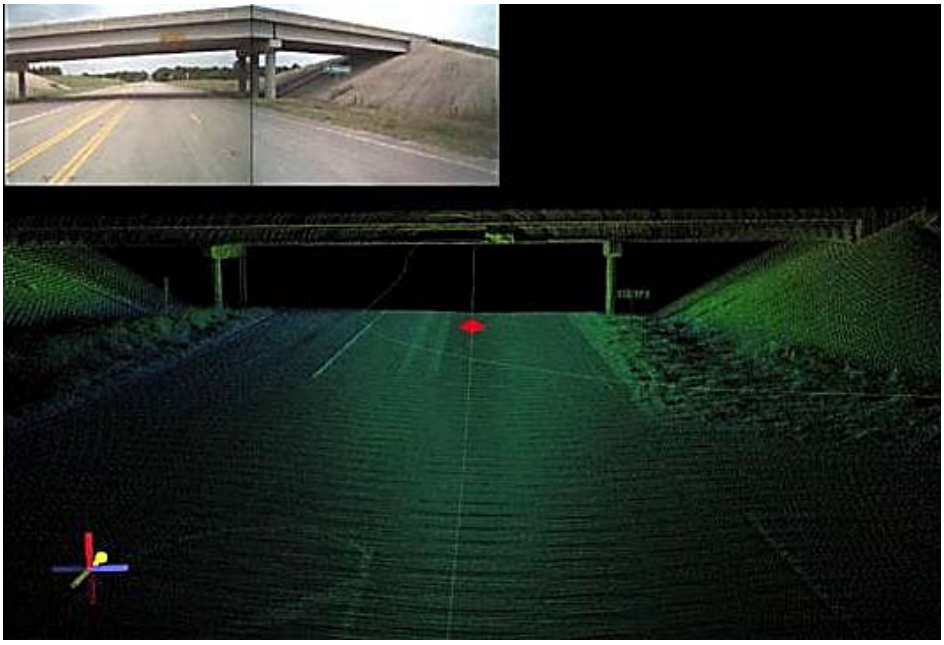

Figure 2. LIDAR creates a point cloud for all roadway assets
Source: ***(25)***

Line and area scanning technologies such as Time Delayed Integration (TDI) cameras, are widely used in high-performance line-scan applications with a high speed and low lighting conditions. This is basically building an amplified 2D image using a single line of sensor pixels. Laser scanning uses laser-sensing technology on a line basis approach without requiring separate illumination, and generates a 2D surface of the scene *(23)*. A pavement surface inspection vehicle equipped with TDI line-scan camera is presented in Figure 3.

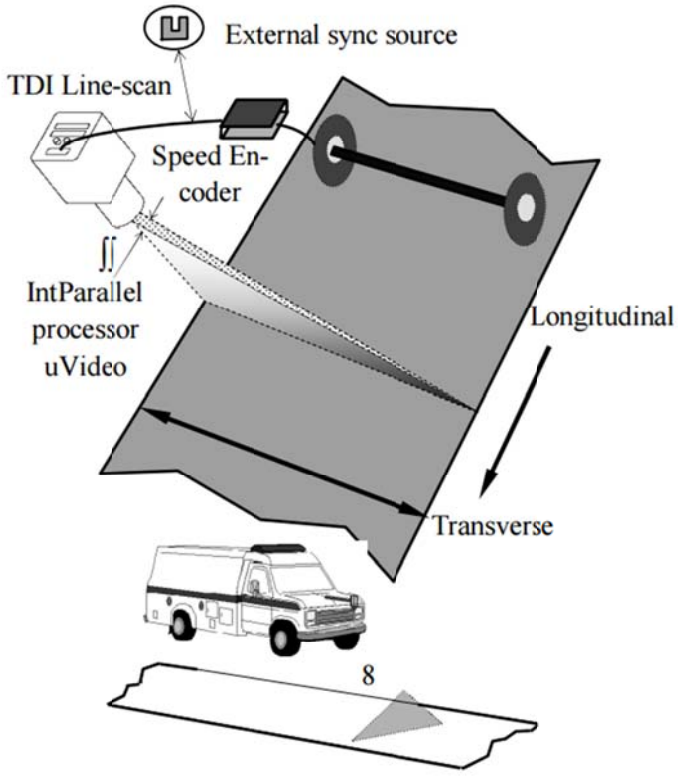

Figure 3. Line-scan camera equipped inspection vehicle
Source: ***(26)***

Ground-penetrating radar (GPR) technology has been applied to pavement and variety of roadway infrastructure elements such as bridge decks and piers to evaluate the deterioration over time. This method transmits electromagnetic waves into the pavement or bridges, and measures the backscattered time delay and amplitude to build information on the properties of the scene. Depending of the need and investigated element, ground-coupled or air-coupled horn antennas could be used for data acquisition, where horn antenna could be more appropriate for pavement and bridge deck evaluations *(27)*. GPR is an effective tool for acquiring subsurface information and thickness evaluation, specifically detecting cracking in airport runways. Successful evaluation of GPR data is relying on data collection and processing speed, availability and appropriateness of the equipment, overall cost (including data processing), and the physical properties of the site. In fact, asphalt pavements and concrete pavements show different characteristics due to its chemical properties and moisture content on GPR evaluations *(27)*. One major limitation of this system is that most GPR applications require lane closures on roadways and bridges *(13, 28)*, which increases the cost for both agencies and travelers. One of the most comprehensive studies on GPR *(29)* presents the advantages and limitations of the technology in detail along with some cost elements.

3.1.3 Overview of Satellite Remote Sensing and InSAR

History of SAR and InSAR

As an active microwave remote sensing system and the base of SAR, radar technologies were first used during World War II for measuring the distances to targets *(30)*, and later used for investigation of topographic features until early 1970s, when first application of airborne InSAR was used for detection of topographic changes over a period of time *(31)*. Later in 1978, spaceborne imaging radars began with NASA satellite SEASAT (launched in 1978 and operated for 100 days), was the breakthrough for geoscience, topographic applications and many others *(31)*. However, there were only few studies conducted due to limited available data until the launch of ERS-1 (1991) and ERS-2 (1995), which triggered the attention to the field and its possible applications *(30, 31)*. Since the early 1990s, tremendous amount of medium-resolution (100ft +) satellite images become available from space agencies, used for different applications in geoscience, environmental research, topographic mapping, hazard monitoring, etc. *(30)*. With the advances in space-based radar technology, current-operating satellites can provide much higher resolution (3-10 ft) and carry more detailed information for in-depth analysis.

How It Works?

A spaceborne or airborne SAR is a microwave imaging system that uses the motion of a satellite to simulate a long synthetic antenna by using relatively small antenna to produce much higher resolution to overcome the limitation of real aperture radar *(5, 32)*.

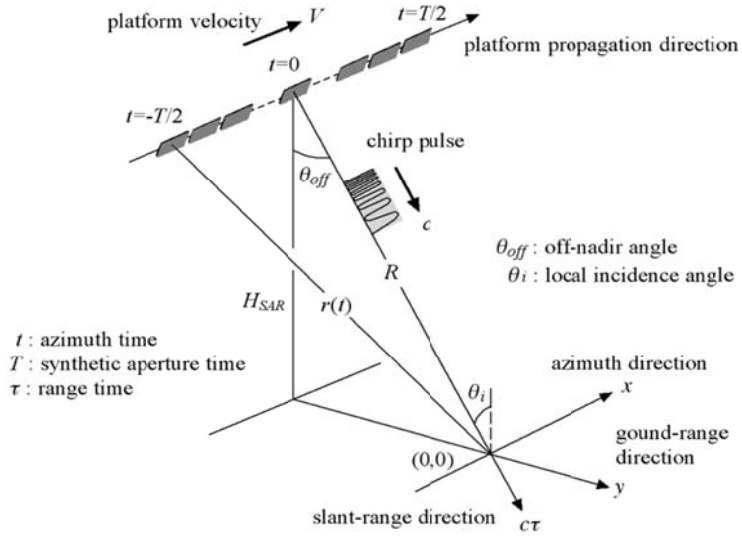

Figure 4**. The geometry of SAR system** *(14)*

As presented in Figure **4**, SAR sensor moving on azimuth direction transmits a serious of pulse called chirp pulse at an off-nadir angle θ_{off} in the direction of line-of-sight (LOS) also called slant-range direction to obtain information about the scene.

SAR imagery is produced by measuring the transmitted and backscattered radiation of the illuminated scene. A radar image contains both amplitude and phase in each pixel. Amplitude is the measure of the radiation backscattered by the objects in each pixel and helps to differentiate the surface characteristics. The amplitude depends more on roughness of the surface and ability to mirror away the radiation *(5)*. Typically, smooth flat surfaces present low amplitude characteristics such as roads, airport runways, storm channels, etc. *(5, 33)*. On the other hand, phase includes information about the distance between radar and scene by measuring the transmitted and received radiation proportional to wavelength (λ), which is successfully used for detection of surface deformations *(5)*. Table 2 presents the selected radar bands and respective wavelength and frequency measures. Most SAR sensors use X, C or L band radars for monitoring surface deformations. Cloud-penetrating capability and day and/or night operating flexibility give SAR superiority over other imaging techniques especially on tough climate locations *(5)*.

Table 2: Examples of radar bands, their frequency and wavelength

Radar Band	Frequency (GHz)	Wavelength (cm)	Satellite
Ka	26 – 40	0.8 – 1.1	
K	18.5 – 26.5	1.1 – 1.7	Military Domain
Ku	12 – 18	1.67 – 2.5	
X	8 – 12.5	2.4 – 3.8	TerraSAR-X, TanDEM-X, COSMO-SkyMed
C	4 – 8	3.8 – 7.5	ERS-1&2, Radarsat-1&2, RISAT-1, Envisat ASAR, ALOS PALSAR-2
S	2 – 4	7.5 – 15	Almaz-1
L	1 – 2	15 – 30	Jers-1 SAR, ALOS PALSAR
P	0.3 – 1	30 – 300	AIRSAR

SAR Interferometry (InSAR) uses two or more SAR images acquired at different times to derive more information about the scene by aligning (co-registration) them in an appropriate order and differentiating magnitude and phase *(5, 30-32)*. The change in the signal phase Δφ is proportional to wavelength and expressed as following equation:

$$\Delta\varphi = \frac{4\pi}{\lambda}\Delta R + \alpha$$

Since R represents the distance between radar and target scene in Figure **4** and Figure **5**, ΔR will be equal to the displacement between two radar acquisitions where λ is the wavelength and α is the phase shift due to atmospheric conditions. Following figure presents the surface deformation detection with phase change on two or more SAR acquisitions. In this figure, T_1, T_2, and T_n represent SAR image acquisition times, and ΔR_{12} and ΔR_n represent surface deformation between respective acquisitions.

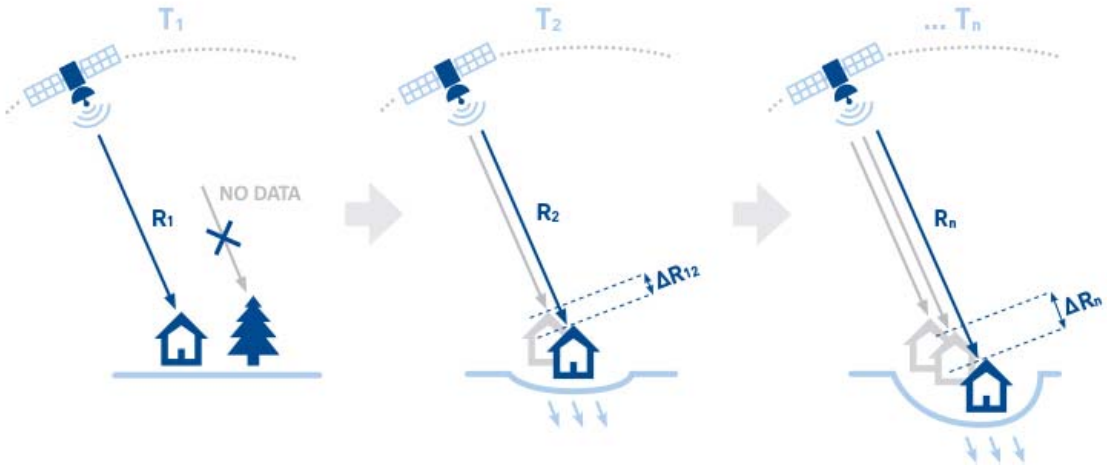

Figure 5**. A Schematic representation of deformation detection with InSAR approach** ***(34)***

The Interferometric phase comparison of SAR images enables creation of Digital Elevation Models (DEM) with meter accuracy and large area surface deformation with subcentimetric accuracy *(6)*. Detection of surface displacement relies on the precise co-registration of images to calculate the phase shift accurately; otherwise, rotation or movement in pixel or sub-pixel level can cause decorrelation *(30)*

Satellites for InSAR Analysis

New generation of SAR data providing satellites such as Radarsat-2, TerraSAR-X, Cosmo-SkyMed, and Sentinel-1 have better orbit control then their previous versions and provide pointable high-resolution data, which make them more suitable for InSAR analysis.

Many satellites carry different sensors for performing multiple tasks such as optical imagery, SAR, weather sensors, etc. Besides spaceborne satellite remote sensing systems, airborne platforms are also used to perform similar tasks. Table 3 provides a list of previous and currently operating satellites that produce InSAR applicable data. Table 4 summarizes three main platforms and their similarities and differences. These three platforms are widely used for transportation related studies and applications.

Table 3: Details of satellites for InSAR analysis

Satellite	*Agency-Country*	*Year of Launch*	*Band*	*Resolution (m)*	*Polarisation*	*Revisit Time (days)*
ERS-1	ESA/Europe	1991	C	5, 25	VV	35
ERS-2	ESA/Europe	1995	C	5, 25	VV	35
JERS-1 SAR	NASDA/Japan	1992	L	6, 18	HH	44
ENVISAT-ASAR	ESA	2002	C	10, 30	dual	3
RADARSAT-1	CSA/Canada	1995	C	8, 8	HH	5
RARDASAT-2	CSA/Canada	2007	C	3, 3	quad	24
ALOS-PALSAR	JAXA/Japan	2006	L	5, 10	quad	7
ALOS-PALSAR-2	JAXA/Japan	2013	C	10, 100	quad	14
Cosmo-SkyMed (4)	ASI/Italy	2007-10	X	1, 1	dual	5
TerraSAR-X	DLR/Germany	2007	X	1, 1	quad	11
TanDEM-X	DLR/Germany	2009	X	1, 1	quad	11
RISAT-1	ISRO/India	2012	C	3, 3	quad	25
HJ-1-C	China	2012	S	5, 20	VV	31
Sentinel-1A	ESA/Europe	2014	C	9, 50	dual	12

Table 4: SAR versus other earth observation instruments *(35)*

	LIDAR	*Optical Imagery*	*SAR*
Platform	Airborne	airborne / spaceborne	airborne / spaceborne
Radiation	own radiation	reflected sunlight	own radiation
Spectrum	infrared	visible / infrared	microwave
Frequency	single frequency	multi-frequency	multi-frequency
Polarimetry	N. A.	N. A.	polarimetric phase
Interferometry	N. A.	N. A.	interferometric phase
Acquisition Time	day / night	day time	day / night
Weather	blocked by clouds	blocked by clouds	see through clouds

Source: (32)

Applications upon SAR (DInSAR, PSInSAR^{TM}, SqueeSAR^{TM}, etc.)

Advanced imaging technologies and data processing capabilities increased the further research on SAR applications, specifically after the InSAR has made possible for using multiple images to retrieve more information about the scene. Increased data availability in 1990s led researchers to develop new methods to overcome the limitations of the technology, improve the calculation models, and explore new fields for InSAR applications.

SAR Interferometry (InSAR) uses two or more SAR images acquired at different times to derive more information about the scene by aligning (co-registration) them in an appropriate order *(6, 30, 31)*. Differential InSAR method (DInSAR), which uses the existing digital elevation information combined with InSAR, has long been used for detection of surface deformations with a millimetric accuracy on larger scale. Both methods have been widely used in many disciplines from ocean studies to hazard monitoring. Some of the transportation and infrastructure related application are listed here: detection of slow-moving landslides *(7)*, observation of volcanic and tectonic activities *(36)*, monitoring of land subsidence due to mining, gas, water, and oil extraction, etc. *(8, 24, 31)*, fire risk monitoring *(37, 38)*, flood monitoring and management *(39)*, urbanization tracking *(40-42)*, environmental studies *(43, 44)*, etc.

Effect of geometrical and temporal decorrelation caused by atmospheric effects and changes in backscattered signal intensity *(45, 46)* has been an active field for SAR related researches (Figure 6). Two of methods developed to overcome this issue are PSInSAR^{TM} *(6)* and a small baseline subset (SBAS) technique *(47)*. Ferretti et al. *(6)* introduced Permanent Scatterers (PS) method (PSInSAR^{TM}) to effectively remove the atmospheric interference by using stable neutral reflectors (buildings, electric poles, transmission towers and similar man-made objects that are consistent in terms of radiation reflectivity) in each SAR image over a series of images taken from same scene and calculated the surface deformations with millimetric accuracy *(6, 48)*. Ferretti et al. *(48)* stated that most cities and urban areas could provide about 2,000 PS/ km^2, which is very desirable *(48)* and currently operating high-resolution SAR satellites such as TerraSAR-X, COSMO-SkyMed, and Radarsat-2 significantly increased the number of detected PSs *(8, 49)*. Additionally, the relative effectiveness of PSInSAR^{TM} method also highly depends on the number of the images used for analysis, called image stack, which consists of 15 or more SAR images significantly contribute to the reliability of the results.

On the other hand, low density of PSs in nonurban and rural areas encouraged researchers to use Distributed Scatterers (DS) to extract more information about the scene where PSInSAR^{TM} is not applicable or not sufficient enough *(45, 46, 49)*. Although DSs do not produce high backscattered radiation as PSs, they are still statistically consistent in a homogenous area called DS Effective Area (EA) to reduce the noise. Developed this method (such as SqueeSAR^{TM}) *(45, 46)* successfully used in pastures, scree, and debris fields to increase the accuracy of results.

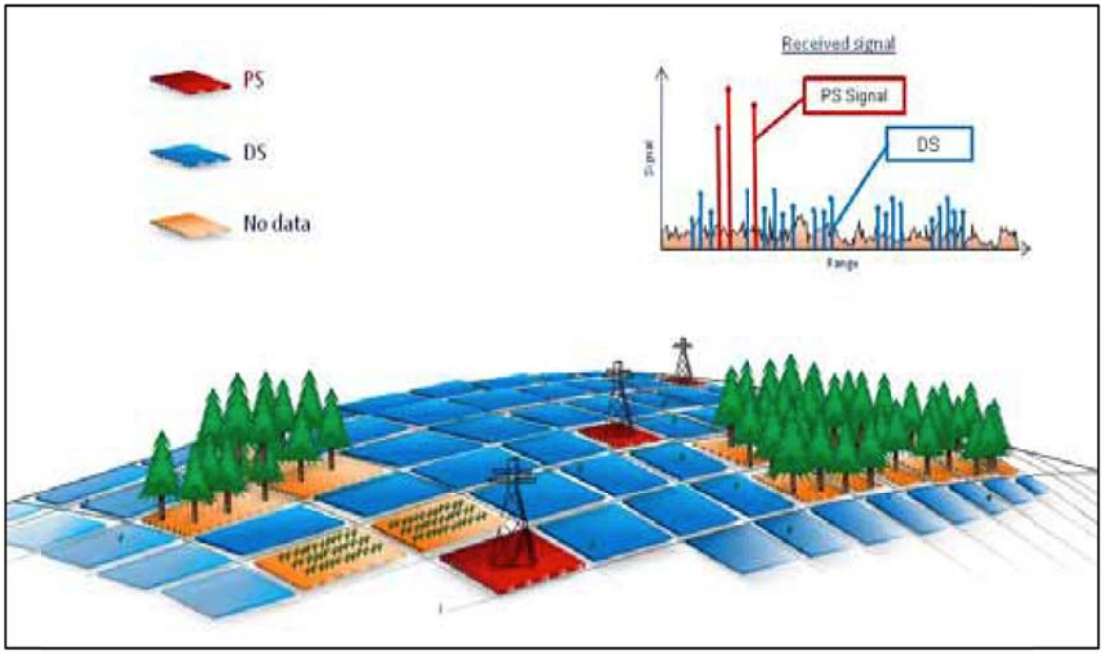

Figure 6. Illustrations of Permanent Scatterers (PS) and Distributed Scatterers (DS) by SqueeSAR™ algorithm
Source: ***(46)***

3.1.4 SAR and InSAR Processing Components

Processing of SAR imagery is highly dependent on available inputs and expected outputs for different cases besides some basic image processing steps. This section briefly introduces most common SAR image processing steps and specifically useful stages for deformation detection through InSAR. The main steps of SAR data processing are illustrated in Figure 7.

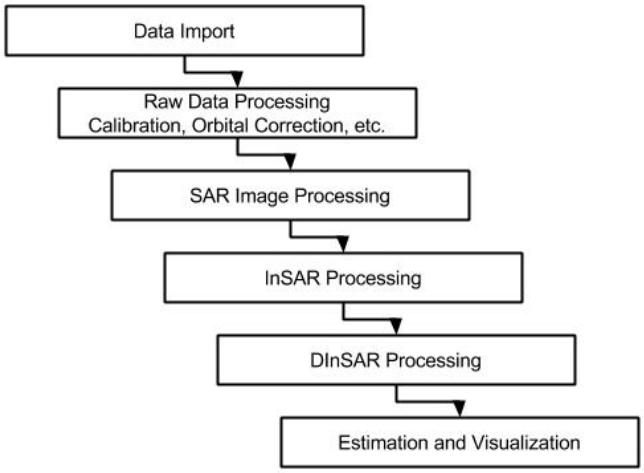

Figure 7. General data processing steps for SAR imagery

Image Selection

Variety of satellite imagery in different levels makes selection of suitable images for InSAR analysis difficult. As a key first step, image selection process has a high impact on the quality of final products. The following criteria should be considered during this process to improve the quality of expected results *(5)*:

- View angle (Ascending or descending)
- Geometric and temporal baseline
- Time of the acquisition
- Coherence
- Metrological Condition

Interferometric Correlation (Coherence)

In SAR imagery, the complex correlation coefficient between two SAR images has been represented with coherence, and carries useful information about the physical properties of the scene. High coherence between two SAR images can be translated as high quality of phase difference while low coherence meaning noisy phase difference *(5)*.

For instance, urban areas mostly show high coherence even after several years due to persistent backscattering signal reflectivity. On the other hand, vegetated areas might show low coherence even after weeks, which make the interferometric analysis difficult to perform. Coherence is mathematically represented as follows:

$$|\rho| \frac{|E\{S_1 S_2^*\}|}{\sqrt{E\{|S_1|^2\} * E\{|S_2|^2\}}}$$

In this equation, S_1 and S_2 represents SAR images, E{x} represents ensemble average, and (*) denotes complex conjugate. It is also important to understand the components contributing the coherence of master and slave images as presented in the following equation. Coherence of images consists of temporal (time between acquisitions), geometrical (orbit errors), volumetric (surface characteristics such as vegetation), and processing effects. Among these four elements, processing errors should be avoided to minimize the coherence loss between images.

$$\gamma = \gamma_{Temporal} * \gamma_{Geometric} * \gamma_{Volumetric} * \gamma_{Processing}$$

Co-registration

The process of co-registration could simply be explained as superimposing the images that have the same orbit and acquisition mode. However, it consists of complicated steps for estimating the cross-correlation between pixels of sub-windows in two SAR images. Without giving technical and mathematical details, it is logical to represent the co-registration process as in Figure 8. Individual SAR images are first calibrated, then available images co-registered consisting of one master and one or more slave images.

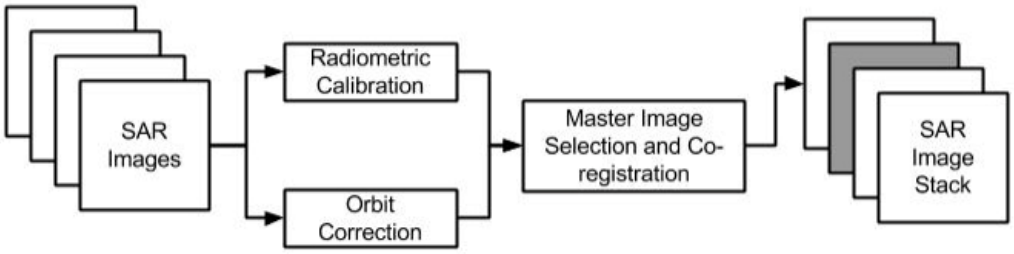

Figure 8. Preparation of Image Stacks in InSAR Process

Orbital Correction

Orbital correction is an essential step for accurately transforming the phase information into real height values. In this procedure, some accurate Ground Control Points (GCP) are used to remove this anomalies. Orbit files can be obtained from satellite agencies' websites little shorter than the generation of the product. Some of the SAR processing software (such as Sentinel-1 toolbox) can automatically download and apply the orbit file without requiring much effort.

Radiometric Calibration

Radiometric calibration is the process of removing the radiometric bias affecting the pixel values in SAR images. Most SAR products distributed as level 1 image, which generally does not include radiometric correction. Therefore, applying this correction for revealing true backscattering value of pixels is necessary, specifically for SAR images acquired from different sensors.

Interferogram Generation

Once the single SAR images are individually processed and co-registered, interferograms could be generated for determining phase change. Interferogram is produced by multiplying two complex SAR images to present the phase difference of acquisitions $r_2 - r_1$, shown in Figure **5**

Table 5: Generation of SAR product based on single/dual channel mode, polarimetry, and interferometry

SAR Intensity Processing	InSAR Processing	PolSAR Processing	PolInSAR Processing
Focusing	Interferogram Generation	Polarimetric Calibration	Co-registration
Multi-looking	Interferogram Flattening	Pol. Speckle Filtering	Interferogram Generation
Co-registration	Interferometric Correlation (Coherence)	Polarization Synthesis	Polarimetric Coherence
Speckle Filtering	Phase Unwrapping	Pol. Signature	Coherence Optimization
Geocoding	Orbital Correction	Pol. Decomposition	
Radiometric Calibration	Phase to Map Conversion	Pol. Classification	
Radiometric Normalization	Phase to Displacement Conversion		
Mosaicing			
Segmentation			
Classification			

Source: (35)

SAR Interferometric Phase Components and Phase Unwrapping

InSAR analysis and deformation detection requires determination of phase difference. Therefore, accurately obtaining phase difference and evaluating the components affecting the overall phase change is essential. Five components have contribution to the phase difference of SAR images as presented below:

$$\Delta\varphi = \Delta\varphi_{displacement} + \Delta\varphi_{elevation} + \Delta\varphi_{flat} + \Delta\varphi_{atmosphere} + \Delta\varphi_{noise}$$

Among these five components, $\Delta\varphi_{displacement}$ is expected to be calculated while removing or minimizing the other effects. Each one of the effects briefly explained below:

- $\Delta\varphi_{displacement}$: contribution of surface deformation to the interferometric phase (The change will be measured)
- $\Delta\varphi_{elevation}$: contribution of topographic effects to the interferometric phase
- $\Delta\varphi_{flat}$: effect of earth curvature to the phase. This effect can be estimated and subtracted.
- $\Delta\varphi_{atmosphere}$: atmospheric contribution to the interferometric phase due to temperature, humidity and atmospheric pressure change between acquisitions
- $\Delta\varphi_{noise}$: the phase noise due to temporal change of the scatterers, and volume scattering, look angles, etc.

The phase of an interferogram is presented in the unit of 2π, which makes the determination of absolute change hard, as presented in Figure 9. The process of converting absolute phase from wrapped phase called "phase unwrapping", simply adding appropriate number of cycles to the measured phase. Several phase unwrapping algorithms have been developed over time such as minimum least squares, minimum cost flow, multi-baseline, residue-cut, etc. *(5, 50)*.

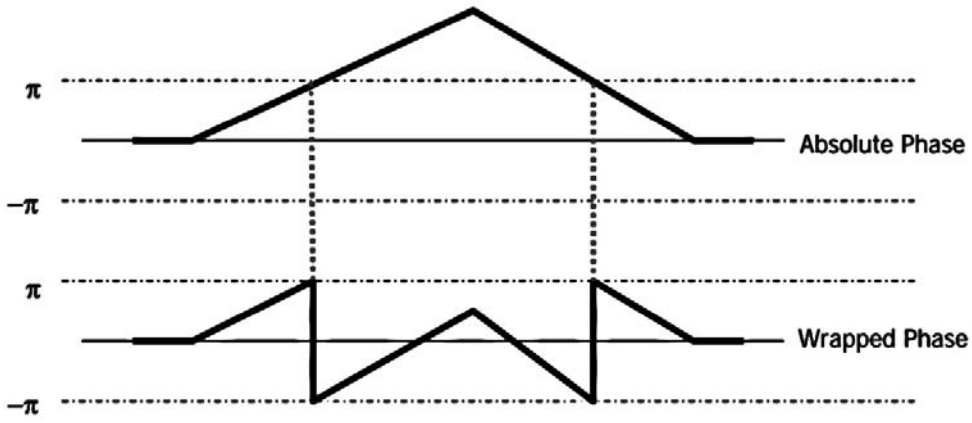

Figure 9. Schematic representation of phase unwrapping

3.1.5 Data Sources and Software Evaluation for InSAR Analysis

Variety of data sources for SAR imagery, and broad application field naturally created different opportunities for data analysis and software development. Only remote sensing

satellite data and possible software options are presented and evaluated in this section to stay within the boundaries of scope by giving priority to freely available options. Some data sources and software are presented with detail to inform readers about the process of obtaining and using the data or software.

Data Sources for SAR Imagery

Remote sensing airborne and satellite data has been available since early 1970s with low-resolution, which is not very useful for transportation and infrastructure purposes. Many studies in this field have begun with the launch of medium-resolution satellites in 1990s such as ERS-1&2, Radarsat-1, and Landsat-1. More interestingly, recent studies that use high-resolution and spot images highlighted the effectiveness of such technology in transportation and civil infrastructure systems. In addition the data sources, there are many software packages available from single image processing to time series of SAR data analysis that might be used based on research needs and data constraints. Some software packages provide detailed analysis for many different satellite inputs to address different users, while some of them only aim at specific type of analysis.

One of the main players in space and earth observations, NASA, provides variety of data sets and images for researchers through EOSDIS (NASA's Earth Observing Systems Data and Information Systems). The information is publicly available through NASA's website with a user-friendly search interface. In terms of InSAR stacks for pavement and infrastructure monitoring, EOSDIS does not provide very useful datasets. However, datasets such as MODIS (Moderate Resolution Imaging Spectroradiometer), ASTER (Advanced Spaceborne Thermal Emission and Reflection Radiometer) and AVIRIS (Airborne Visible / Infrared Imaging Spectrometer) might be useful complimentary data sources for transportation related applications.

One of the main sources of SAR data is European Space Agency (ESA). Since the breakthrough satellites ERS-1 and ERS-2 completed their journey in the space, ESA makes most of the datasets from both satellites available to interested researchers upon proposal submission and approval. Although the medium-spatial resolution SAR datasets are not very suitable for pavement and infrastructure monitoring, combining ESA-1&2 datasets with recent high-resolution SAR data might provide opportunity for long-term historical analysis of the area of interest. Following figure presents the screenshot of ESA's one of the data access portal for viewing, selecting and downloading different type of satellite remote sensing data. Access to the portal for catalog browsing requires free registration; however, ordering the data is only possible after the proposal submission through ESA Earth Online account.

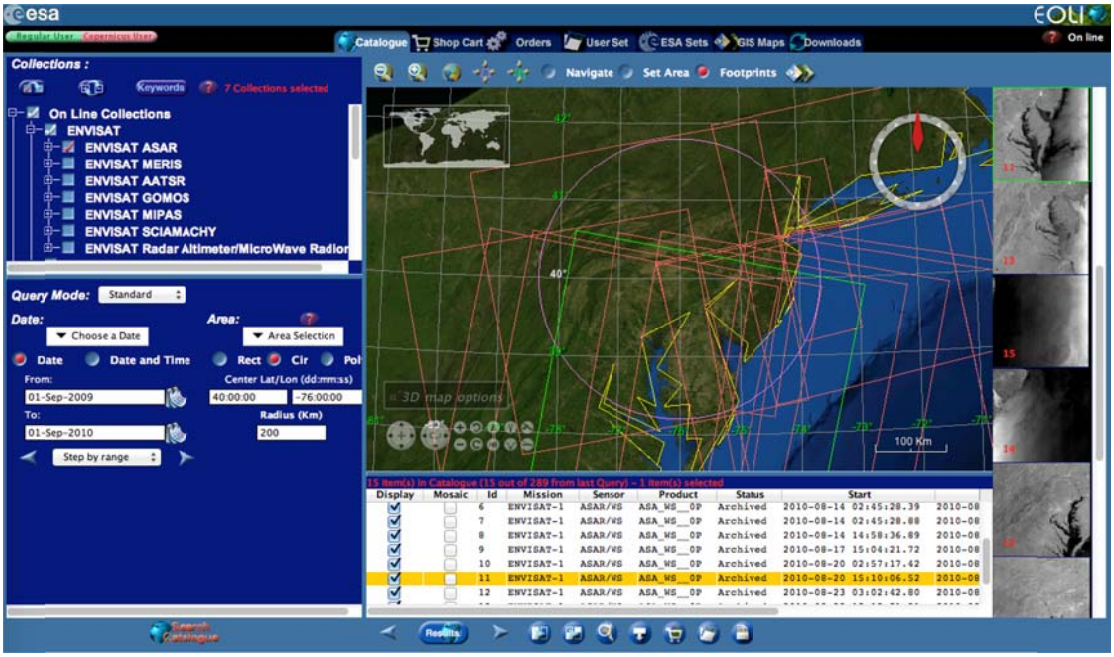

Figure 10. Eoli-sa (ESA Data Access Portal)

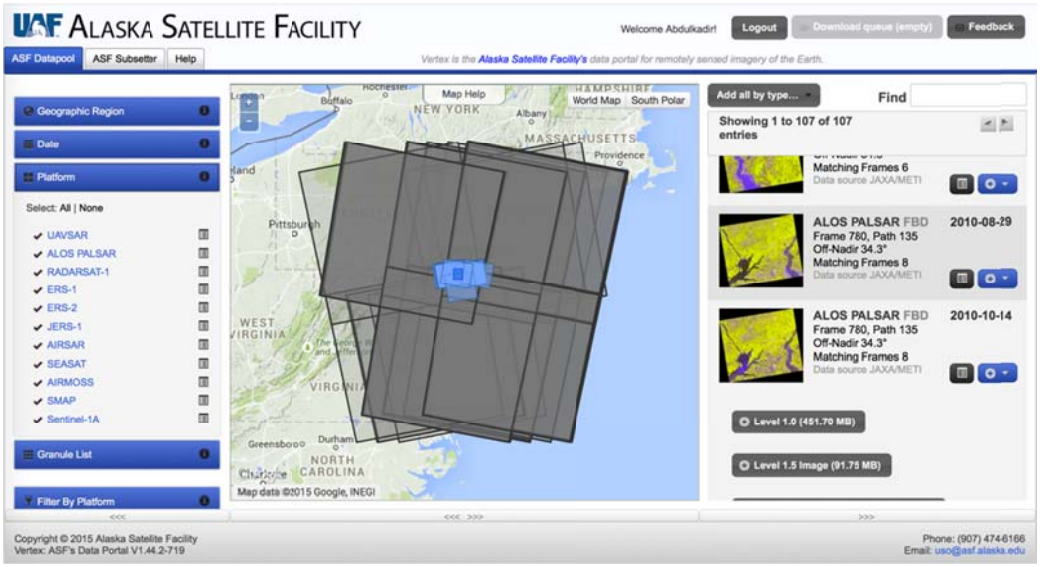

Figure 11. Alaska Satellite Facility data access portal

Alaska Satellite Facility (ASF) provides variety of satellite remote sensing data including ERS-1&2, RADARSAT 1, ALOS PALSAR, recently launched Sentinel-1n and more. Easy to use data access portal facilitates the selection and download of data by users.

Selected datasets freely distributed through the portal whereas some datasets provided upon proposal submission and approval. In this case, data users might pay for acquisition and some level of data preparation based on data users' need. Figure 11 shows a screenshot of data access portal of ASF.

ASF also provides another data access portal as illustrated in Figure 12 and Figure 13. In this User Remote Sensing Access portal, users have an option for only selection InSAR stacks that are suitable for SAR Interferometry analysis, which eliminates a complicated data selection process for non-experienced users. However, in this portal, users must have the required credentials such as approved proposal and financial account linked to the research for obtaining the data. In Figure 13, available SAR acquisitions in the InSAR stack are presented in a temporal baseline graph to facilitate the selection of appropriate datasets.

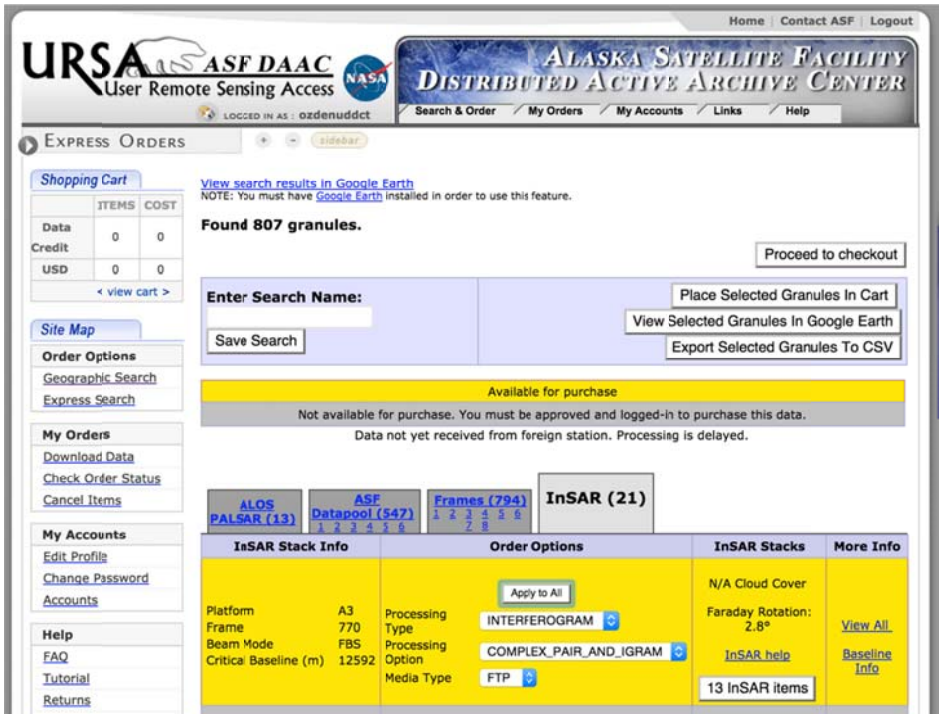

Figure 12. Alaska Satellite Facility InSAR data access portal

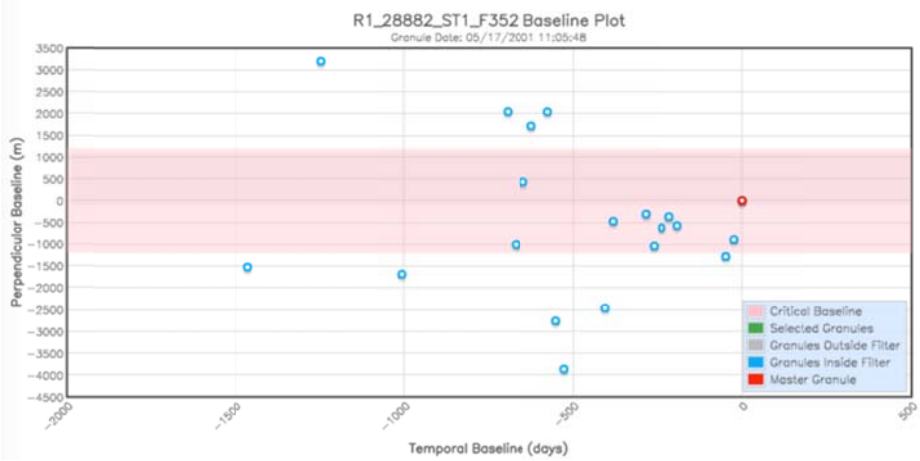

Figure 13. ASF InSAR data stack selection

Many other regional organizations and consortiums such as UNAVCO (a non-profit university-governed consortium) and WInSAR (Western North America InSAR Consortium) use and provide SAR data to their members and interested 3rd party researchers. Besides mentioned data sources, some agencies or companies provide most-recent SAR image and data processing for a fee for interested users. The cost of image acquisition and data processing may vary by image type, area of interest, expected outcomes, etc. and is comprehensively provided in cost-benefit analysis section of the report. Additionally, in some cases, users are able to request new acquisitions for the area of interest for a specific time frame.

Freely Available Software for SAR Data Analysis

There are many open source and commercially developed software packages available for SAR data analysis. Due to broad range of satellite remote sensing data types and different level of data products, selection of data processing tool requires serious attention specifically for non-experienced users. It is important to note that this selection is vastly related to the goal of the project and needed outputs as well as the prior knowledge of data analysis personnel. Some code based SAR data processing applications might provide a simple and quick solution if the objectives and data output needs overlap with what the application offers.

Most of the open source software packages have been developed by researchers who are working in the field of SAR Interferometry. Therefore, many of these non-commercial packages are code based and require basic knowledge on compiling and running the program in a suitable environment. Although these tools are mainly used internally, they also contribute to the research community by providing stand-alone modules for interested users. In the field of SAR data processing for InSAR analysis, following software packages or toolboxes have been found useful and recommended for a possible data analysis tool:

European Space Agency's Sentinel-1 Toolbox is one of the most powerful software packages developed for SAR data analysis that handles most data types from different satellites including recent high-resolution SAR imagery from Cosmo-SkyMed and TerraSAR-X. Comprehensive and detailed analysis is possible with Sentinel-1 toolbox such as: calibration, topographic correction, speckle filtering, co-registration, InSAR analysis, etc. This comprehensive package replaced the previous version NEST, and provided freely as ESA's many other data analysis tools through their website. This recently announced toolbox is quickly adopted by experienced users and the users of previous version, NEST.

GRASS (Geographic Resources Analysis Support System) is another powerful, open source GIS and geospatial data management and analysis application. It provides both graphical user interface and command line syntax to accomplish many different image processing, spatial modeling, and data visualization, operations. The platform uses both raster and vector formats for data analysis, GIS capability of platform is one advantage for quick visualization of end products. As a well-known GIS and data processing application, GRASS is a possible tool for SAR data analysis.

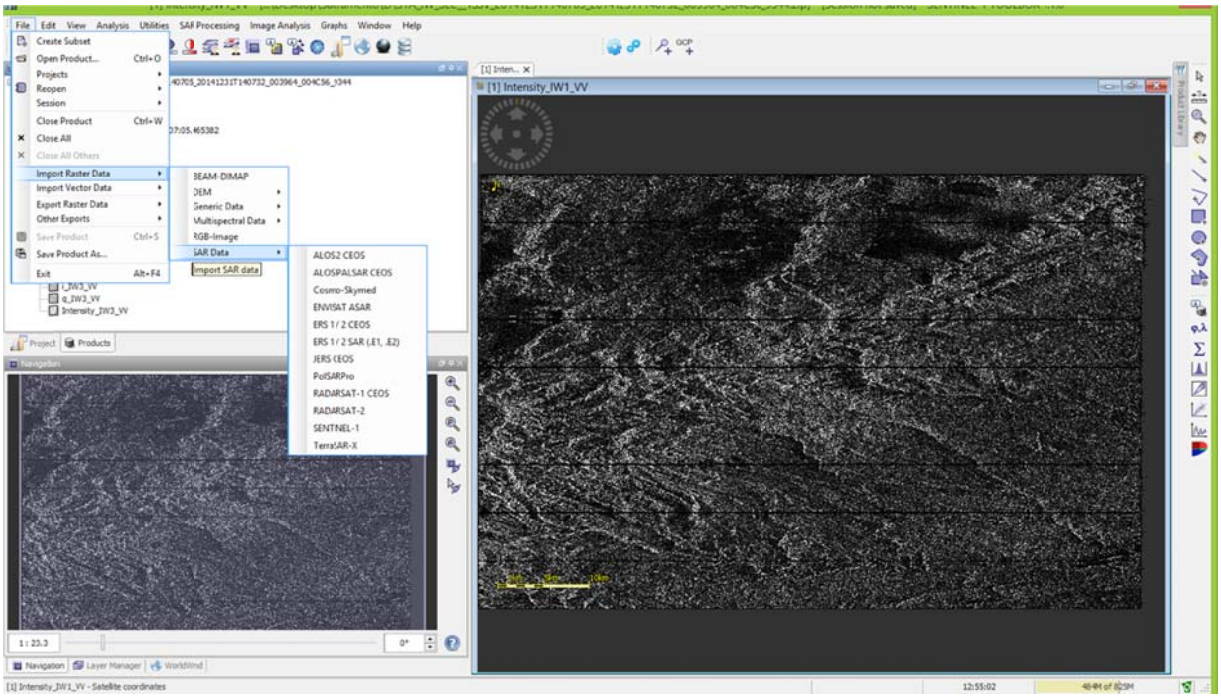

Figure 14. Screenshot of Sentinel-1 toolbox

SAGA (Systems for Automated Geoscientific Analysis) is an open source and cross-platform GIS software, which enables users to work with computational methods for raster, vector and tabular data by using C++ and python. SPRING is another GIS and

remote sensing image-processing software developed by Brazil's National Institute of Space Research (INPE/DPI). SPRING is able to process LANDSAT, SPOT and ERS-1 images. OFGT (Open Foris Geospatial Toolkit) is another command-line tool aimed at simplifying the process of L0 level satellite imagery.

ROI_PAC (Repeat Orbit Interferometry PACkage) is an open source software package that process variety of SAR data and specifically useful for L0 level data and InSAR applications. This code-based package developed by Caltech and JPL (Jet Propulsion Laboratory) and currently maintained by Cornell University research groups. ISCE is another Caltech/JPL & Stanford initiated open source SAR data processing software package that has been licensed and managed by UNAVCO on behalf of WINSAR.

DORIS (Delft Object-oriented Radar Interferometry Software) developed by the Delft Institute of Earth Observation and Space Systems is another useful tool for generating of interferometric products such as DEMs and displacement maps. DORIS uses Single Look Complex (SLC) data from ERS-1&2, ENVISAT, JERS-1 and RADARSAT-1 satellites for the generation of interferograms and other SAR end products.

GMTSAR is another open source SAR data processing tool that is used by researchers who are familiar with Generic Mapping Tools (GMT). The C programming language based code could be used for variety of tasks including preprocessing satellite data to convert the native format and orbital information into a generic format; aligning image stacks and forming complex interferograms for InSAR processing; and determining line-of sight displacements based on GMT. This code based data analysis package is mainly managed by Scripps Institution of Oceanography, University of California San Diego and collaborators from other universities.

Besides mentioned freely available software packages, there are many powerful commercial software packages for different level and type of SAR data processing. Gamma (Gamma Remote Sensing), ENVI SARScape (Exelis), DIAPASON (Altamira), and IMAGINE Radar Mapping Suite (ERDAS) are some of the packages that are suitable for SAR image processing. These packages are designed to appeal to a broad range of users as in many other commercial software packages.

3.1.6 Current Transportation Infrastructure Practices of SAR Remote Sensing

In this section, studies related to pavement monitoring and bridge assessment will be presented since SAR remote sensing has been increasingly investigated in these two fields. Recent studies highlight the effectiveness of InSAR methods in pavement and infrastructure monitoring along with its potential and limitations. Cascini et al. *(8)* compared medium- and high-resolution SAR images for detection of undergoing settlements in an urban area in Naples, Italy. They used PSInSAR^{TM} method for detection

of deformation and determination of deformation velocities on a high-speed railway line and a close by highway section in the area of interest. Results present that availability of high-resolution SAR images can significantly increase the accuracy of the results and level of detail for detection of deformations.

Hoppe et al. *(10)* used both DS along with SqueeSAR™ technique and Temporary Scatterer (TS) approach (a by-product of SqueeSAR™) to evaluate the use of satellite remote sensing for transportation infrastructure. First, they found that PSs and DSs are densely populated along highways, railways and infrastructure elements, which make satellite remote sensing valuable on infrastructure monitoring. They also found that both methods are very useful for detection of sinkhole formations, progressive settlements on bridges and dangerous rock slopes *(9, 10)*. In the same study, they evaluated the pavement surface distress detection with TS raster data and highlighted the possible use of such technique and recommended further exploration targeting pavement surface distress detection as presented in the Figure 15 and Figure 16 *(10)*. One of the common results in these studies was that researchers were not able to identify the type of pavement surface distress or settlement problem without further investigation on site. This is mainly the result of limited research and available methods in the field of transportation and infrastructure monitoring. InSAR has recently gained attention by transportation and infrastructure researchers for further investigations.

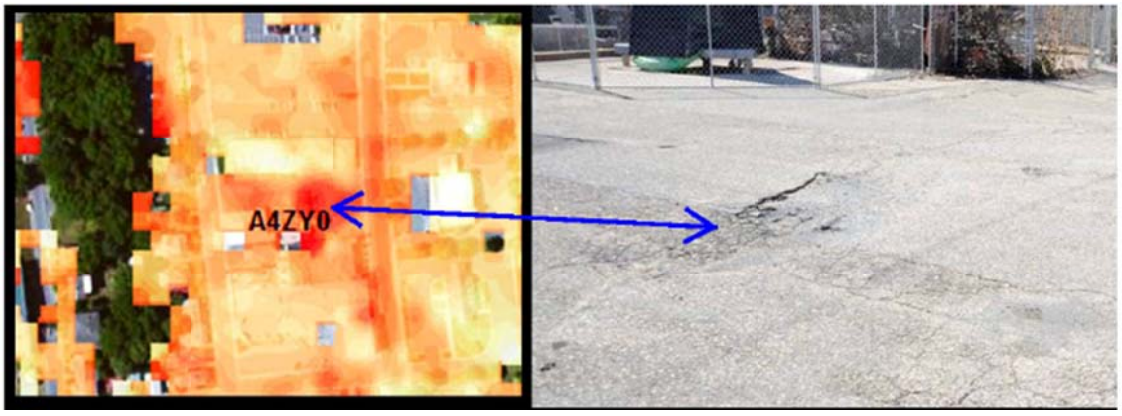

Figure 15. DS and TS data indicating surface deformation

Source: ***(10)***

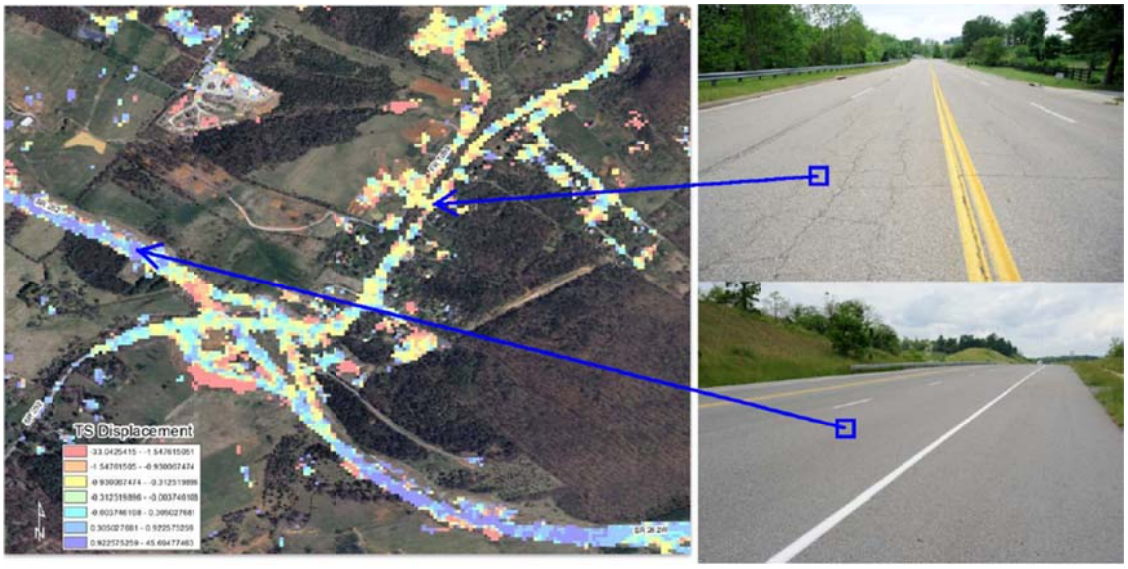

Figure 16. Pavement surface deformation detection with TS

Source ***(10)***

In another study, Hoppe et al. *(11)* used InSAR analysis technique for evaluating an ongoing water intrusion problem at both approaches of Monitor-Merrimac Memorial Bridge-Tunnel in Virginia. InSAR analysis is used to examine if the water intrusion caused by consolidation settlement. 46 SAR images acquired between 2001 and 2010 were processed with SqueeSAR^{TM} method. Evaluation of the results revealed that there is no significant settlement at the tunnel boat sections to cause a water intrusion problem *(11)*. The study presents a good example of medium-resolution historical SAR data with recent high-resolution acquisitions for a long-term historical analysis.

Goel and Adam *(49)* presented the use of high-resolution SAR data for mapping the surface deformations in their study. Results also revealed the potential of such technology for detection of pavement surface deformations as shown in Figure 17. However, many of these studies did not specifically focused on detection of pavement deformations and presented as a possible contribution of such technology. Therefore, further research investigating the effective use of SAR based applications for pavement monitoring might reveal more reliable information regarding the use of technology in pavement management.

Figure 17. Detection of deformations using Distributed Scatterer Interferometry

Source: ***(49)***

In another study, *(51)* used Phase Array type L-band SAR (PALSAR) to evaluate the pavement condition in a section of a highway in Thailand. Preliminary analysis resulted that HH and VV backscatter values are correlated with condition of the pavement where increase in HH backscattering indicates poor condition. Validation with International Roughness Index (IRI) along the analyzed section shows that the accuracy of the prediction of the highway surface condition was 97% *(51)*.

3.2 CASE STUDY 1: MONITORING URBAN GROWTH WITH SAR TIME SERIES

UNESCE-Bilko project was started in late 80s to provide open-source software and training data for those who study coastal and marine remote sensing. Low-cost computer requirements, easy to use interface supported by training lessons, and availability of all components free of charge were the main reasons to increase the popularity of tool over time. Since the software was widely used by education and training purposes in early years, users started improving the content and adding data, which became available and useful for other fields such as land development.

Bilko supports many common image formats such as GeoTIFF, USGS Mapgen formats, data from ESA satellites (ERS, SMOS), and also from Envisat and Jason-2 besides some others. The software also supports 8-bit, 16-bit, 32-bit and floating point data for the use

of image processing. Bilko currently does not support recent satellite imagery (Radarsat, TerraSAR-X, Cosmo-SkyMed, etc.) for image processing and InSAR analysis, which might change in the future. However, ESA supported open source SAR software Sentinel-1 Toolbox can process most recent SAR-based images which is demonstrated in Case Study 2.

In this demonstration, freely available datasets from "*Learn Earth Observation with ESA"* website was used. Following section presents step-by-step procedure with visual representation for urban monitoring with SAR time series using Bilko software. Dataset contains 10 Envisat ASAR images of Rome, Italy. Images were acquired from 2004 to 2010, and details are provided in Table 6. The spatial resolution of images is 30m.

Table 6: ASAR images and acquisition dates

Image	Acquisition Data
ASA_IMP_1PNDPA20040110…_0439.N1	10 Jan 2004, at 20:53 UTC
ASA_IMP_1PNDPA20040214…_0440.N1	14 Feb 2004, at 20:53 UTC
ASA_IMP_1PNDPA20040703…_0443.N1	03 July 2004, at 20:53 UTC
ASA_IMP_1PNDPA20040911…_0444.N1	11 Sep 2004, at 20:53 UTC
ASA_IMP_1PNDPA20041016…_0445.N1	16 Oct 2004, at 20:53 UTC
ASA_IMP_1PNDPA20100227…_0462.N1	27 Feb2010, at 20:53 UTC
ASA_IMP_1PNDPA20100508…_0463.N1	08 May2010, at 20:53 UTC
ASA_IMP_1PNDPA20100717…_0464.N1	17 July 2010, at 20:53 UTC
ASA_IMP_1PNDPA20100821…_0465.N1	21 Aug 2010, at 20:53 UTC
ASA_IMP_1PNDPA20100925…_0466.N1	25 Sep 2010, at 20:53 UTC

SAR image processing is performed by using following steps:

- Opening and displaying SAR data
  - Reading basic information from header files
  - Displaying individual SAR imagery in Bilko
- Calibration of SAR images
  - Converting Digital Numbers (DN) image values into backscattering coefficient values
  - Converting backscattering values into decibel (dB) units
- Co-registration of images
  - Selection of master and slave images
  - Ground control points

    - Resampling of images
- Speckle reduction
    - Frost method
    - Lee method
- Determination of change detection
    - Backscattering analysis
    - Evaluation of backscattering changes with colour composite
    - Time series analysis of selected pixels

3.2.1 SAR Metadata and Displaying SAR Images

Individual images can be opened either using "Open" command in the toolbar or dragging and dropping the image into Bilko software. If image contains header files and metadata, which most images do, user will have a similar window as in Figure 18 containing product headers and bands. Product headers (MPH and SPH) and other fields in metadata include information about the SAR imagery such as acquisition time and location, polarization, orbital information (ascending/descending), number of azimuth and range looks, azimuth and range spacing, real and absolute orbits, etc.

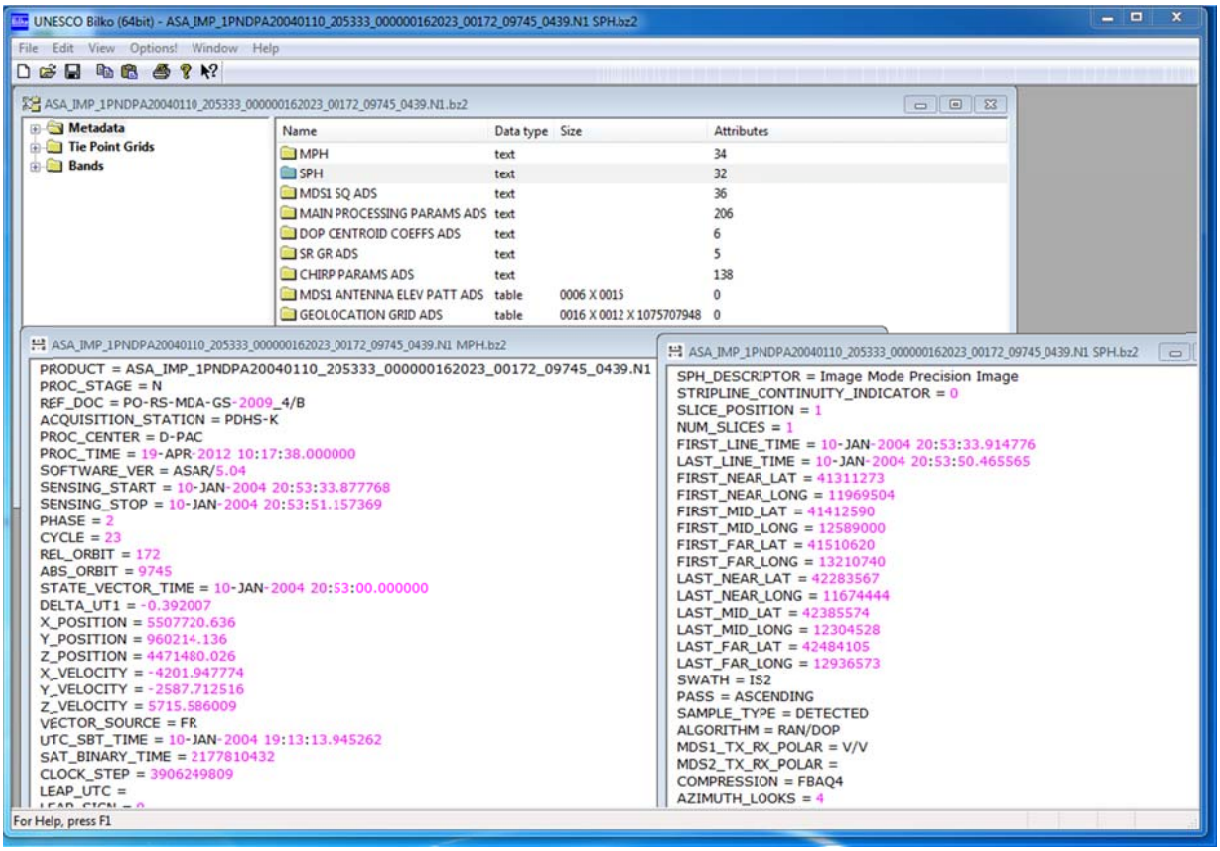

Figure 18. Metadata and product headers of SAR imagery

After reviewing the information about the acquired SAR imagery, actual image could be opened by double clicking the product in "Bands" folder (See Figure 19). Then, the image can be displayed in different view by right-clicking the image and using zoom options.

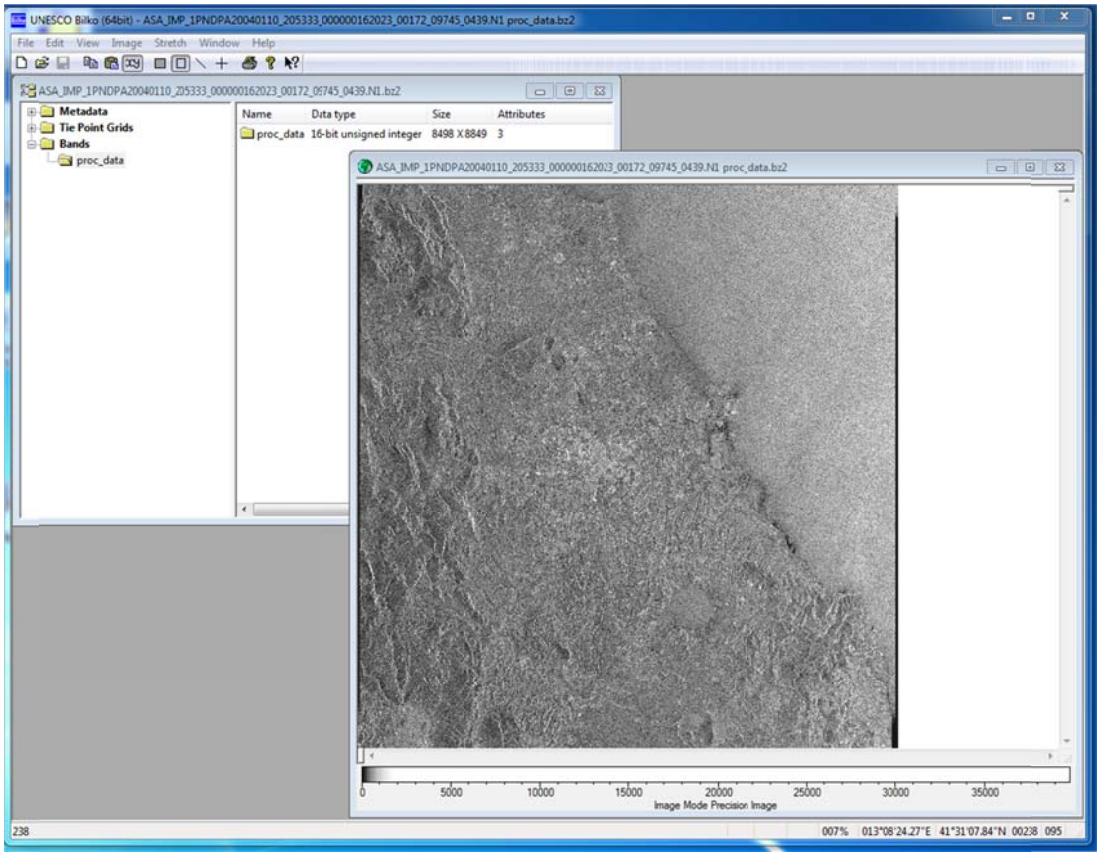

Figure 19. Opening and displaying SAR imagery

3.2.2 Calibration of SAR Images

First, individual SAR images are opened and radiometric calibration applied to assign backscattering coefficient to each pixel. SAR imagery is expressed as Digital Numbers (DN) in general, and need to be converted into backscattering coefficient values, decibel (dB) in most cases. In Bilko software, this calibration is possible in two steps:

For the first step, following formula is applied in all images to convert DNs into backscattering coefficients. By using "copy" and "paste" commands in Bilko, users can copy the formula and paste in onto the image, and calibration of the data will be performed automatically.

```
# Bilko formula to calibrate ASAR SAR images
# This formula can be indifferently applied to a single image or to a stack
```

```
# NB: Output options must be set to floating point data
set output 32f;     #output is 32 bit float
CONST k=297166.59375;
CONST a=0.4274;
# The calculations below will create a new, corrected image on the fly.
for i=1,_last

@[i]=sin(a)*(@[i]^2)/k;
```

Then, calibrated data should be converted into decibel (dB) by using the formula below. Again, using "copy" and "paste" commands in Bilko toolbar automatically perform the calibration on image. Un-calibrated and calibrated SAR imagery is presented in Figure 20.

```
# This formula can be indifferently applied to a single image or to a stack
# NB: Output options must be set to floating point data
set output 32f; #output is 32 bit float
for i=1,_last

if (@[i]>0)  @[i]=10*log(@[i]) else @[i]=0;
```

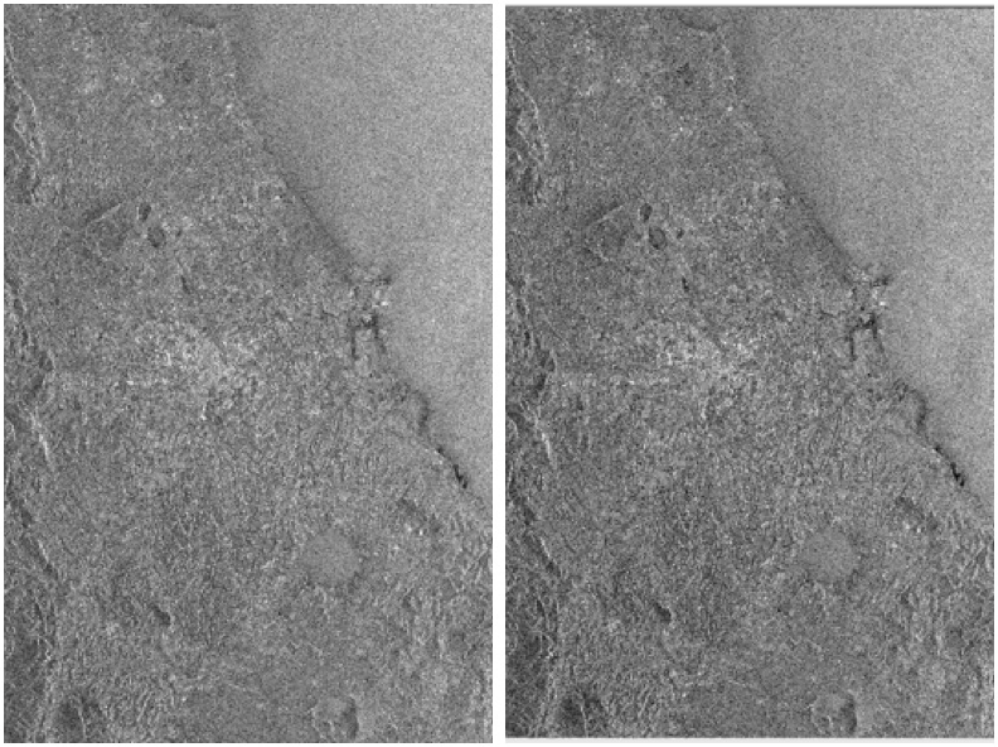

Figure 20. Radiometric calibration of SAR imagery: Un-calibrated (left) and calibrated (right)

Now, the individual images are ready for co-registration. This step requires selection of master and slave images and using Ground Control Points (GCP) for successfully co-

registering the images. GCPs are selected among the pixels that are clearly identifiable in both master and slave images, and preferred 20 or more that are spread on different sections of the scene. In this process, first "Rectify" command is used under "image" command in the toolbar. Then, user should identify master and slave images in the opening window, which will open a table list for entering GCPs. Figure 21 presents the selection of two GCPs in master and slave images.

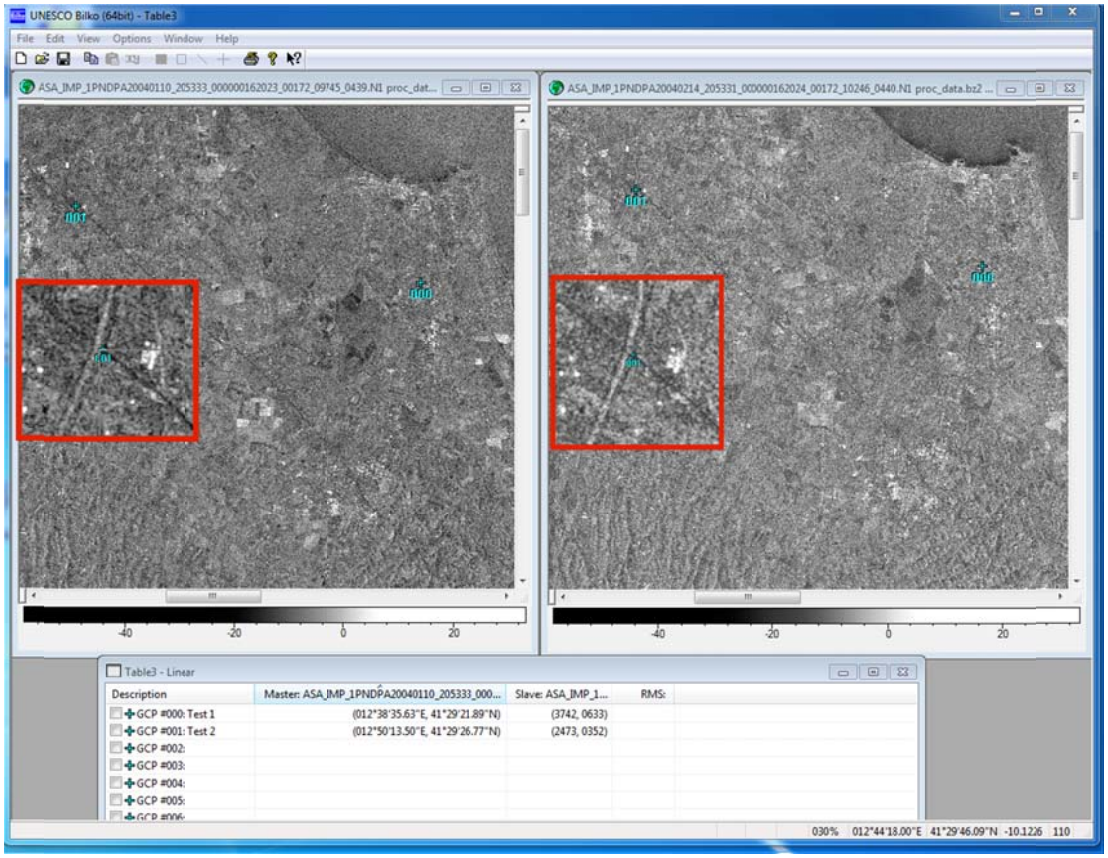

Figure 21. Selection of GCPs in master and slave images (Zoom-in views presented in boxes for GCP #1)

GCP #1 is selected as an intersection of two highways, which is clearly visible when zoomed in. The remaining table could be filled out by following the same procedure before co-registration process. After entering the GCPs, the GCP table should be copied and pasted onto the slave image to fix the pairs. Then, resampling process should be carried out for viewing the image in its correct size and position. Nearest neighbor method could be used to resample the images. This step can be performed by using "image" and "Resample" commands. Figure 22 presents the resampled master and slave images that will be co-registered in the next step.

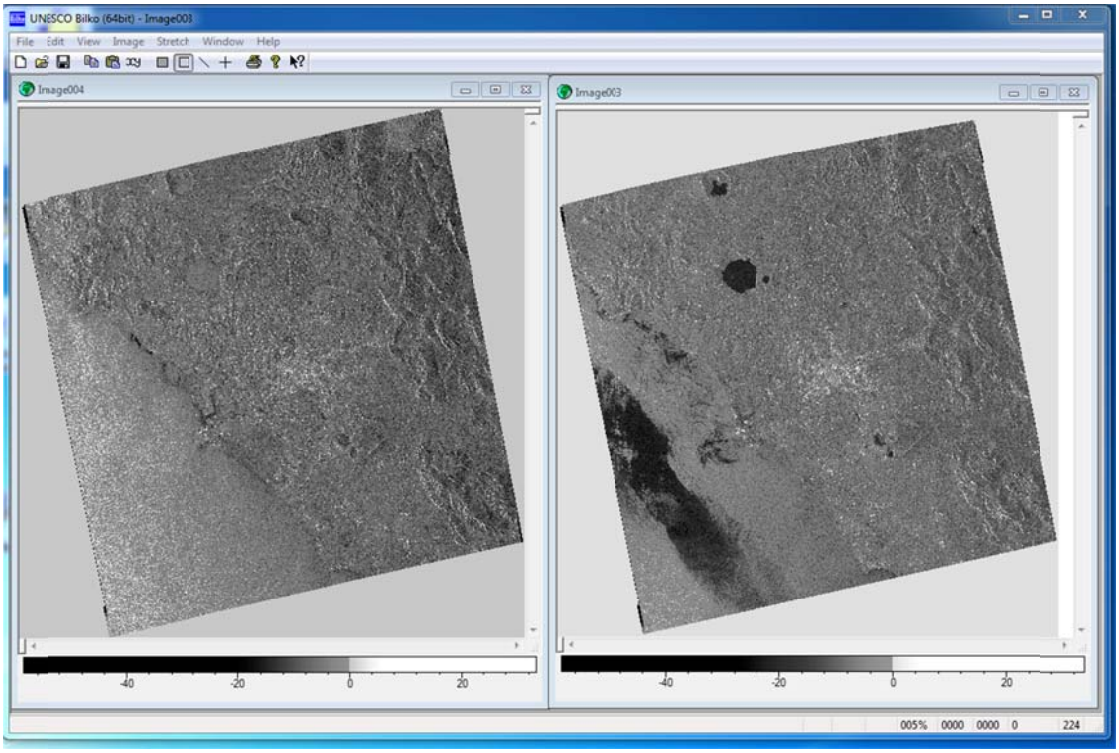

Figure 22. Resampled master (left) and slave (right) images

3.2.3 Co-registration of Images

After the calibration, GCP selection and resampling process, SAR images are ready for co-registration. This simple step could be performed by using “Image” and “Connect” commands. Then, user should select the available SAR images ready for co-registration from the menu, and click “OK” while “stack” option is selected. Bilko will automatically co-register the selected images and open as a new window. User can navigate between images by using “tab” key from their keyboards or using dropdown menu on the screen.

Figure 23 shows the individual SAR images to construct image stack for further analysis. 10 Envisat ASAR images are co-registered based on previously listed steps.

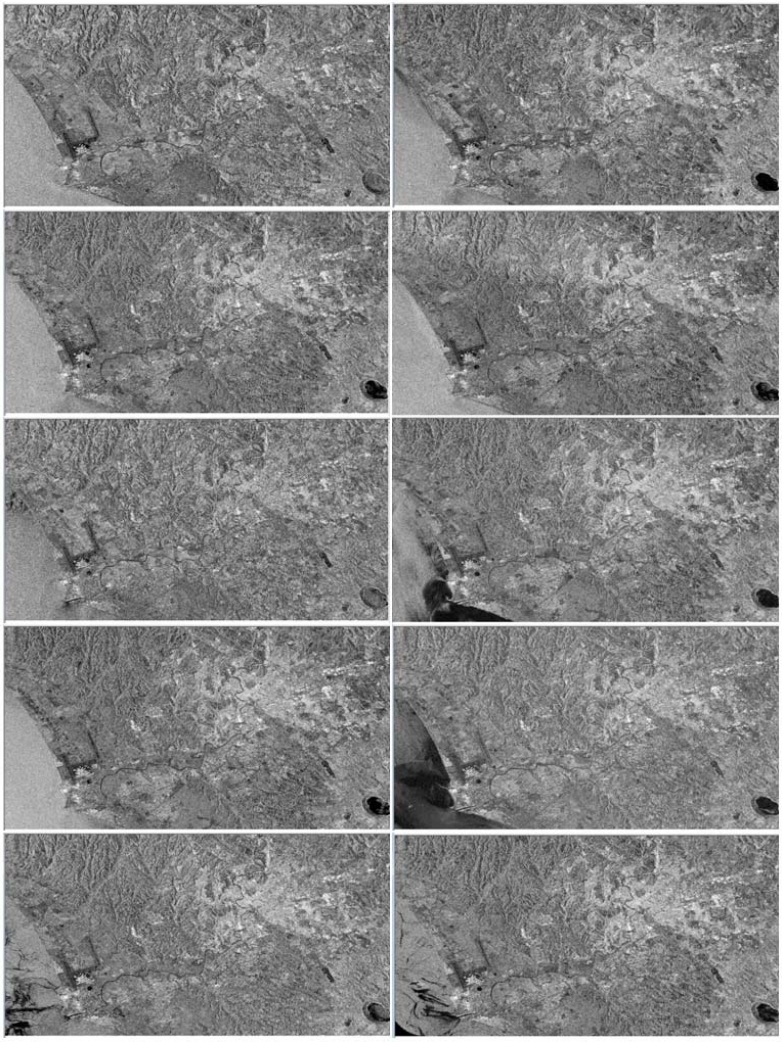

Figure 23. Individual Images Constructing SAR Image Stack

3.2.4 Speckle Reduction

After successfully co-registering the images, speckle reduction could be performed to remove the noise in the images. This could be performed by using Frost or Lee speckle filtering methods in Bilko. Speckle filtering is applied by using "image/filter/Frost (or Lee)" in the toolbar menu. One important point here is to determine the filter sizes and number of looks to perform the process. This decision should be made based on characteristics of the scene and expected outcomes as well as filter type. Picchiani and Del Frate *(52)* mentioned that using larger window sizes might be useful for uniform and large areas but this might also cause smoothing the small objects and features such as narrow roads and small buildings. From this perspective, window size should be defined by users. On the other hand, the second input "equivalent number of looks" could be found in the metadata of the image under the Specific Product Header (SPH) folder. In our case study, azimuth look is 1 and range look is 4, where equivalent number of looks

becomes the multiplication of looks, 4. Figure 24 shows the effect of the speckle filtering in both methods. The top image presents the scene without any filter while middle and bottom images presents the Frost and Lee speckle filtering respectively for 3*3 window size and 4 equivalent number of looks.

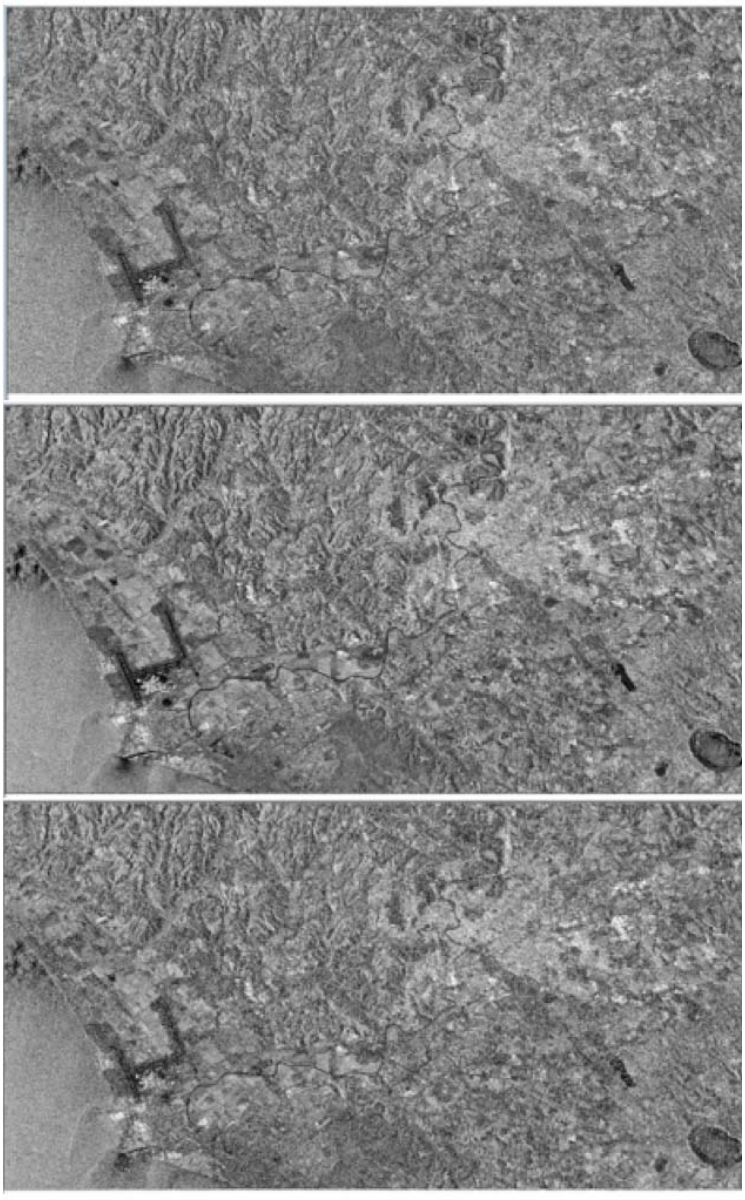

Figure 24. Speckle filtering: no filter (top), Frost filtered (middle), Lee filtered (bottom)

3.2.5 Determination of Changes and Feature Extraction

Once the SAR images are calibrated and co-registered appropriately, the image stack can be used to perform further evaluation for change detection. First, backscattering differences could be observed for different surface characteristics. For this demonstration, one pavement and one green area were chosen to compare the backscattered radiation differences. Asphalt pavement was chosen around the runway of Leonardo da Vinci International Airport, and green area was chosen from downtown Rome. Figure 25 and Figure 26 presents the backscattering signal intensity and associated statistics in graphs. Figure 25 is from asphalt pavement surface that mostly backscatters the radiation away meaning there is fewer signals backscattered to the radar. Same conclusion can be drawn from low mean values (-15.99 dB) of selected area. On the other hand, Figure 26 presents the volume backscattering, which is cause by trees and farmlands. In volume scattering, mean value of backscattered signal is observed as -9.80 dB, relatively higher than asphalt backscattering mean values. This is basically due to more signals backscattered to the radar in volume scattering.

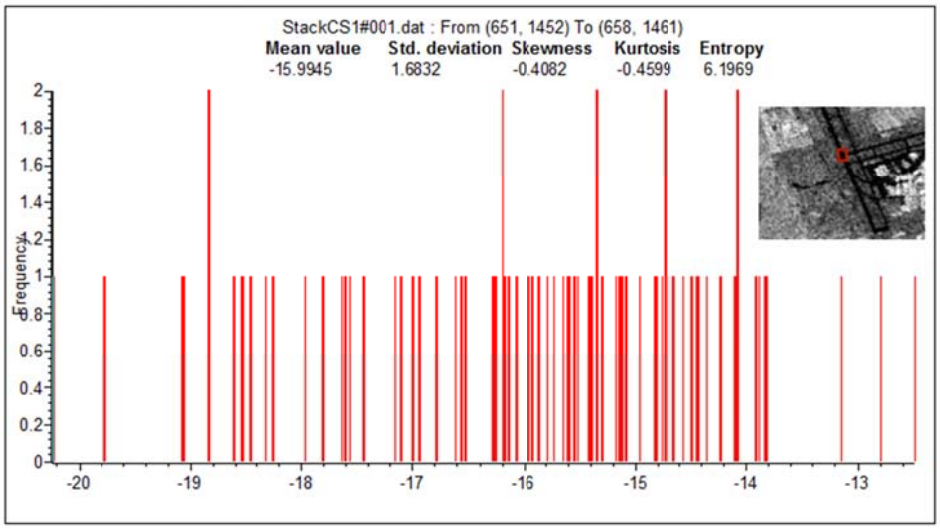

Figure 25. Smooth and low backscattering surface (pavement)

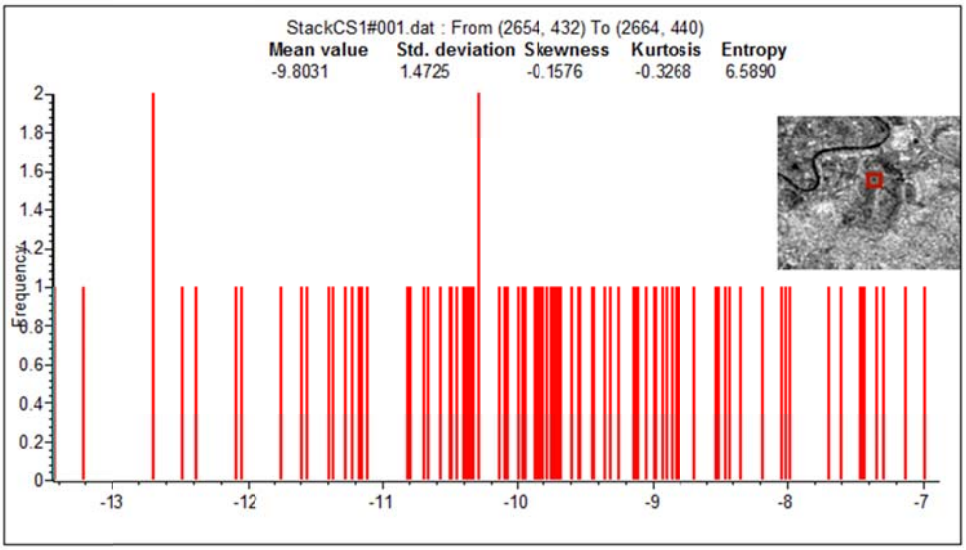

Figure 26. Volume backscattering surface (vegetation-trees)

The backscattering intensity could also be analyzed by color composites in Bilko. This simple method is useful specifically for monitoring the seasonal changes in a quick way. This might be a helpful way for determining the vulnerable areas for sudden changes that affect the moisture content of surface such as rain, snow, etc. Since backscattered intensity does not significantly change for persistent scatterers (such as buildings, roads, and other man-made objects), they will mostly appear in light colors in color composite image. On the other hand, farmlands and green areas such as trees and grass might show different backscattering intensities due to surface and soil characteristics and moisture content.

Following two examples presents the backscattering changes in different time frames. Figure 27 presents the changes in three summer dates where there is not much change expected. The blue, red and green colored pixels show significant change in backscattered signal intensity between 3 July, 17 July, and 21 August 2004.

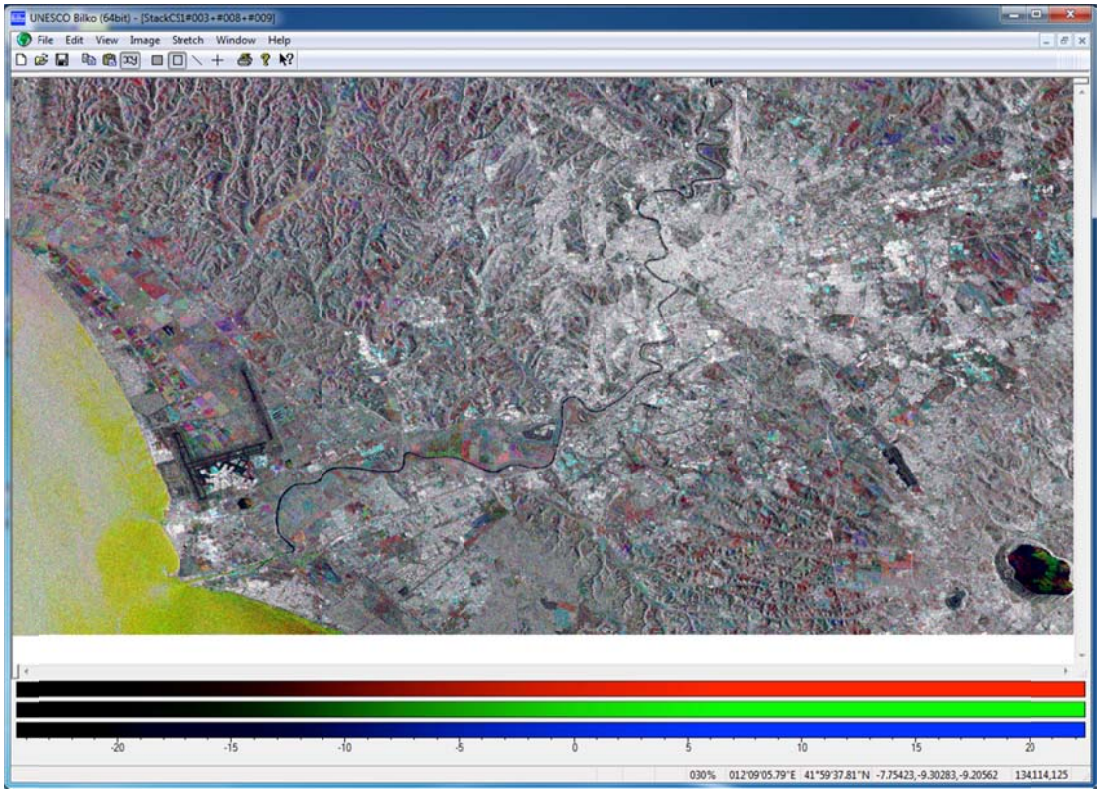

Figure 27. Color composite or radar signal backscatter intensity (same season)

Similarly, Figure 28 also presents changes in backscattered signal intensity for three different dates. However, these dates were chosen in different seasons to increase the variation in backscattered signal intensity. The dates were chosen as 14 February, 8 May and 25 September. Comparing two images can clearly highlights the effect of backscattered signal intensity for determination of changes in surface characteristics.

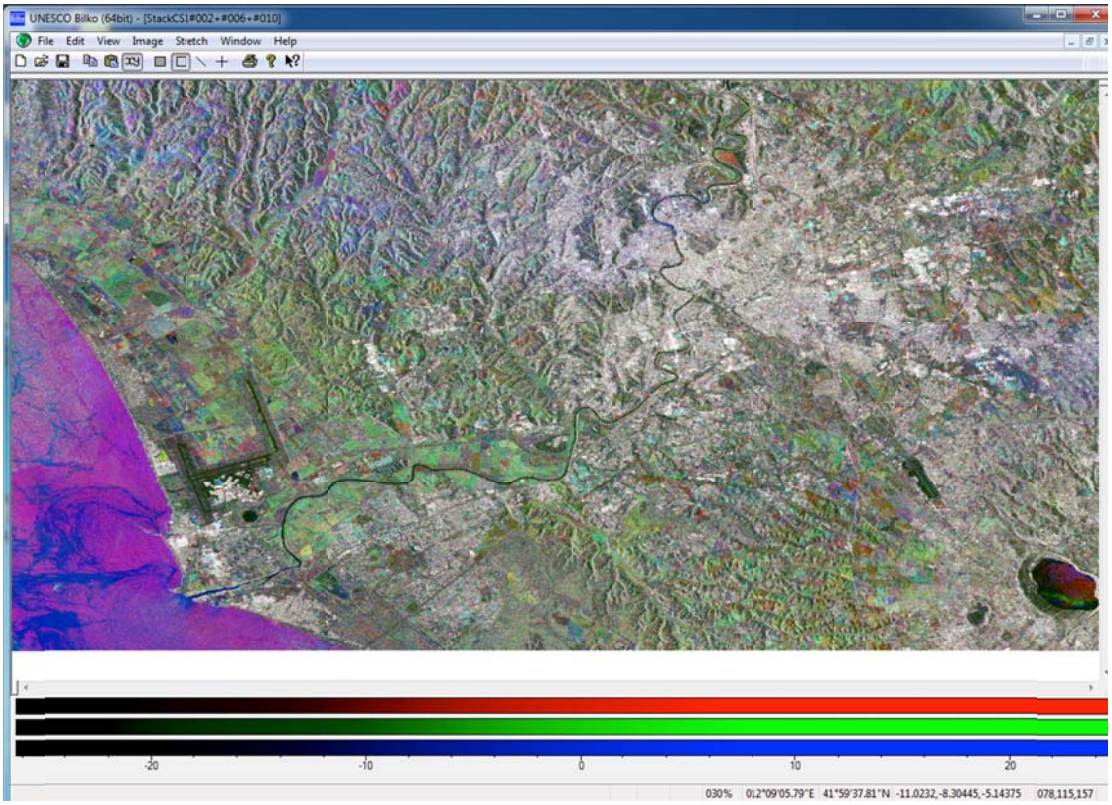

Figure 28. Color composite of radar signal backscatter intensity (different season)

It is also possible to extract time series of backscattered signal intensity change for a selected pixel in Bilko. This could be done by selecting the point of interest and using New/Transect commands. For instance, two pixels with different characteristics were chosen to compare their backscattered signal intensity change over monitoring period. First point was chosen from a green area (012°23'54.22"E, 41°48'22.66"N) that expected to present variation in signal intensity. Second point was chosen from a pavement surface (012°14'04.00"E, 41°48'57.97"N), which expected to show little or no variation in backscattered signal intensity.

Evaluation of figures presents the distinction between surface elements that show difference in backscattered signal intensity. In Figure 30, backscattered signal intensity was mostly consistent with a little variation towards the end of monitoring period. This could be due to changes in surface characteristics such as rutting, surface deformations, or pavement markings, etc.

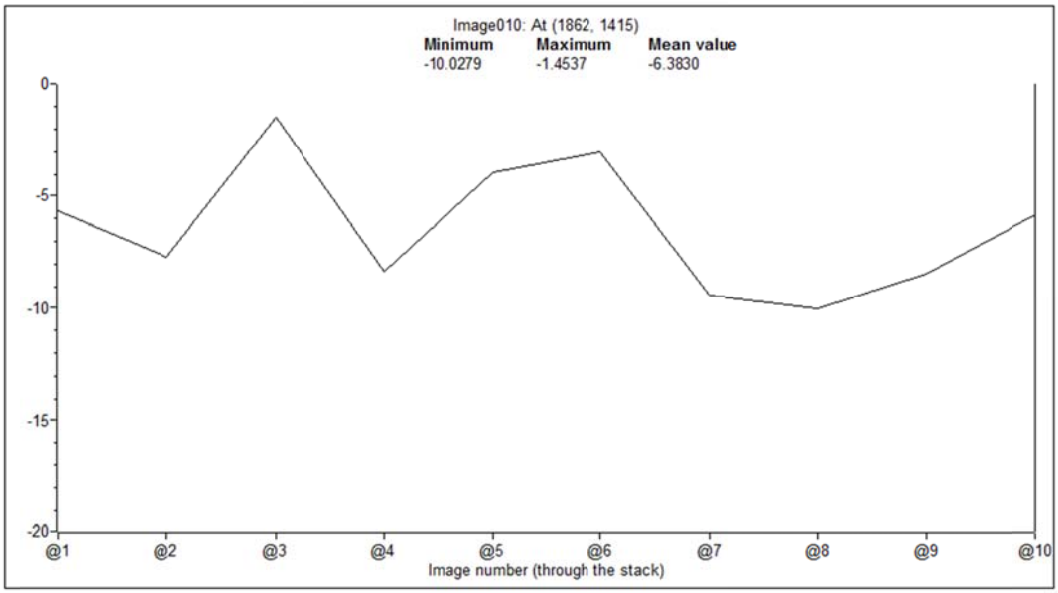

Figure 29. Time series of a pixel with variation in backscattered signal intensity (vegetation-green area)

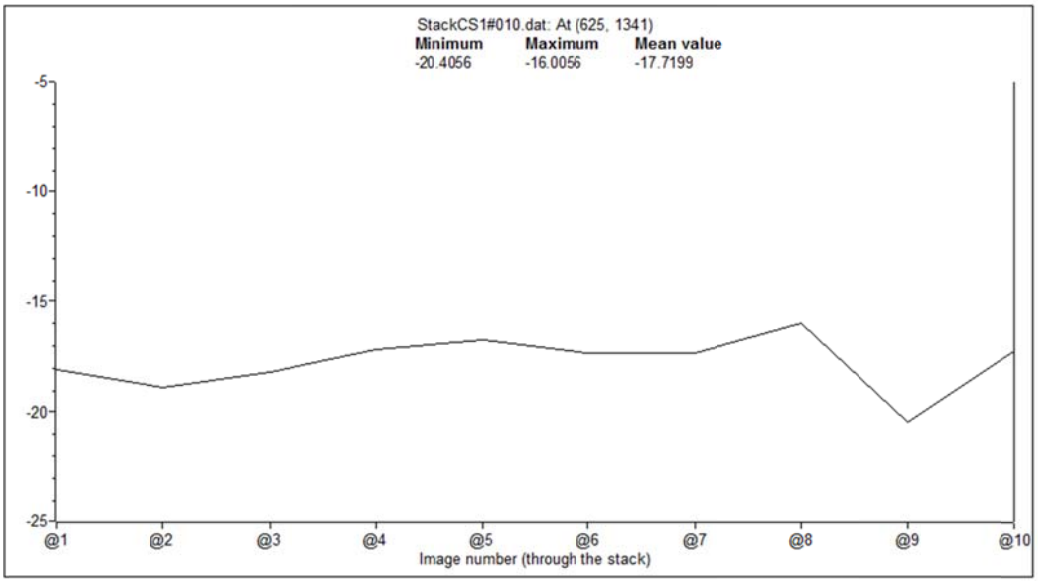

Figure 30. Time series of a pixel with no variation in backscattered signal intensity (asphalt pavement)

Finally, urban growth monitoring could be performed in a small scale for comparing the classified pixels. This process could be performed by using Image/Classification/Supervised comments in Bilko software and assigning different

surface characteristics by different colors. Leonardo da Vinci International Airport is selected to present the detection of new building between 2004 and 2010. In the selection menu, “blue” has been assigned to pavement, “red” has been assigned to buildings and “green” has been assigned to vegetation/green area, as presented in Figure 31.

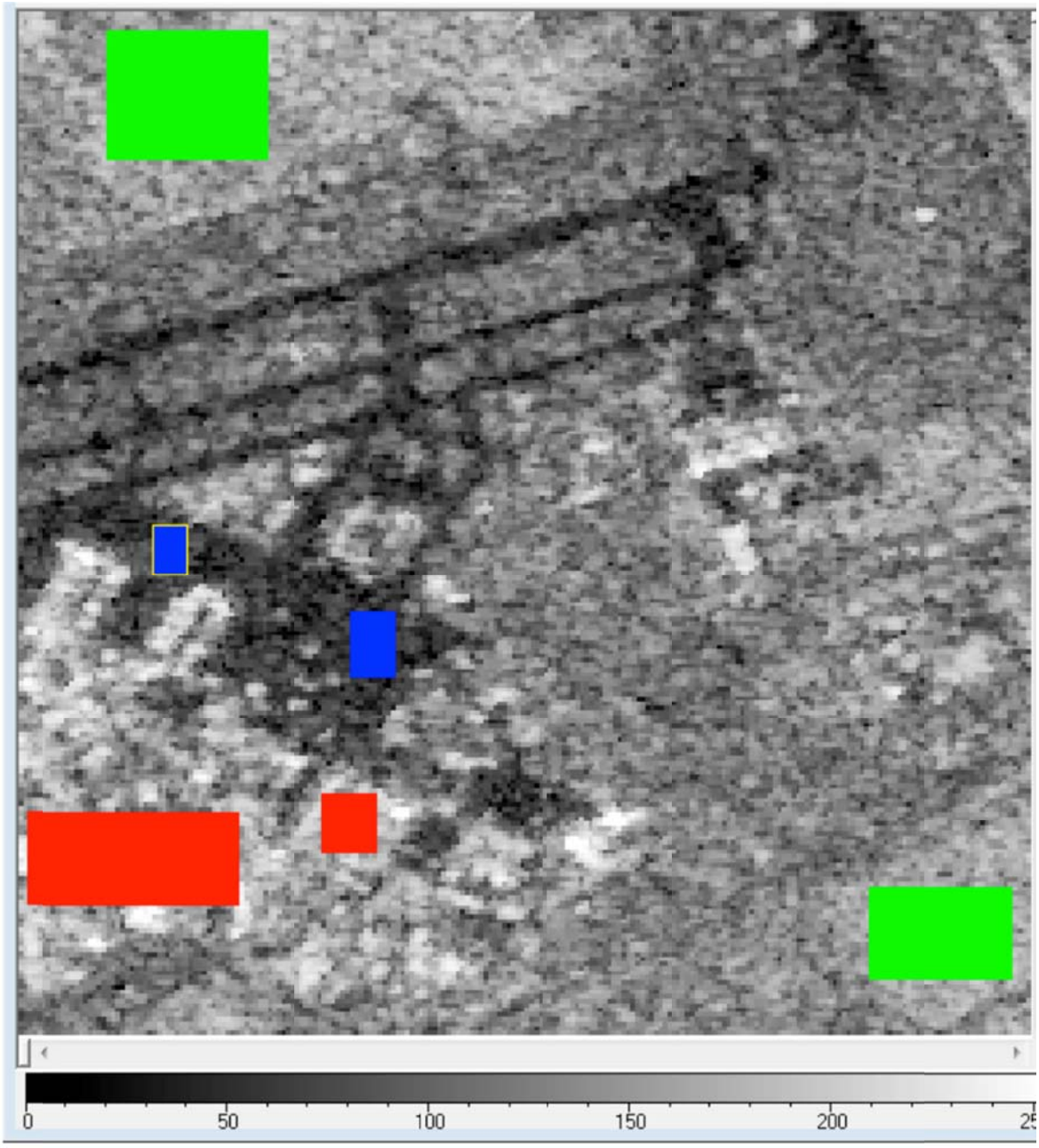

Figure 31. Color assignments to different surface characteristics

After assigning the colors to surfaces, backscattering changes of a small section of airport by using the "parallelepiped" classification method between 2004 and 2010. Following Figure and table present the changes in the selected area. The new addition to airport affected the classification of surface characteristics between 2004 and 2010, and is clearly identifiably in optical imagery.

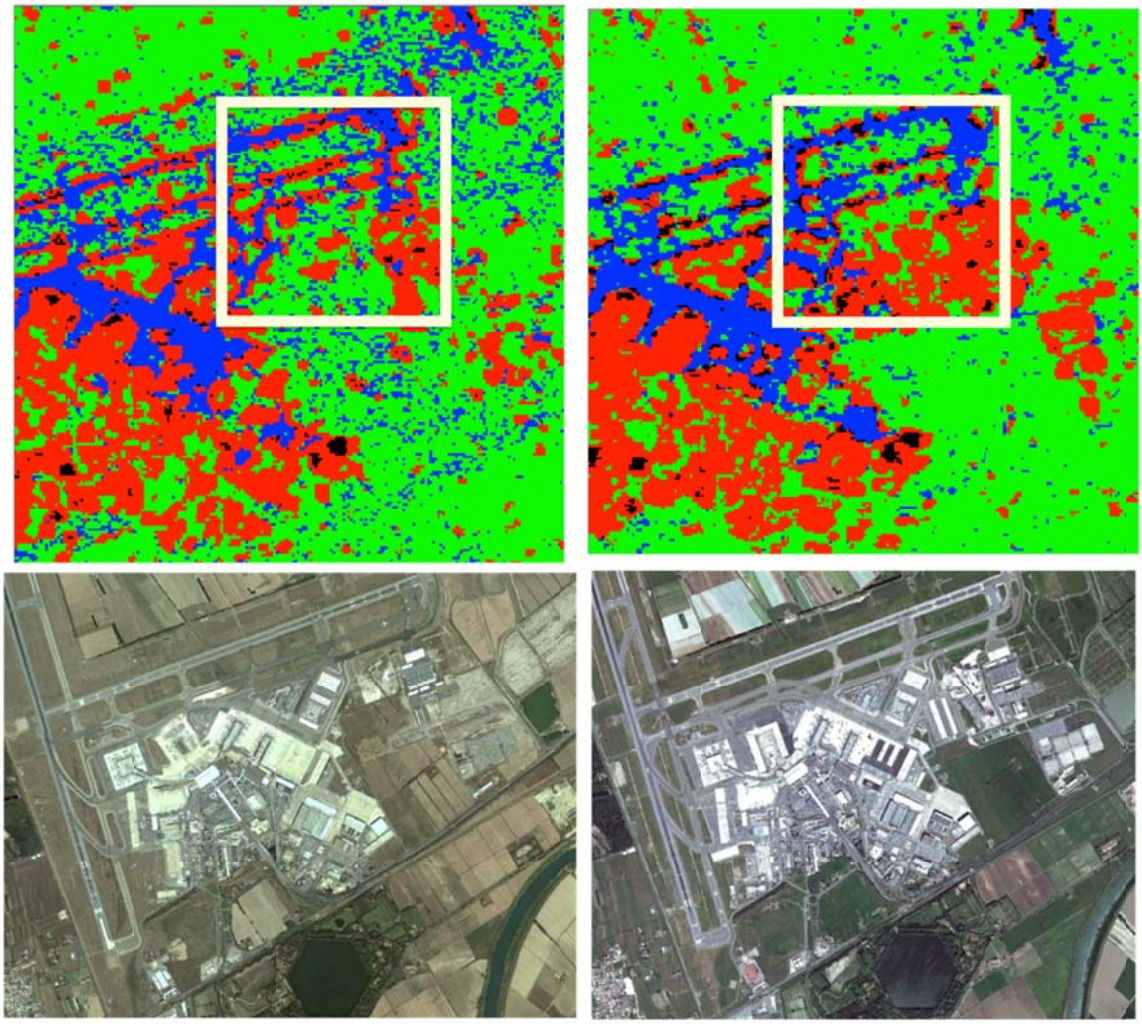

Figure 32. Urban growth tracking by using surface changes

(top-left: 2004 surface classification), (top-right: 2010 surface classification), (bottom-left: October-2004 optical imagery of area), (bottom-right: April-2011 optical imagery of area)[1]

[1] Optical images acquired from Google Earth by using closest available dates

Table 7. Distribution of surface characteristic between 2004 and 2010 in selected area

	2004	*2010*
Blue (Pavement)	% 15.1	% 21.4
Red (Buildings)	% 29.3	% 57.1
Vegetation (Green area)	% 55.6	% 21.5

3.3 CASE STUDY 2: RECENTLY INTRODUCED SENTINEL-1 FOR INSAR ANALYSIS

3.3.1 Overview of Sentinel-1 Toolbox

Sentinel-1 has been introduced by ESA and replaced its ancestor NEST in late 2014. State of the art SAR processing software, Sentinel-1 can currently import most raster and vector data products including data from Cosmo-SkyMed, TerraSAR-X, and Radarsat-2. Due to broad range of inputs, it also performs variety of analysis from image texture analysis to InSAR. Figure 33 shows possible raster data inputs for Sentilen-1 Toolbox and an already imported Single Look Complex (SLC) Sentinel-1 product.

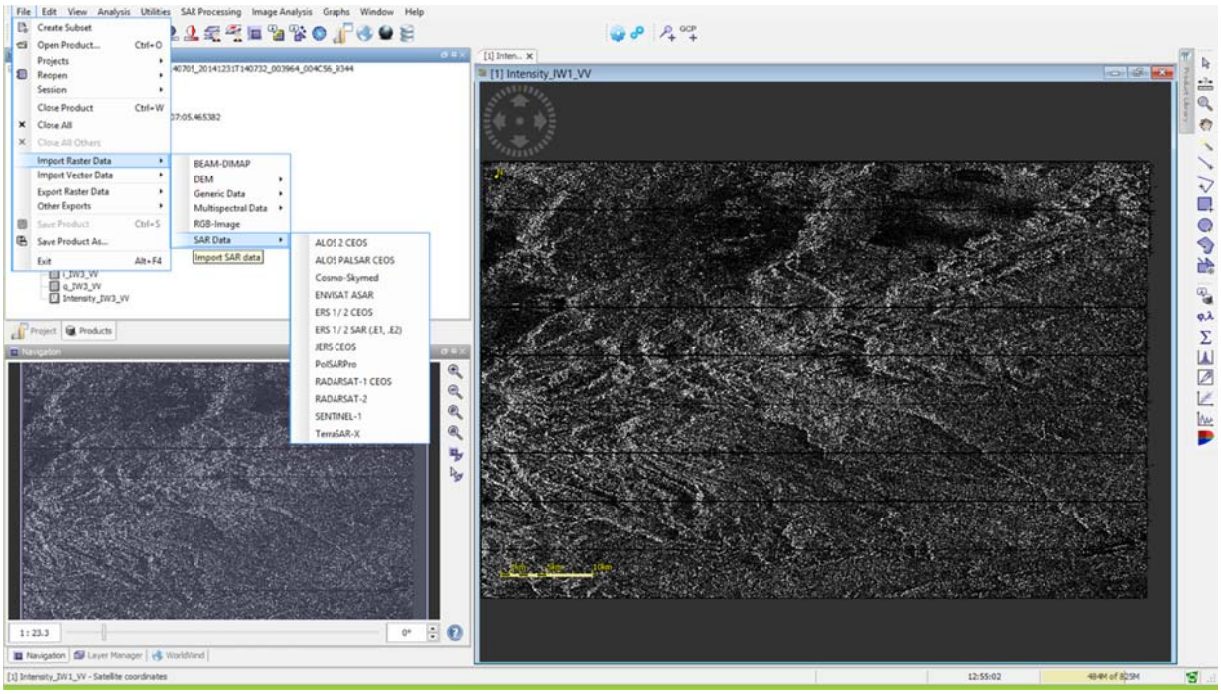

Figure 33. Possible Raster Data Inputs for Sentinel-1

Imported SAR imagery can be evaluated via its metadata and product header similar to Bilko software used in previous demonstration. The product header includes all details regarding the SAR imagery, some of which are critical for selecting suitable images for co-registration and InSAR analysis. Users can view the acquisition time, date, view angle, orbital information, etc. through the metadata folder. Figure 34 shows the abstracted metadata of a Sentinel-1 product.

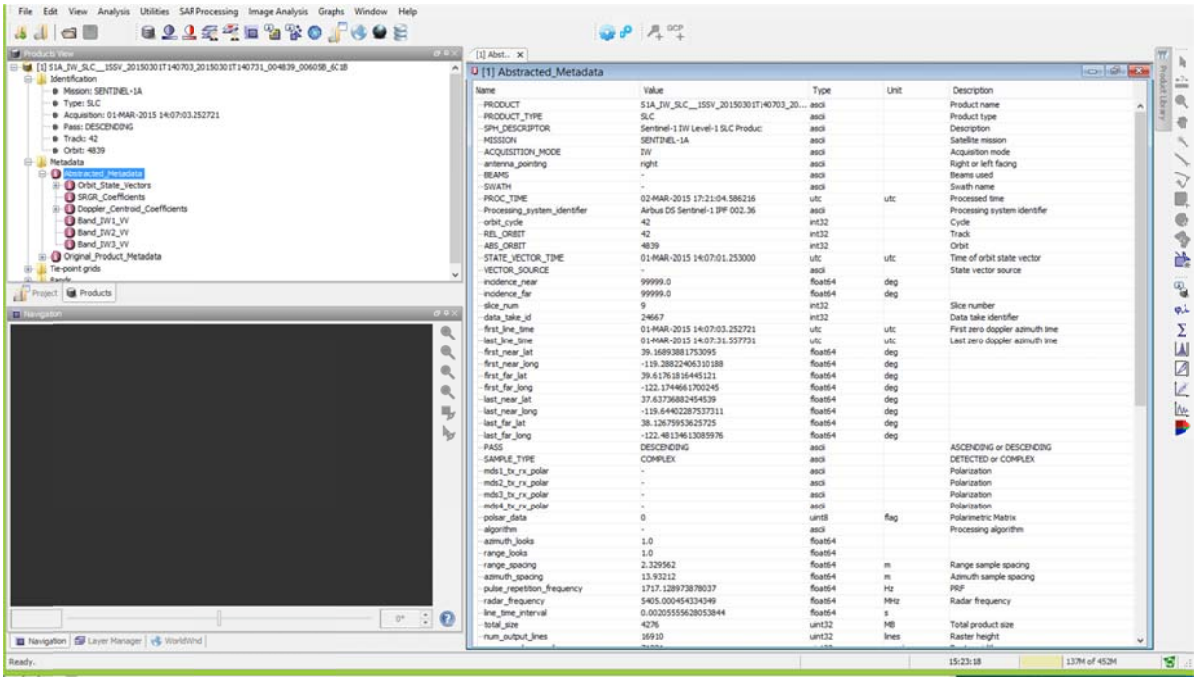

Figure 34. SAR Image Metadata and Product Header

This recently developed toolbox has also facilitated many processes by automatizing them via "graph builder" feature. By using this feature, users can easily automate the processes for multiple images, such as calibration, terrain correction, etc. Moreover, there are prebuild processing chains (called graph) for many common SAR processing steps. Following figure presents some common built-in graphs useful for SAR processing and InSAR. The list of built-in graphs can be viewed at "graphs" menu in the toolbar.

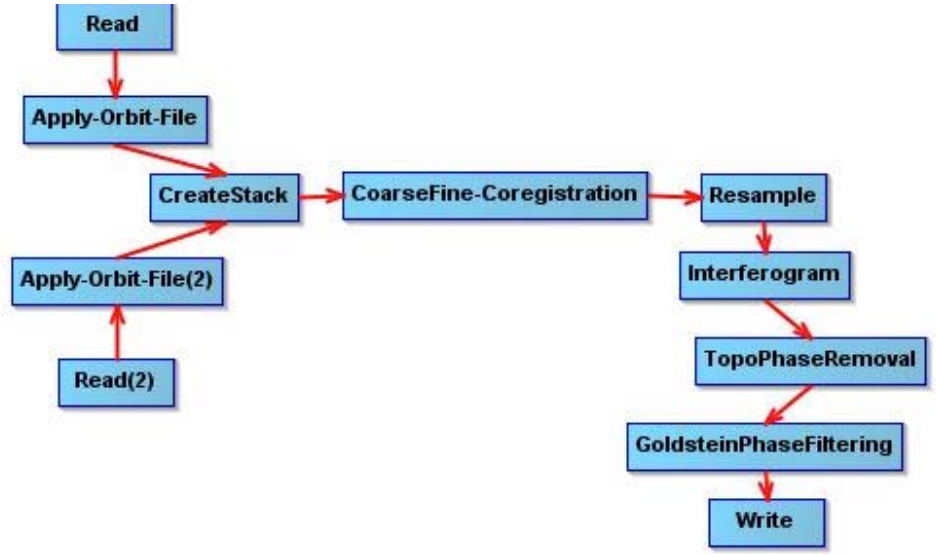

Figure 35. InSAR Deformation Pre-processing in Graph Builder

3.3.2 Interferometry Analysis with Sentinel-1 Toolbox

In this section, step-by-step procedure is provided for detecting deformation by using two or more Sentinel-1 Stripmap SLC products in Sentinel-1 Toolbox. Same procedure with slight differences can be applied to SLC products from other satellites such as RADARSAT-2, TerraSAR-X, ENVISAT ASAR, ERS-1&2, Cosmo-SkyMed, and ALOS PALSAR-1&2.

Step-1: Opening and viewing product metadata

The SAR products can easily be opened in toolbox either using the menu items in toolbar or dragging and dropping the products onto the software product view window. Once all SAR products are opened, product information of each SAR image should be checked by using “Identification” and “Metadata” folders to make sure all products have appropriate view angle, orbit, and polarization bands for InSAR analysis.

Step-2: Co-registration of SAR images (Creating image stack)

Interferometric process requires co-registration of two or more images into a stack. This could be easily done by using “InSAR Optimized Coregistration” command as shown in Figure 36. Users should select and add images in “InSAR Coregistration” window. It is also possible for selecting optimal master image automatically if multiple images are used in InSAR stacking process. Users have an option to change the different settings in this window such as number of GCPs, Resampling parameters, and output files. A preview of the window is presented in Figure 37.

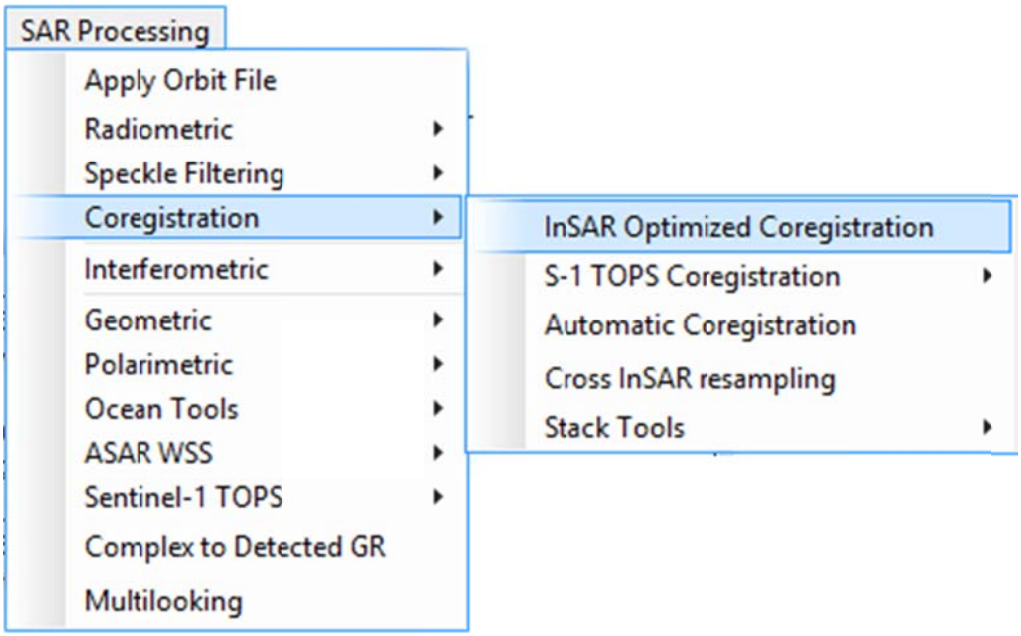

Figure 36. InSAR Optimized Co-registration Command

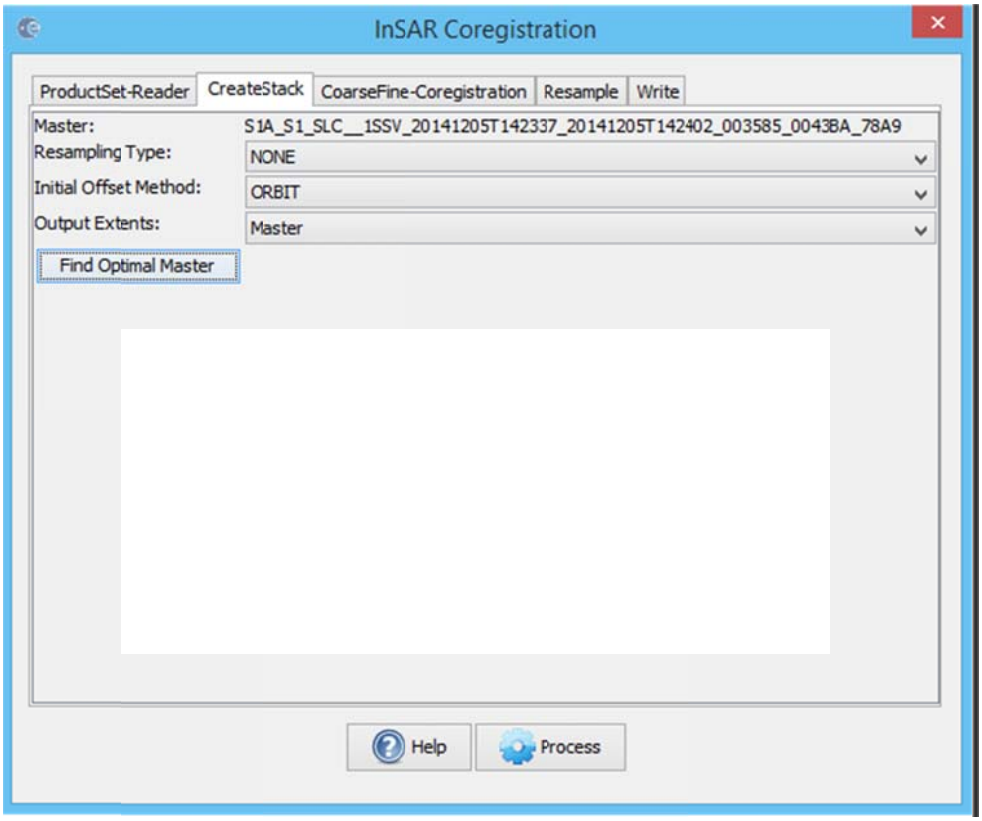

Figure 37. InSAR Co-registration Window

Once the co-registration process is completed, users can view the intensity bands in created co-registered stack. There should be one intensity band for each individual image in the new stack. For a quick view of change detection, SAR stack can be displayed in RGB view. This option presents similar results as in Figure 27 and Figure 28 in Bilko demonstration. RGB view can be opened by right clicking the SAR stack and selecting "Open RGB Image View" in the following menu. Then, user should select up to three intensity bands for displaying the differences in backscattered signal intensity between selected dates. The following two figures present the screenshot of RGB view window and RGB Image respectively.

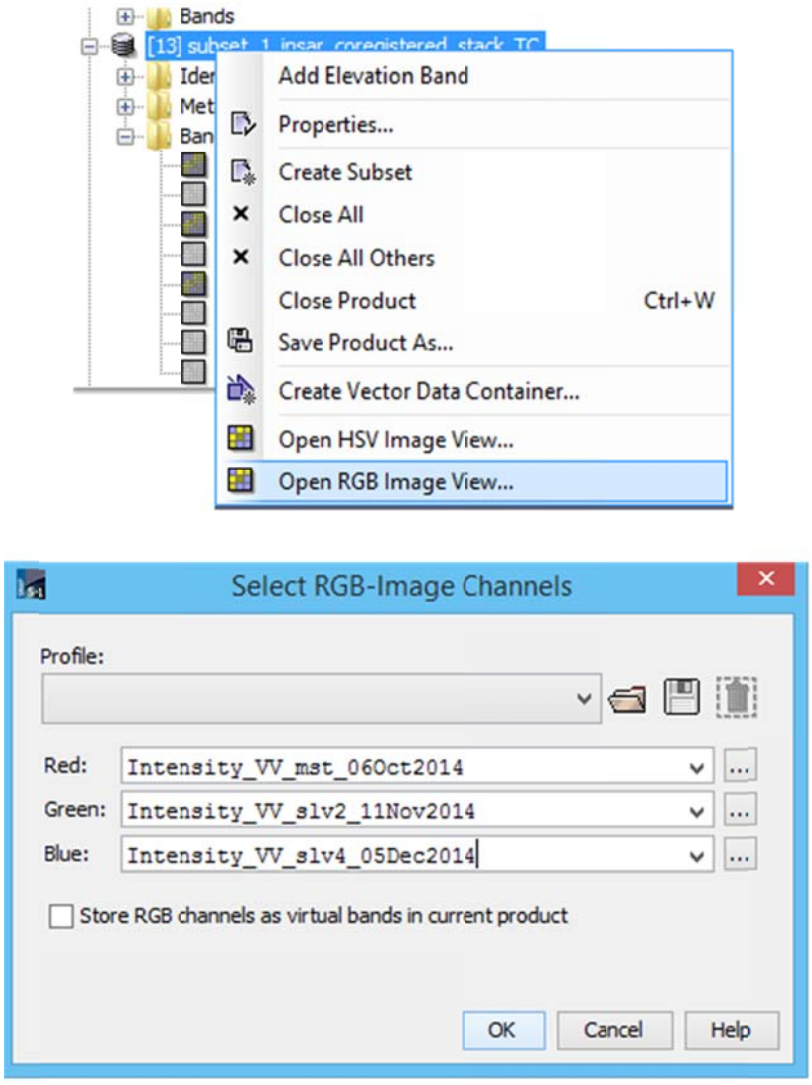

Figure 38. RGB View Window in SAR Image Stack

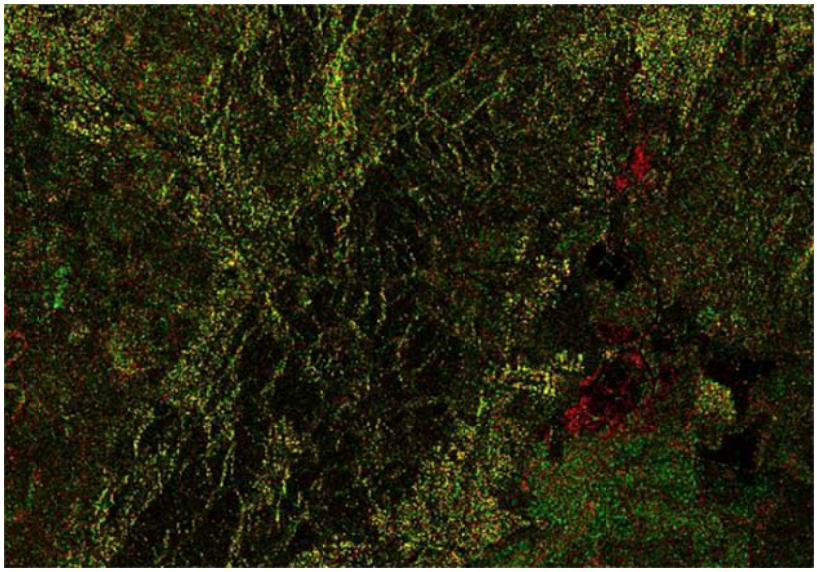

Figure 39. Displaying Change Detection in RGB Image View

Step-3: Interferogram Generation

After co-registration of SAR images, interferometric formation should be performed. This process could be executed by using built-in processing chains in Sentinel-1 Toolbox. This automated process can be accessed from Graphs/InSAR Graphs/BandSelect-Coreg-Interferogram-Filter command in toolbar.

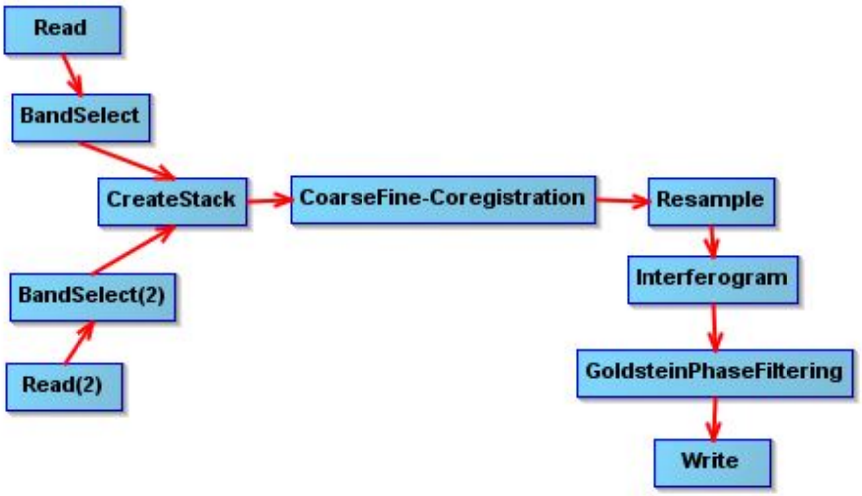

Figure 40. Interferogram Generation of SAR Images

3.4 COST-BENEFIT ANALYSIS

In many cost-benefit analyses that investigate monetary effects of a possible new technology or data collection method, it is common to evaluate the cost in two parts: capital costs and maintenance/operating costs. Capital costs include one-time expenses such as adaptation of system and associated technical infrastructure, computer and software costs, new personnel, etc. On the other hand, maintenance/operating cost includes ongoing or scheduled expenses during the time where system is in use such as continuous SAR imagery acquisition, data processing cost, etc. In this perspective, cost-benefit analysis of adopting satellite-based pavement and infrastructure monitoring should be approached similarly. In most cases, cost of SAR-based monitoring system is dominated by the cost of SAR imagery where operational cost (personnel time, data storage and data processing time) would be much lesser compared to image cost *(13)*.

Vavrik et al. *(53)* evaluated manual and automated pavement distress data collection methods to help Ohio Department of Transportation (ODOT) for deciding whether the transition from manual to semi- or full-automated systems is reasonable. In this study, inputs from 6 vendors and 18 state agencies helped providing comprehensive and reliable data for a comparative analysis, including a detailed cost analysis.

In a study conducted by Hong et al. *(28)*, commercial remote sensors are economically evaluated in order to quantify and compare the eight widely used technologies for bridge health monitoring, including BridgeViewer Remote Camera System (BVRCS), LIDAR and SAR etc. First, a basic comparative analysis conducted based on literature and field expert interviews. Then, a detailed analysis on cost elements such as cost of data collection system, data collection vehicle, data storage, data processing time, contractor's charge, etc. are conducted and 7 currently available technologies are compared cost-wise, excluding SAR technology. Although the study excluded the cost analysis of SAR technology, they presented the benefits and limitations of method briefly. SAR method found useful for detection of bridge settlements and determination of road and bridge surface roughness. Limitations of this technology include the necessity of continuous acquisition of SAR data to evaluate the before and after situations, and need for high quality SAR images for roughness analysis *(28)*.

In another study, Vaghefi et al. *(13)* reviewed commercially available bridge monitoring technologies in detail and rated based on cost, availability of instruments, data processing complexity, traffic disruption, etc. with a score between 0 and 16, where score 16 means all criteria are met with high scores. InSAR method found very useful for determining global metrics of bridges such as bridge length, bridge settlement, bridge movement, surface roughness and vibration with a score of 12 and above for all criteria *(13)*.

In this study, cost-benefit analysis of SAR-based pavement and infrastructure monitoring is evaluated. It is assumed that SAR-based monitoring will be complementary rather than replacing current monitoring efforts. It is expected that the SAR-based monitoring will be reducing unnecessary vehicle-based inspection trips to the sites and prioritizing the monitoring effort with a continuous SAR imagery for timely detection of pavement and infrastructure problems. It is also important to note that, no previous study has evaluated and quantified the possible reduction in routine vehicle-based inspection trips in result of SAR-based continuous monitoring. Therefore, some assumptions will be used here to give an insight for further studies.

In our cost-benefit analysis, finding from *(53)* used to estimate the cost of pavement distress monitoring.

3.4.1 Cost Scenarios

Unit Costs of Developing Technical Infrastructure for SAR Data Analysis

Computer and software purchase are the main elements of this capital cost for SAR-based monitoring. Considering many DOTs are already equipped with high-processing capability computers and common software such as GIS and CAD, these cost items might not be included in the CBA. However, unit cost of computer and software purchase are assumed $10,000-$15,000. The computer and software cost will be accounted for every 5 year due to technological advancements and licensing.

Data storage cost will also be accounted for since the SAR imagery and byproducts will require between 5-10 GB per image. If the agency decides obtaining historical data while adopting the system, initial data storage will be necessary. Cost of data storage is estimated by *(28)* as $10 per GB per year. Assuming each SAR image reserve 5-10 GB including some processing byproducts, $1500 data storage cost per year is considerable safe for 20 SAR images with a $3,000 capital cost for the storage of historical data. This process might also be excluded based on the data storage availability of agencies.

Another capital cost at the beginning stage of adopting the SAR-based monitoring will be training personnel for data processing. This cost is estimated as $50,000 for one-time expense.

Unit Costs of SAR Image Acquisition and Processing

Costs of SAR images and data processing may vary depending on the technical features of the image (medium- or high-resolution), size of the Area of Interest (AOI), and data processing methods (InSAR, PSInSAR^{TM}, SqueeSAR^{TM}, TSInSAR, etc.). Some agencies prefer outsourcing the image acquisition and processing, and receive end products as GIS

and/or CAD files to further the evaluation for a specific project. However, due to possible high cost for outsourcing the process, an agency might prefer establishing necessary technical infrastructure for image acquisition and processing, which might significantly reduce the operational cost in long-term.

Additionally, if the SAR-based monitoring method will be used for a specific project or temporarily for a period, then Power et al. *(32)* suggests conducting feasibility study for testing the coherence of images before proceeding further to reduce the cost of image acquisition. It is stated that 4 images could be used for coherence testing in a feasibility study.

High-resolution satellite imagery often preferred to increase the accuracy and provided level of detail in the end products, specifically for pavement and infrastructure monitoring. Image cost of currently operating Cosmo-SkyMed and TerraSAR-X satellites, which provide suitable high-resolution images for InSAR analysis, are acquired from companies that might also process the data.

Agencies might also prefer obtaining historical SAR data to establish a SAR-based database while establishing the monitoring system. This might provide obtaining quick and reliable results without waiting to increase the number of images over time. Although this step will add some capital cost, the archived SAR data will cost much lesser than the new acquisition. Each new acquisition will then be added to this dataset to detect new or to monitor continuing deformations.

Airbus Defence & Space *(54)* provides cost information as of 2014 for high-resolution satellite images along with data processing cost. Cost of image acquisition varies depending on requested product (SpotLight, StripMap, ScanSAR, etc.), scene size and delivery options, where customers might request fast or urgent delivery for a fee. In terms of InSAR analysis, SpotLight InSAR and StripMap InSAR data stack are available for purchase. Data provider also requires minimum purchase of 5 scenes for the stack packages for the following discounted InSAR stack prices:

(1) SpotLight InSAR: € 2,500 per scene (minimum of 5 scene)
(2) StripMap InSAR: € 1,250 per scene (minimum of 5 scene)

As similar to most InSAR contractors, *(54)* also quotes the cost of image acquisition and data processing as a package based on customer needs and physical properties of AOI due to complexity of the data processing and availability of analysis methods. Cost of such package is mostly determined based on the discussions between customer and contractor. In some cases, contractors perform preliminary site analysis and evaluation of coherence before providing the cost to the customers. It is also possible to see fixed base-

price by contractors for InSAR analysis independent from the complexity of the project *(32)*. Cost of high-resolution Cosmo-SkyMed SAR image and data processing acquired as follows including data processing cost, excluding fast processing and delivery fees which may vary *(55)*:

(3)	Spotlight-2 (7x7 km, 1m resolution)	€ 9,450 (new)	€ 4,725 (archive)
(4)	Spotlight-2 (10x10 km, 1m resolution)	€ 6,150 (new)	€ 3,075 (archive)
(5)	Stripmap (40x40 km, 5m resolution)	€ 3,600 (new)	€ 1,800 (archive)

Note: 1 Euro equals to 1.11 US$ (2015)

Medium-resolution SAR images cost less compared to high-resolution images for InSAR analysis. However, these types of images are mostly preferred for large-scale deformation analysis and historical monitoring. Power et al. *(32)* stated that historically archived data covering average of 3-5 years time frame with minimum of 15 or more images can produce high accuracy results for monitoring programs. Some archived medium- and low-resolution SAR images could even be acquired free of charge as few agencies open their databases to consumers. ESA, JPL, USGS, ASF and some other agencies and organizations provide certain types of SAR data products freely (some of them require registration and proposal submission) for research, education and other peaceful purposes. However, this cost saving attempt requires certain level expertise for finding appropriate data stacks among many satellite products. On the other hand, resolution level of these products might not provide enough detail for pavement analysis.

(32) reported the estimated cost of medium-resolution images as follows:

- ERS/ENVISAT: $1,000 per image (100 x 100 km (60 x 60 mi))
- RADARSAT-1: $2,500 per image (50 x 50 km (30 x 30 mi))

Cost of image acquisition highly depends on the total number of images purchased and significant discounts such as 50% - 75% might reduce the overall cost with increased quantity.

Power et al. *(32)* reported the estimated cost of image processing as follows:

- Feasibility Study:
  - SAR imagery (ERS or ENVISAT): 4 x $1,000 = $4,000
  - Generation of coherence images: 2 person-days $2,000
  - Generation of Feasibility Study Report: 2 person-days $2,000

- Ongoing cost per monitoring interval

    - Ground movement maps generated using RADARSAT-1
    - SAR imagery: 2 x $2,500 = $5,000
    - InSAR deformation map generation: 2-10 person-days $2,000 to $10,000

    - Ground movement maps generated using ERS/ENVISAT
    - SAR imagery: 2 x $1,000 = $2,000
    - InSAR deformation map generation 2-10 person-days $2,000 to $10,000

Costs not included in our model

Cost of building a technical infrastructure for data processing unit in agency such as network connections, printers, scanners, etc. are ignored since most of these items are already used in most agencies and/or cost insignificant amount compared to other capital costs.

3.4.2 Benefit Scenarios

As in all pavement and infrastructure monitoring applications, primary goal of using satellite remote sensing technology is early detection of problems that might affect the safety and serviceability of the transportation network, and cost much higher later for maintenance and rehabilitation. In this perspective, benefits of such technology to the community will be crucial in addition to the benefits to the responsible agency.

Direct Benefits to Agency

Utilization of satellite remote sensing technology might reduce the routine pavement and bridge inspection trips by regularly monitoring the transportation infrastructure system in network-level. This helps the agency prioritize the necessary vehicle-based inspection trips and reduce the use of other technologies, specifically if other technologies are contracted.

For instance, *(28)* estimates the contractor's charge for bridge health monitoring as $1,300 and $1,800 for Mobile-Lidar and Ultra Wide Band Imaging Radar System (a form of GPR) respectively. Due to limited data availability, it is assumed that SAR-based pavement and infrastructure monitoring might reduce the routine vehicle-based inspection trips by 5% - 20%. On the other hand, agencies that are not outsourcing pavement and infrastructure data collection might own less number of vehicles or operate

already purchased vehicles less than usual due to efficiency of pavement and infrastructure monitoring system. This eventually contributes to reducing the operational cost in the agency.

Indirect Benefits to Society

One of the main expected benefits of satellite remote sensing technology is to maintain the high level of service (LOS) on roadways. This is possible due to early detection of problems that might later cause major rehabilitation/maintenance issues, which eventually bring time, energy and money loss. Chatti et al. *(56)* enhanced the initial studies on the effect of pavement surface condition to fuel consumption, tire wears, repair and maintenance cost, and operating cost of vehicles. Cost adjustment factors are presented based on IRI change from 1m/km to 6 m/km with 1 m/km increments for 3 speed categories (35, 55 and 70 mph) and different vehicle class. It is reported that an increase of 1m/km (63.4 in./mi) IRI increase the fuel consumption by 2% for passenger vehicles and by 1% - 2% for heavy trucks, repair and maintenance cost by 10% for passenger vehicles and heavy trucks after a certain level of roughness *(56)*.

Some pavement and infrastructure data collection techniques require closure of shoulders and/or lanes, which disturbs the traffic and might cause the congestion. Although possible cost of the extra congestion caused by the closure might vary depending on the weather, time-of-day, and site-specific criteria, etc. Hong et al. *(28)* used the cost estimation of shoulder closure $125 and both shoulder and lane closure $625 per lane. In satellite remote sensing technology, this would be considered benefits of not using intrusive data collection techniques.

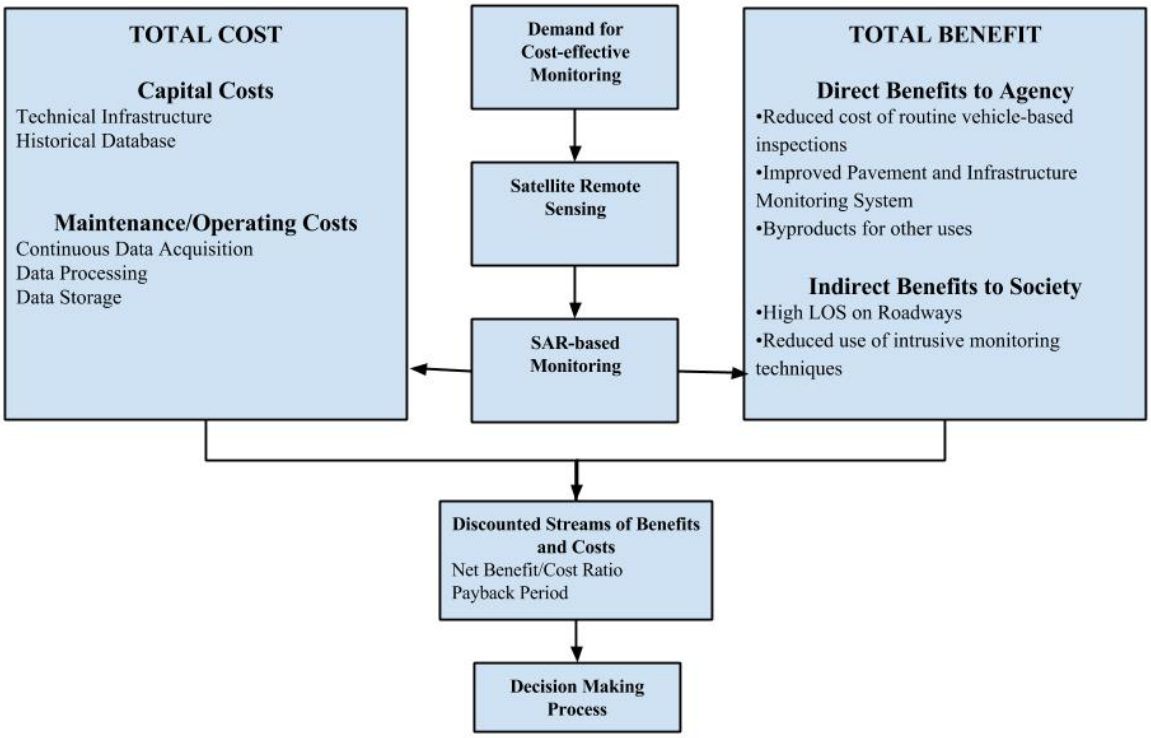

Figure 41. Conceptual framework of the cost-benefit analysis

Indirect benefits not quantified in our model

One major problem for evaluating the benefits of satellite remote sensing technology might be that the broad use of technology. Many departments and units might benefit from end products of satellite-based monitoring program such as transportation planning, land development, environmental offices, etc. These indirect benefits are not included in this study. Only benefits that might directly be related to evaluating pavement and bridge condition are included.

As an example to the indirect benefits, the State of Idaho started using satellite imagery to monitor water use in the irrigation districts. 15 Landsat images were used to monitor water right in growing season and cost $30,000 annually including staff time compared to half a million dollars for conventional methods used previously *(57)*.

3.4.3 Case Study for CBA

Investment on a new technology or method such as satellite remote sensing requires a careful evaluation of costs and benefits associated with it, especially if the technology isn't designed for a specific purpose and could be used in a broad range of disciplines. In order to accurately quantify the benefits and costs, it is crucial to evaluate wide range of

parameters. It is considered that there are direct and indirect benefits and costs to both responsible agency such as DOTs and society.

In our case study, applicability of satellite remote sensing technology is evaluated for all bridges and federal-aid highways in the New Castle County (NCC) in the State of Delaware. This will help understand the costs and benefits associated with SAR-based pavement and infrastructure monitoring. It is assumed that SAR-based monitoring will reduce routine vehicle-based monitoring effort for pavement surface distress and bridge health monitoring. Although it is difficult to quantify the reduction percentage in conventional methods, it is assumed that even small changes might affect the overall cost of monitoring efforts. In the case study, only direct benefits to agency, which is reduction in routine vehicle based inspections accounted in calculations as benefits. Costs include capital and maintenance/operating costs as previously mentioned.

New Castle County contains majority of the traffic and road network as well as the population in the State of Delaware. Since satellite remote sensing technology will be used, box area of the NCC will be used for cost estimation. NCC is approximately 24 mi (40 km) wide and 37 mi (60 km) long. Considering Cosmo SkyMed SAR images comes in 40x40 km scenes, area of NCC will require minimum of two scenes to cover all roadways.

State of Delaware has 492 state-owned NBI-length bridges in New Castle County (NCC), where 21 of them are structurally deficient and 96 of them are functionally obsolete as of 2014 *(58)*. State also maintains 40.6 miles of interstate, 1,874 miles urban and 579 miles rural roadways in NCC *(59)*.

Under the Highway Performance Monitoring System (HPMS) program, it is required that all state DOTs must submit their state Highway Performance Monitoring Report to the Federal Highway Administration (FHWA) each year, which are used by the FHWA in the analysis of the highway network system as a basis for supporting FHWA's responsibilities to the public, and especially the Biennial Condition and Performance Report submitted to the Congress every two years *(60)*.

DelDOT performs pavement condition surveys and pavement condition index calculations once every two years to identify type of pavement, severity of distress in pavement and extent of distress in pavement *(16)*. Currently, the field survey has been outsourced to Data Transfer Solutions (DTS) by utilizing right-of-way cameras on DTS's Mobile Asset Collection (MAC) vehicles to perform a pavement distress survey, assess pavement condition data using Earthshaper™ software and deliver pavement data through a geodatabase to the DelDOT pavement management system to calculate the pavement serviceability index and DelDOT's annual PCI values *(61)*.

Manual walking survey uses devices such as rod and level instrument, dipstick profiler, California profilograph etc *(62)*.

Figure 42. Study Area - New Castle, Delaware

The cost estimates were developed by calculating rough quantities and applying unit costs. Costs were then translated into per mile or per category costs. All adjusted cost values were normalized to a base year of 2016. Inflation factors were developed based on Producer Price Index for Highway and Street Construction from the 1986–2010 data to convert unit costs from 2016 levels to the build year.

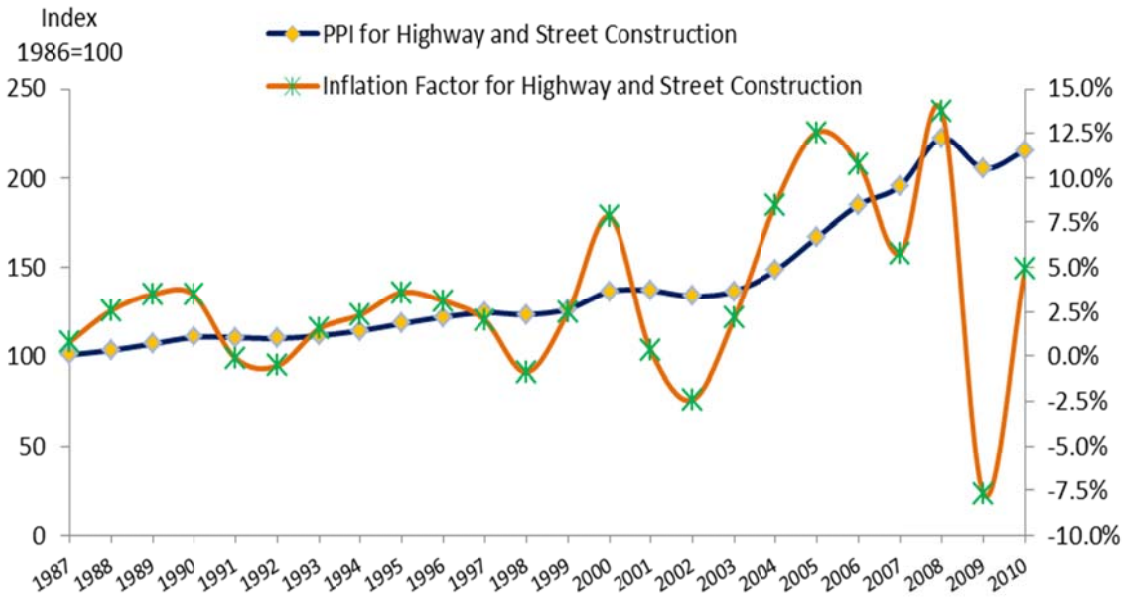

Figure 43. Producer price index for highway and street construction, 1987-2010
(Data source: Bureau of Labor Statistics)

In this study, cost alternatives are investigated based on three options and three resolution levels as follows:

Option 1: Purchasing data & in-house data processing
Option 2: Purchasing data & outsourcing data processing
Option 3: Outsourcing data collection & data processing

H: High-resolution (7x7 km, 1m resolution) € 9,450 (new) € 4,725 (archive)
M: Medium-resolution (10x10 km, 1m resolution) € 6,150 (new) € 3,075 (archive)
L: Low-resolution (40x40 km, 5m resolution) € 3,600 (new) € 1,800 (archive)

Estimation of the costs in this study involves several assumptions, including:

- Costs are based on standard facilities constructed in the United States and are represented in year 2016 dollars. They may change due to future economic conditions.
- Discount rate=5%, with a standard time horizon of 20 years (2016-2035).

Scenario 1H **(Purchasing 7*7 km data & in-house data processing)**

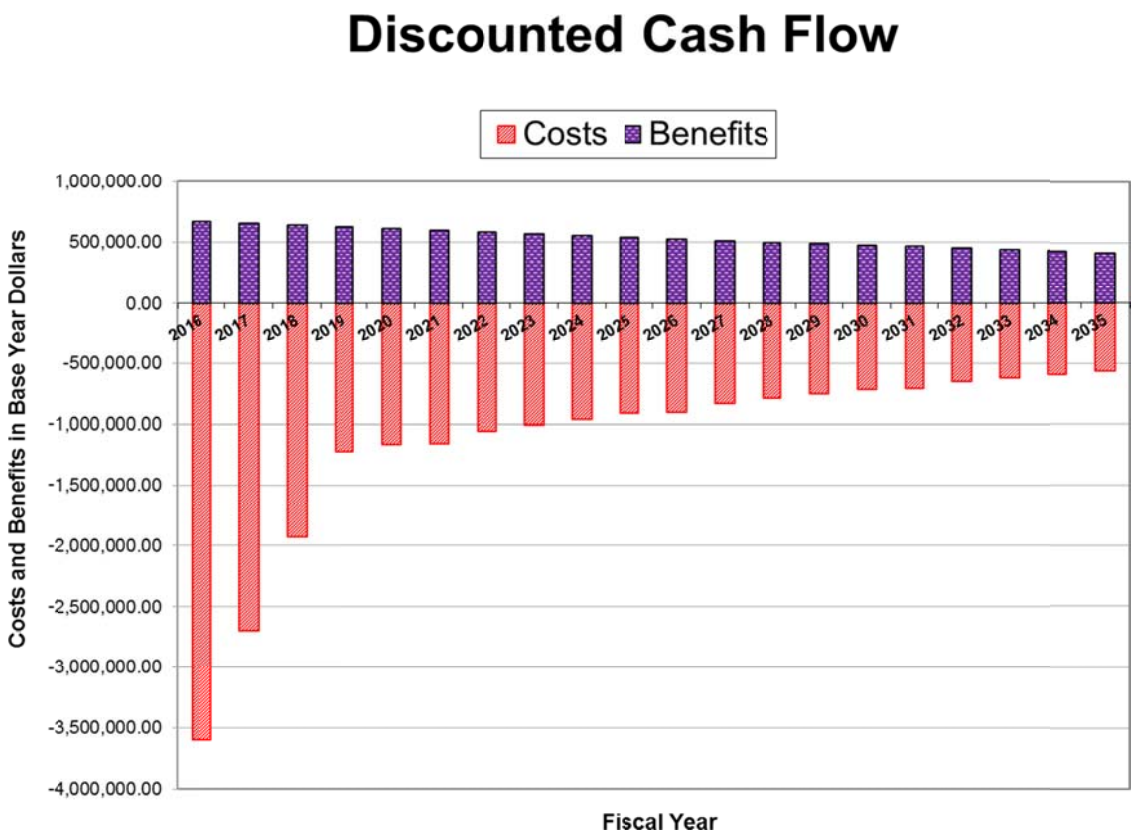

Figure 44. Discounted cash flow – 1H (Discount rate=5%)

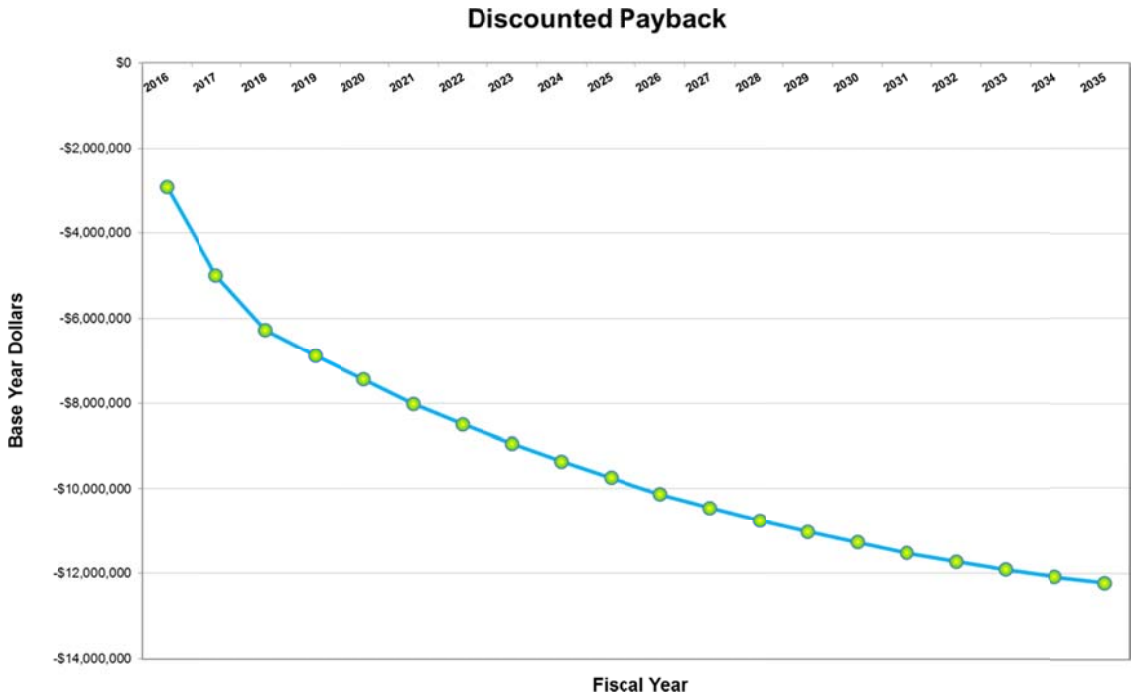

Figure 45. Estimated discounted payback period -1H

Since this scenario takes longer to payback, it should be rejected (Figure 45).

Table 8. Benefit and cost components of investments -1H (2016-2035)

Benefit (present value)	Value ($)
Reduced costs	16,891,509
TOTAL BENEFIT	16,891,509
Costs (present value)	
Computer and software purchase	40,000
Data storage cost	60,000
Training personnel	200,000
Image purchase	32,569,898
Image processing	0
Total budget costs	32,869,898
Tax-cost factor, 20% of budget costs	6,573,980
TOTAL COST	39,443,877
Benefit/cost ratio	0.43

As shown in **Table 8**, Benefit/cost ratio equals to 0.43, which means that the costs outweigh the benefits.

Scenario 1M **(Purchasing 10*10 km data & in-house data processing)**

Figure 46 shows discounted cash flow in different periods.

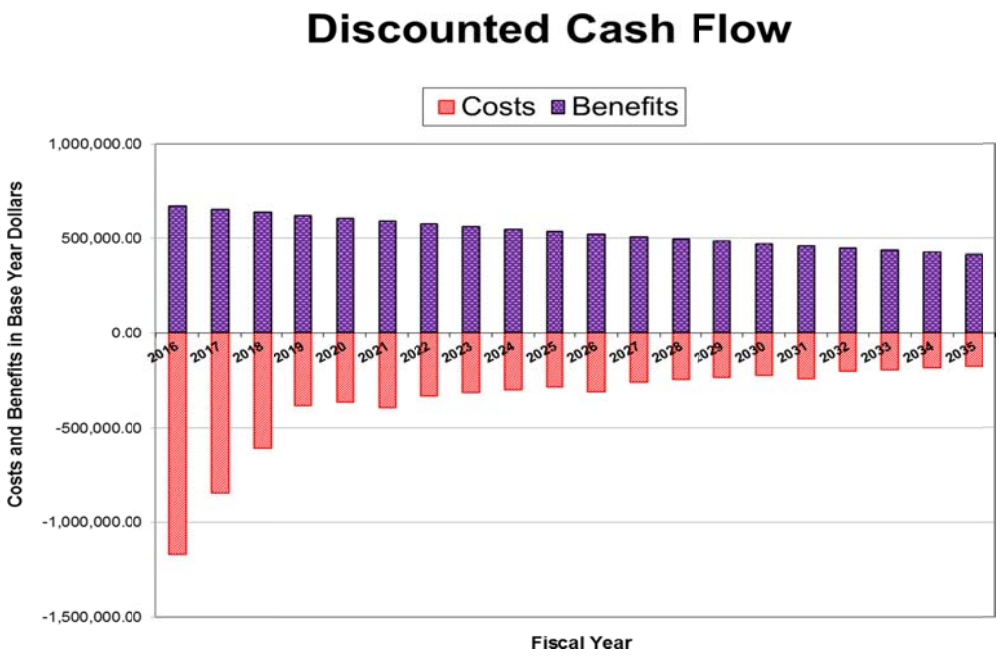

Figure 46. Discounted cash flow – 1M (Discount rate=5%)

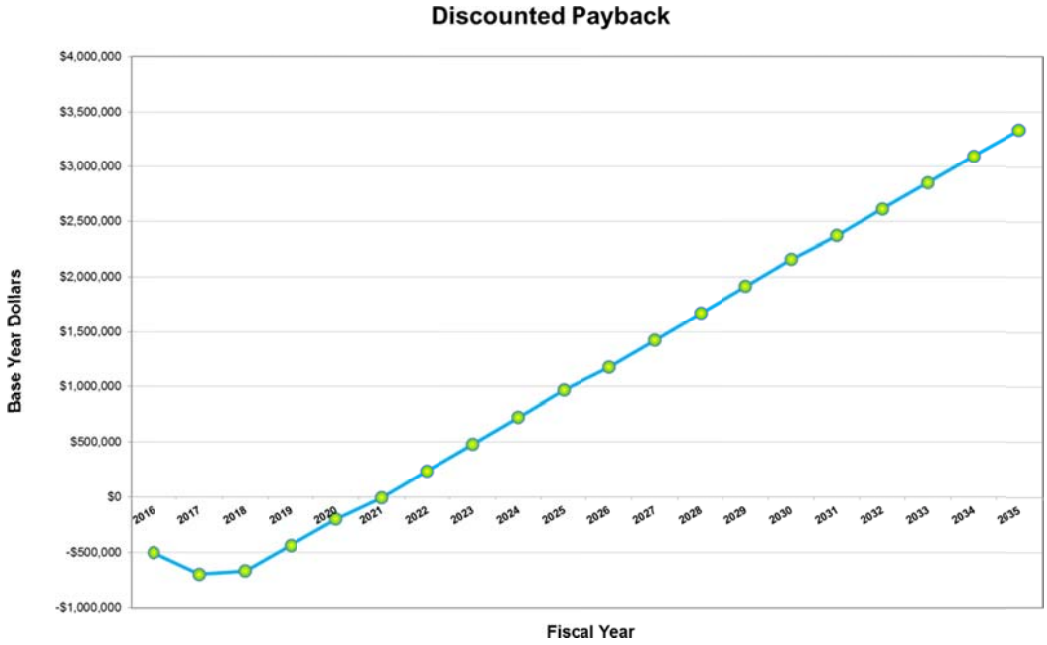

Figure 47. Estimated discounted payback period – 1M

As shown in Figure 47, the project has been fully paid back in 2021.

Table 9. Benefit and cost components of investments 1M (2016-2035)

Benefit (present value)	**Value ($)**

Reduced costs	16,891,509
TOTAL BENEFIT	16,891,509
Costs (present value)	
Computer and software purchase	40,000
Data storage cost	60,000
Training personnel	200,000
Image purchase	10,205,618
Image processing	0
Total budget costs	10,505,618
Tax-cost factor, 20% of budget costs	2,101,124
TOTAL COST	12,606,741
Benefit/cost ratio	1.34

As shown in Table 9, B/C ratio equals to 1.34, which means that this scenario leads to appealing results for investments.

Scenario 1L **(Purchasing 40*40 km data & in-house data processing)**

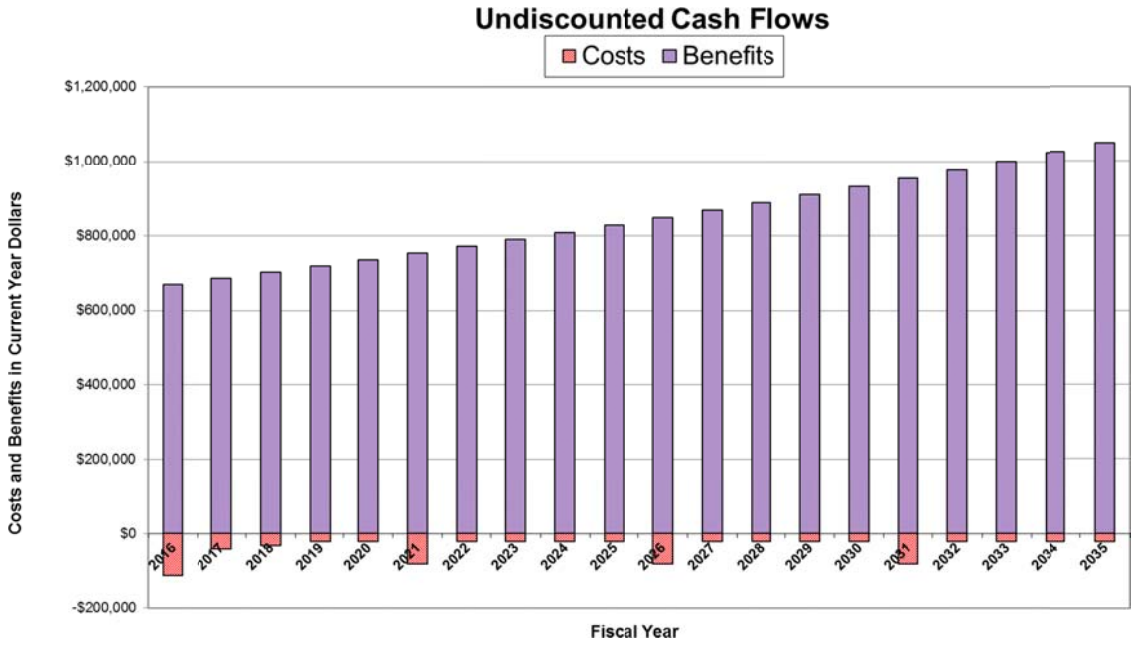

Figure 48. Discounted cash flow – 1L (Discount rate=5%)

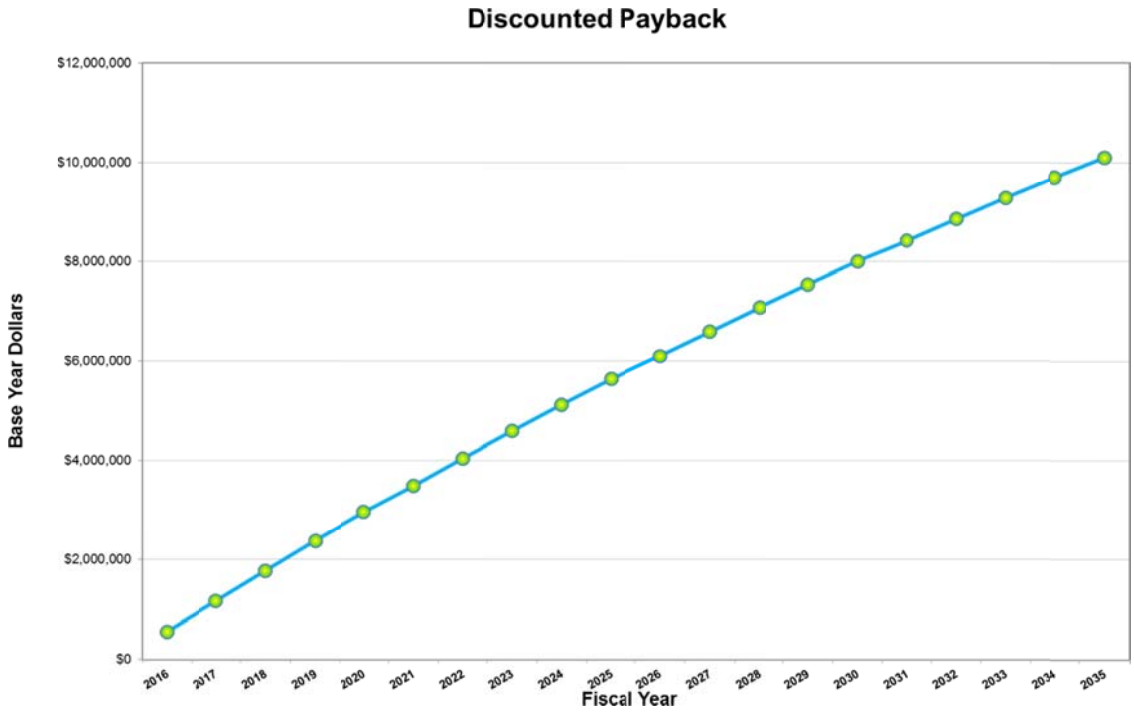

Figure 49. Estimated discounted payback period – 1L

Table 10. Benefit and cost components of investments – 1L (2016-2035)

Benefit (present value)	**Value ($)**
Reduced costs	16,891,509
TOTAL BENEFIT	16,891,509
Costs (present value)	
Computer and software purchase	40,000
Data storage cost	60,000
Training personnel	200,000
Image purchase	459,540
Image processing	0
Total budget costs	759,540
Tax-cost factor, 20% of budget costs	151,908
TOTAL COST	911,448
Benefit/cost ratio	18.53

Scenario 2H **(Purchasing 7*7 km data & outsourcing data processing)**

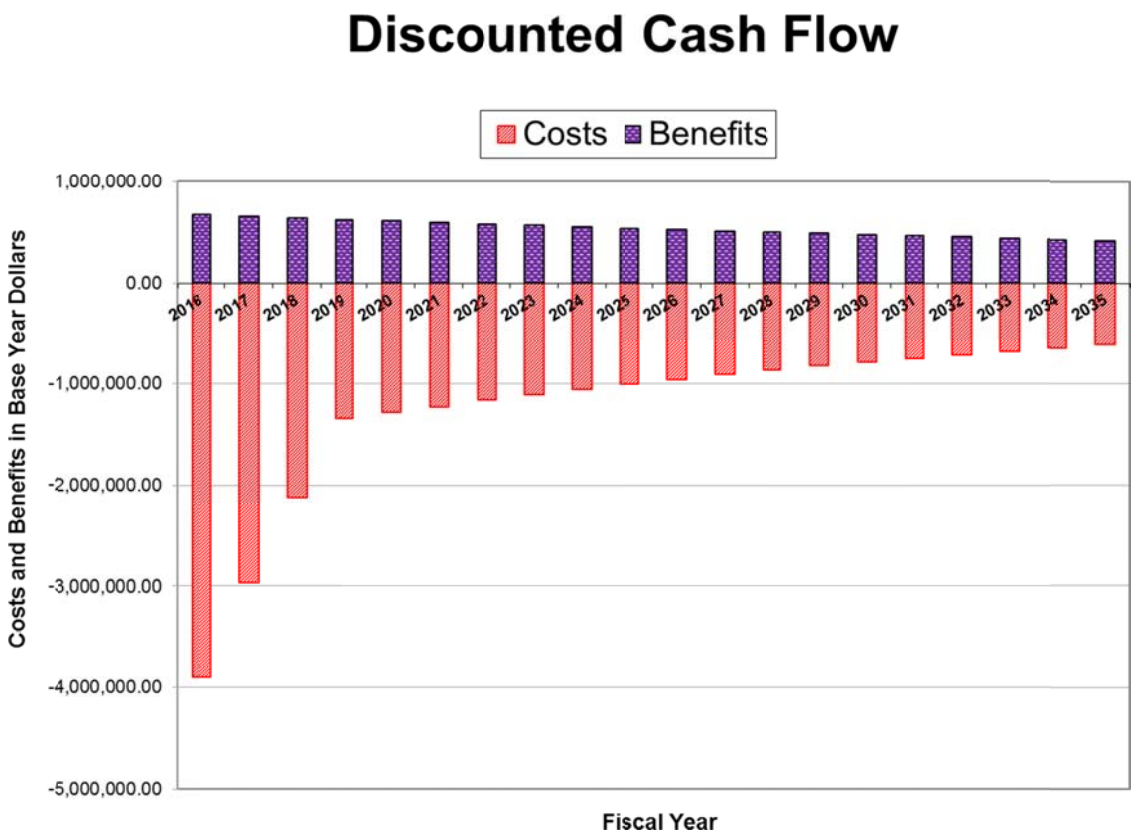

Figure 50. Discounted cash flow – 2H (Discount rate=5%)

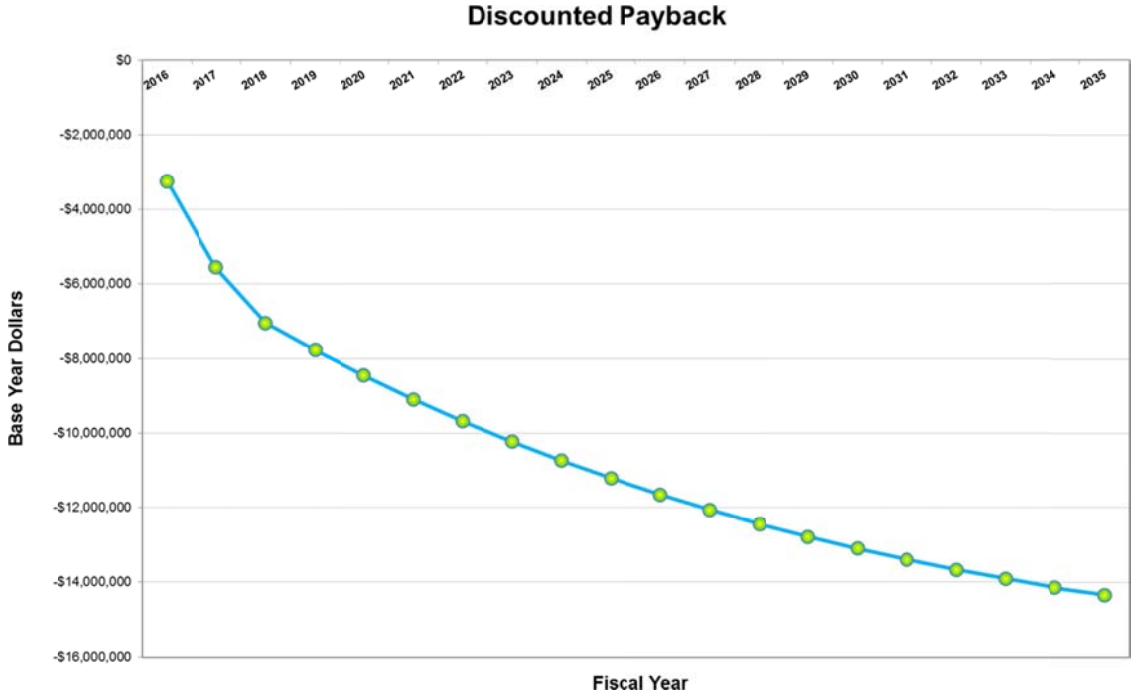

Figure 51. Estimated discounted payback period – 2H

Table 11. Benefit and cost components of investments – 2H (2016-2035)

Benefit (present value)	**Value ($)**
Reduced costs	16,891,509
TOTAL BENEFIT	16,891,509
Costs (present value)	
Computer and software purchase	0
Data storage cost	60,000
Training personnel	40,000
Image purchase	32,569,898
Image processing	3,256,990
Total budget costs	35,926,887
Tax-cost factor, 20% of budget costs	7,185,377
TOTAL COST	43,112,265
Benefit/cost ratio	0.39

Since this scenario takes longer to payback, it should be rejected (Figure 51). As shown in Table 11, Benefit/cost ratio equals to 0.39, which means that the costs outweigh the benefits.

Scenario 2M **(Purchasing 10*10 km data & outsourcing data processing)**

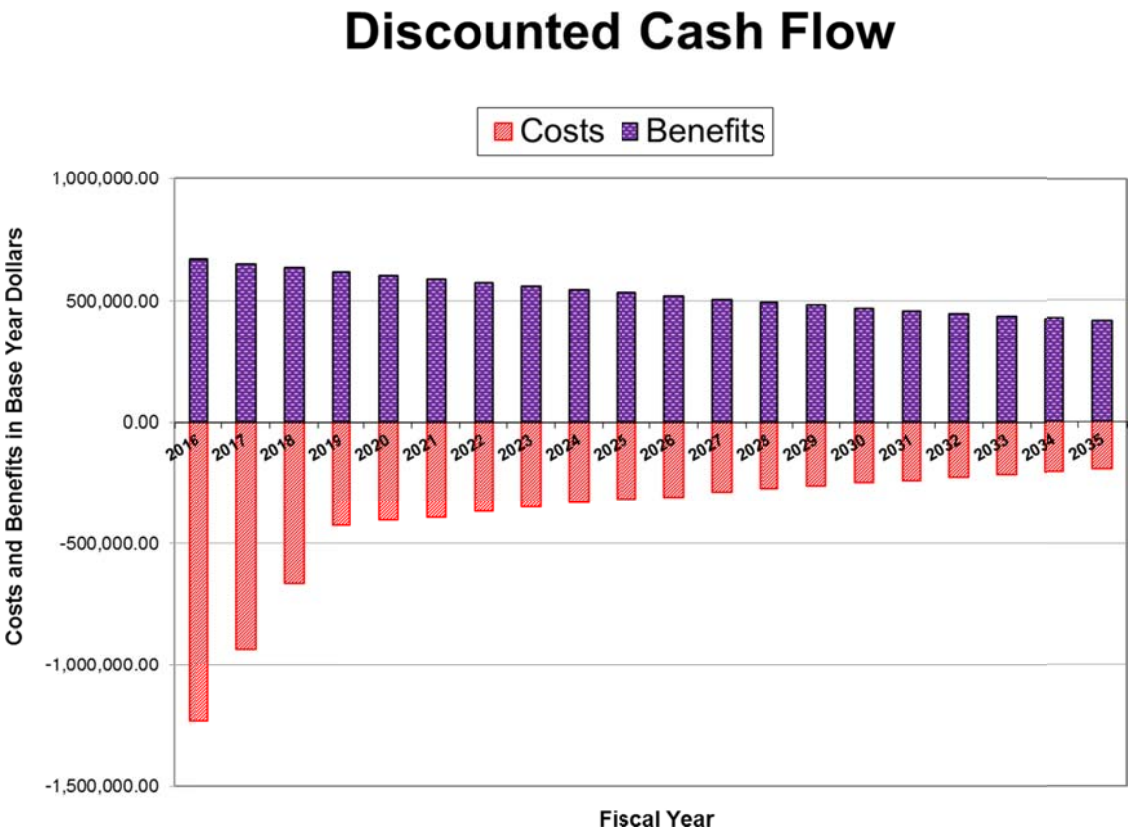

Figure 52. Discounted cash flow – 2M (Discount rate=5%)

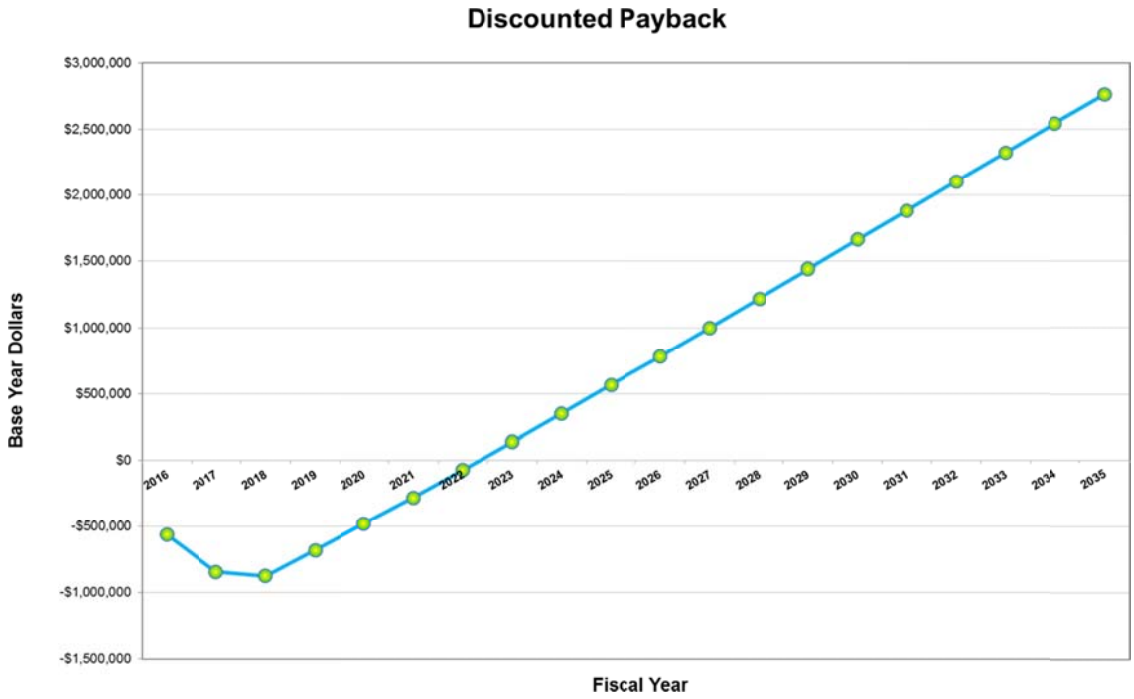

Figure 53. Estimated discounted payback period – 2M

As shown in Figure 53, the project has been fully paid back in 2022.

Table 12. Benefit and cost components of investments - 2M (2016-2035)

Benefit (present value)	**Value ($)**
Reduced costs	16,891,509
TOTAL BENEFIT	16,891,509
Costs (present value)	
Computer and software purchase	0
Data storage cost	60,000
Training personnel	40,000
Image purchase	10,205,618
Image processing	1,020,562
Total budget costs	11,326,179
Tax-cost factor, 20% of budget costs	2,265,236
TOTAL COST	13,591,415
Benefit/cost ratio	1.24

As shown in Table 12, B/C ratio equals to 1.24, which means that this scenario leads to appealing results for investments.

Scenario 2L (Purchasing 40*40 km data & outsourcing data processing)

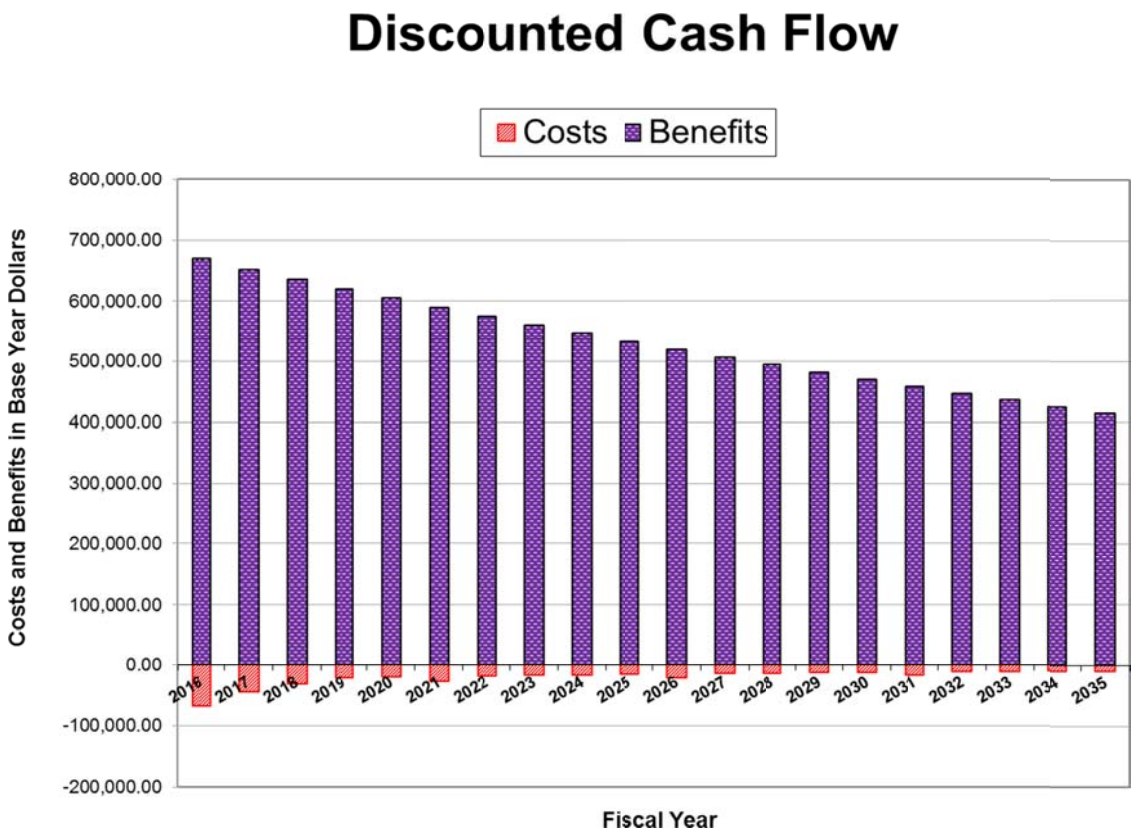

Figure 54. Discounted cash flow – 2L (Discount rate=5%)

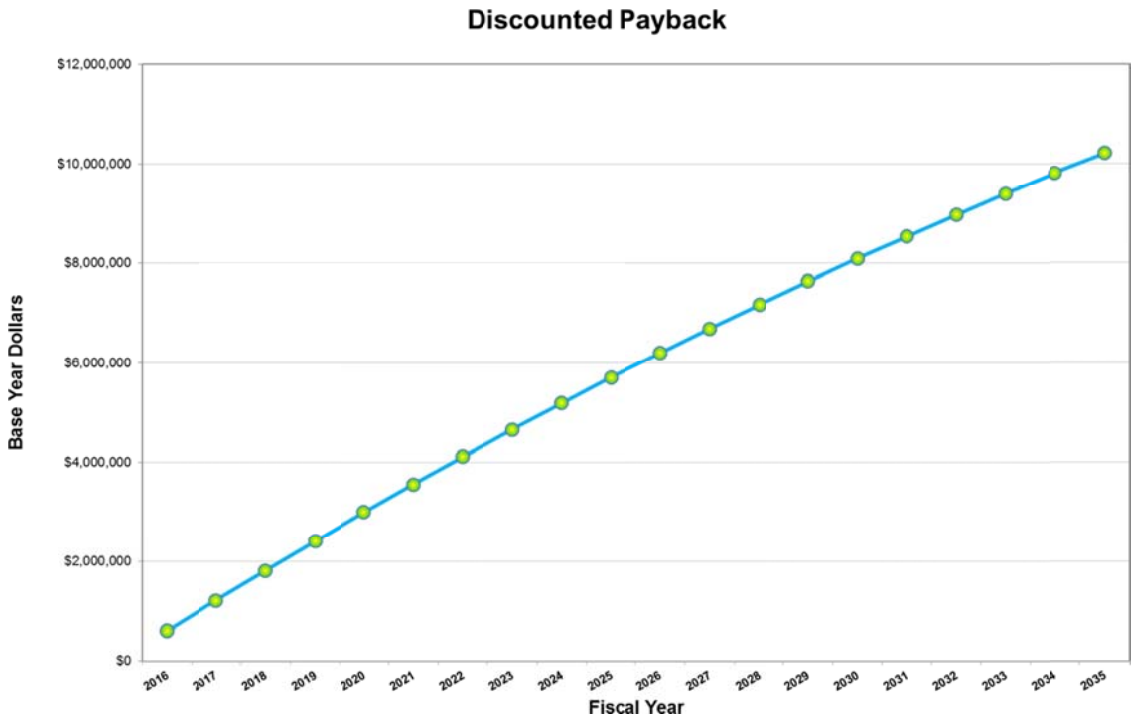

Figure 55. Estimated discounted payback period – 2L

Table 13. Benefit and cost components of investments – 2L (2016-2035)

Benefit (present value)	**Value ($)**
Reduced costs	16,891,509
TOTAL BENEFIT	16,891,509
Costs (present value)	
Computer and software purchase	0
Data storage cost	60,000
Training personnel	40,000
Image purchase	459,540
Image processing	45,954
Total budget costs	605,494
Tax-cost factor, 20% of budget costs	121,099
TOTAL COST	726,593
Benefit/cost ratio	23.25

Scenario 3H **(Outsourcing 7*7 km data collection and data processing)**

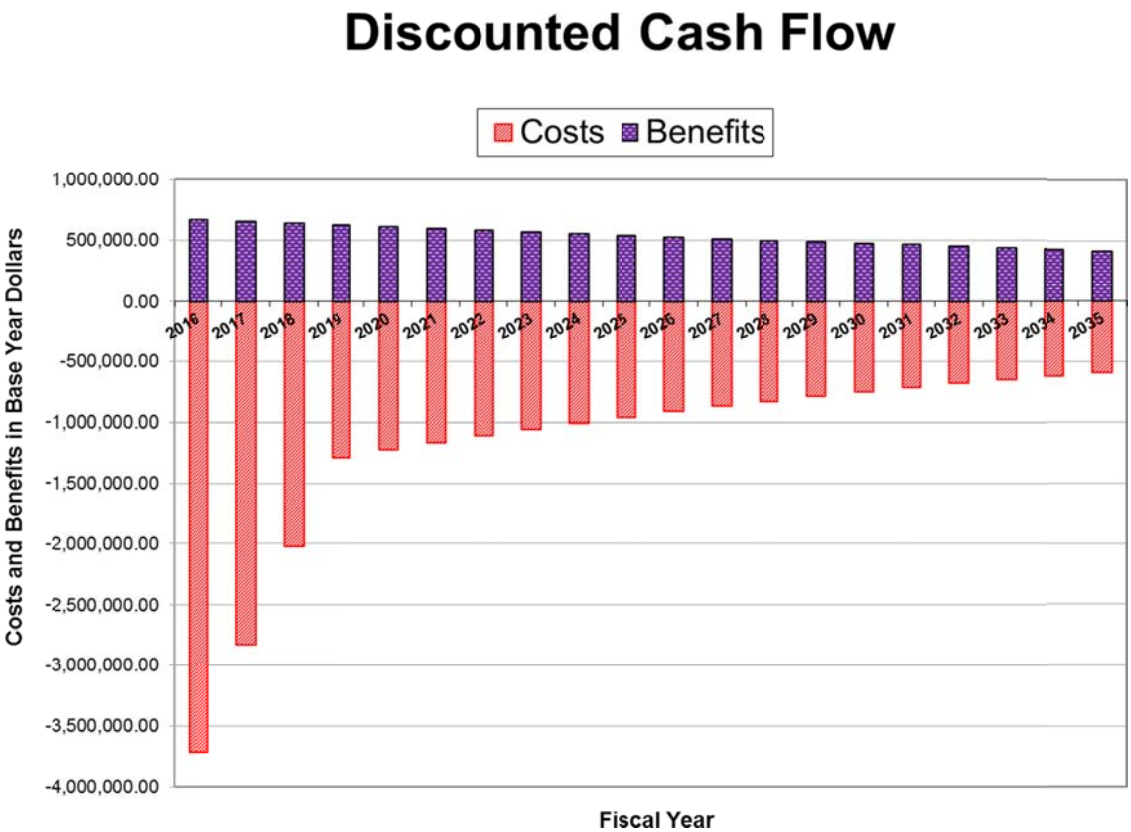

Figure 56. Discounted cash flow – 3H (Discount rate=5%)

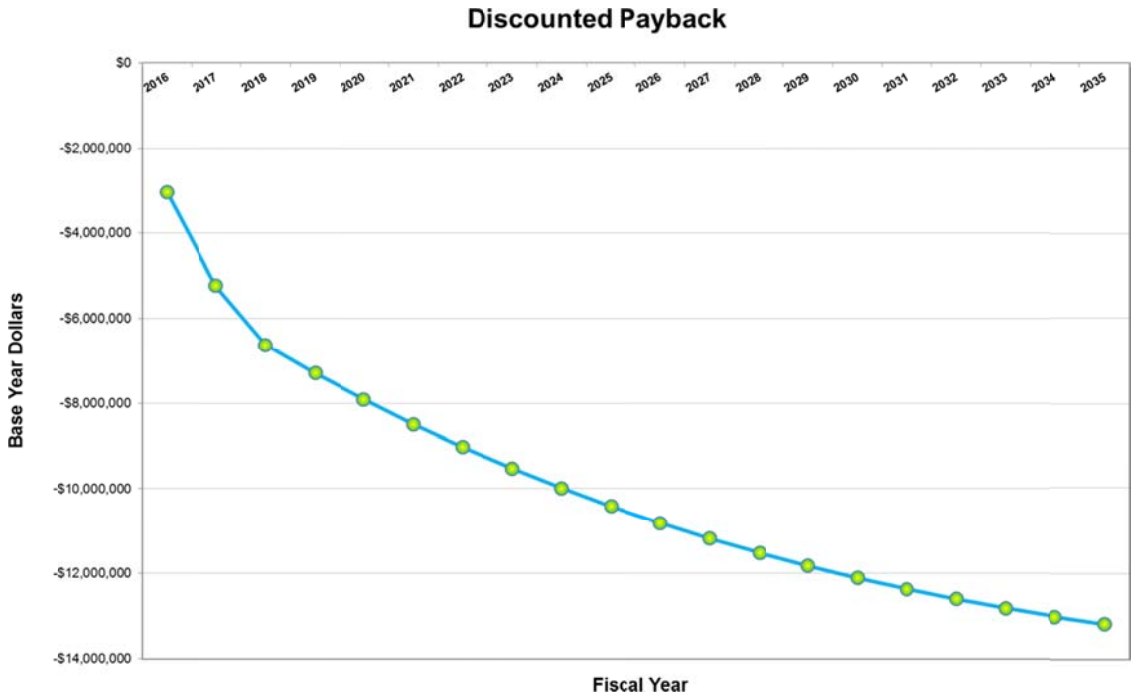

Figure 57. Estimated discounted payback period – 3H

Since this scenario takes longer to payback, it should be rejected (Figure 57).

Table 14. Benefit and cost components of investments – 3H (2016-2035)

Benefit (present value)	**Value ($)**
Reduced costs	16,891,509
TOTAL BENEFIT	16,891,509
Costs (present value)	
Computer and software purchase	0
Data storage cost	60,000
Training personnel	4,000
Image purchase	32,569,898
Image processing	1,628,495
Total budget costs	34,262,392
Tax-cost factor, 20% of budget costs	6,852,478
TOTAL COST	41,114,871
Benefit/cost ratio	0.41

As shown in Table 14, Benefit/cost ratio equals to 0.41, which means that the costs outweigh the benefits.

Scenario 3M **(Outsourcing 10*10 km data collection and data processing)**

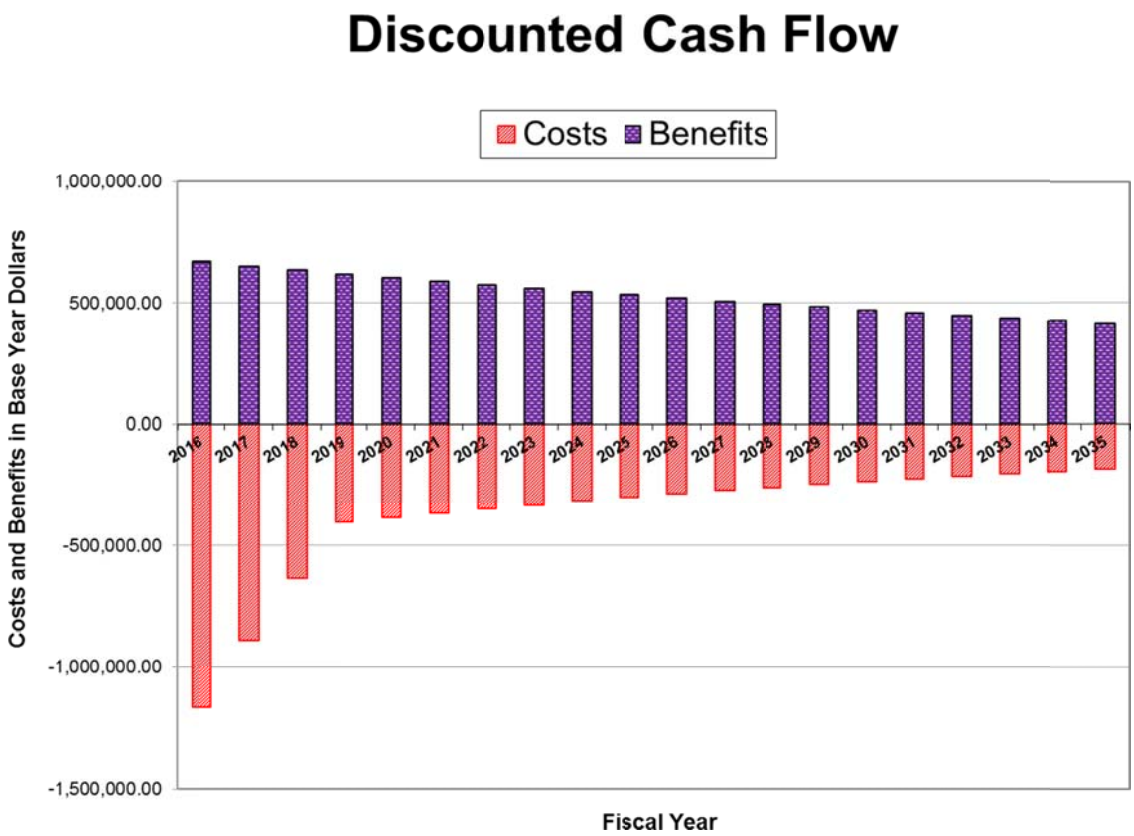

Figure 58. Discounted cash flow – 3M (Discount rate=5%)

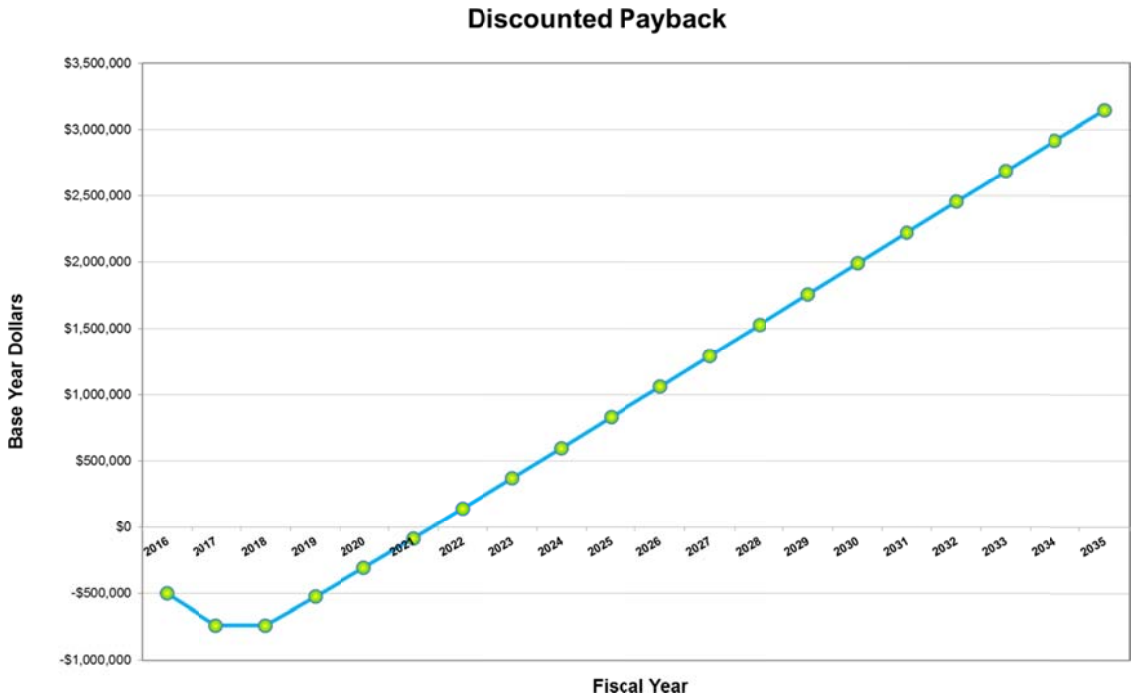

Figure 59. Estimated discounted payback period – 3M

As shown in Figure 59, the project has been fully paid back in 2022.

Table 15. Benefit and cost components of investments – 3M (2016-2035)

Benefit (present value)	**Value ($)**
Reduced costs	16,891,509
TOTAL BENEFIT	16,891,509
Costs (present value)	
Computer and software purchase	0
Data storage cost	60,000
Training personnel	4,000
Image purchase	10,205,618
Image processing	510,281
Total budget costs	10,779,898
Tax-cost factor, 20% of budget costs	2,155,980
TOTAL COST	12,935,878
Benefit/cost ratio	1.31

As shown in Table 15, B/C ratio equals to 1.31, which means that this scenario leads to appealing results for investments.

Scenario 3L (Outsourcing 40*40 km data collection and data processing)

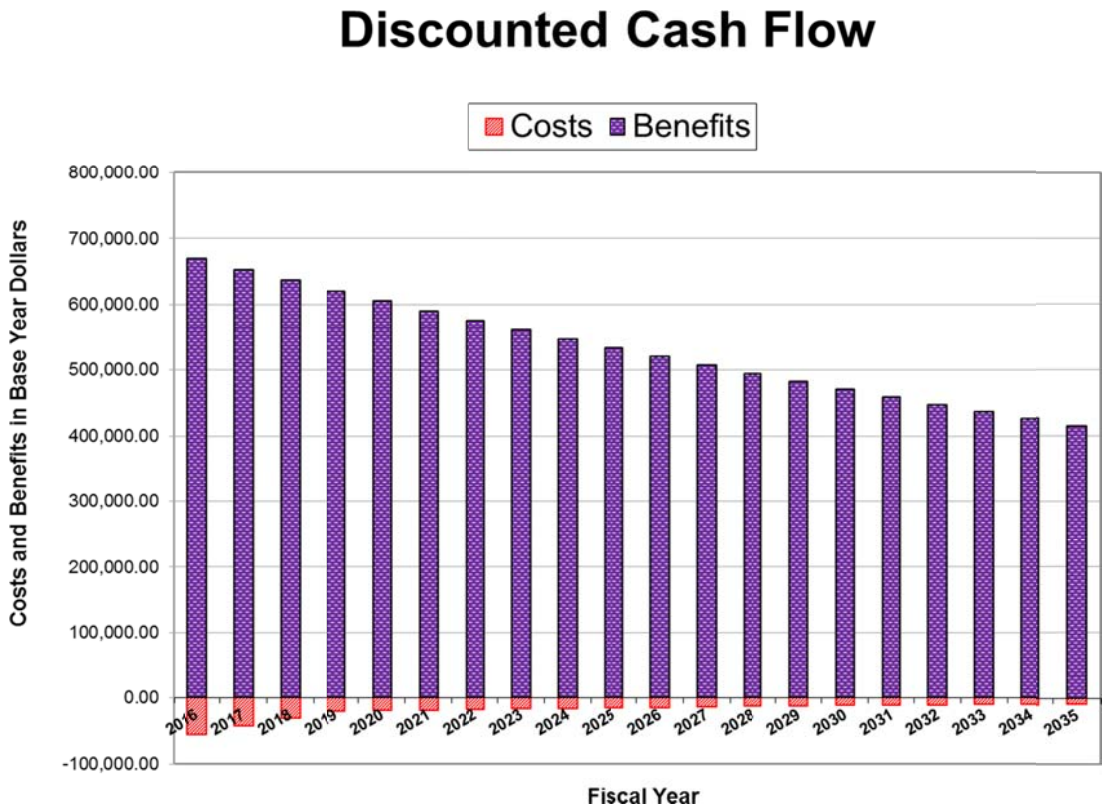

Figure 60. Discounted cash flow – 3L (Discount rate=5%)

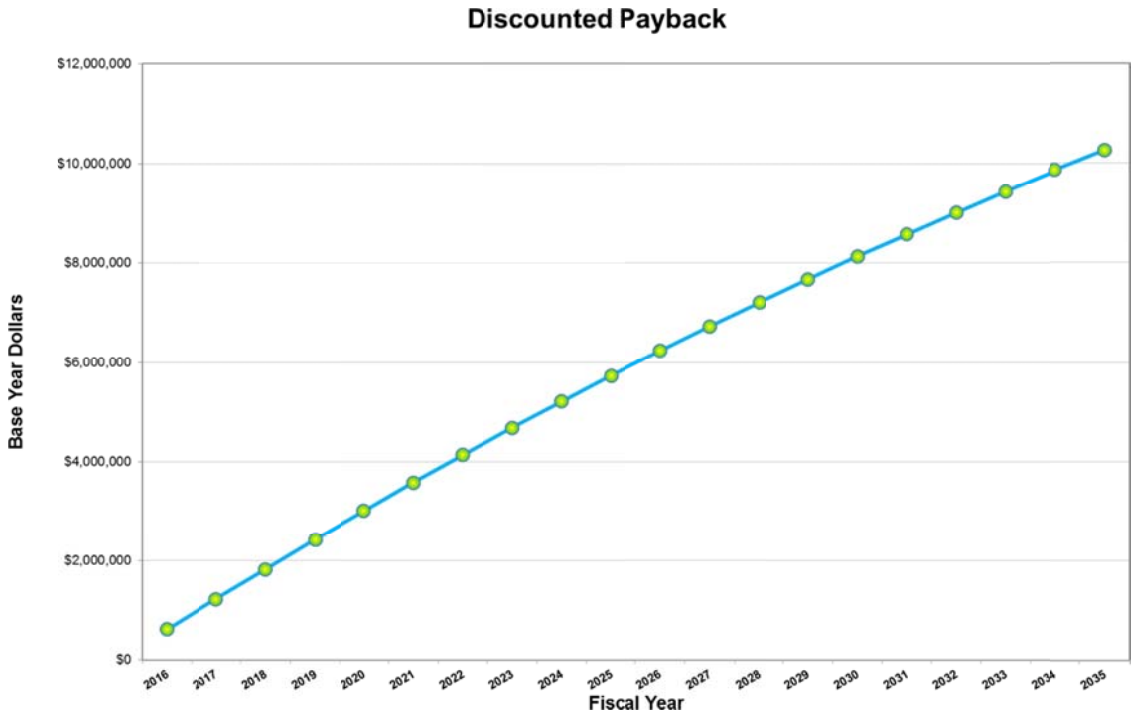

Figure 61. Estimated discounted payback period – 3L

Table 16. Benefit and cost components of investments – 3L (2016-2035)

Benefit (present value)	**Value ($)**
Reduced costs	16,891,509
TOTAL BENEFIT	16,891,509
Costs (present value)	
Computer and software purchase	0
Data storage cost	60,000
Training personnel	4,000
Image purchase	459,540
Image processing	22,977
Total budget costs	546,517
Tax-cost factor, 20% of budget costs	109,303
TOTAL COST	655,820
Benefit/cost ratio	25.76

Table 17. Summary of B/C ratio

			Option 1	Option 2	Option 3
	Size	**Resolution**	**Purchasing data & in-house data processing**	**Purchasing data & outsourcing data processing**	**Outsourcing data collection and data processing**
H	**7x7 km**	1m	0.43	0.39	0.41
M	**10x10 km**	1m	**1.34**	1.24	1.31
L*	**40x40 km**	5m	18.53	23.25	25.76

***** Despite the fact that low-resolution (40x40 km, 5m resolution) has highest B/C ratio, it is only useful for detection of sinkhole formations. Low-resolution images cannot be used to clearly identify the distress type in pavement surface).

Investigation of B/C ratios presents that SAR-based monitoring systems could be cost-effective and quickly pays back for 10*10 km and 40*40 km products. Considering the spatial resolution and high B/C ratio, purchasing the SAR imagery and in-house processing option would be a good option for SAR-based monitoring. This option pays back in five years considering 20 year time horizon as presented in Figure 47.

4 SUMMARY, CONCLUSIONS AND RECOMMENDATIONS

4.1 SUMMARY

Satellite remote sensing technology, specifically SAR has been widely used in many disciplines for decades. Both availability of data and developed methods for data analysis have increased over time and attracted researchers from different fields. In the meantime, technological developments have increased the potential in satellite systems and led much higher resolution capable SAR images. With these advancements, SAR-based monitoring has become potentially useful instruments for advance infrastructure monitoring.

Recent studies present the effectiveness of SAR-based monitoring in pavement and infrastructure management both in historical analysis and current practices. These studies have presented the effective use of SAR-based methods for detecting deformation and deformation velocities for highway and railways, sinkhole formations, dangerous rock slopes and pavement surface roughness in a series of SAR images. In this project, case studies have presented the use of backscattering signal intensity changes for the evaluation of surface characteristics. It is presented that this evaluation could be performed both in pixel level and large-scale. Specifically, pixel level analysis might yield identifying pavement surface deformations due to backscattering signal intensity anomalies.

Aforementioned studies and current researches indicate the effectiveness of SAR-based monitoring to determine the location and severity of pavement and infrastructure problems at certain level. However, determining the type of problems require additional information. This is due to pavement related methods and algorithms are still in its development stage and require further research for pavement and infrastructure monitoring. Evaluation of applications from other disciplines might help developing algorithms to overcome these limitations.

Since some disciplines are mature in SAR-based analysis, there are many data sources and data analysis tools available for research community. Historical data sources (ERS-1&2, ALOS PALSAR, etc.) might be freely available for educational and research purposes, however, recent SAR image acquisitions (Cosmo-SkyMed, TerraSAR-X, etc.) are costly. In terms of data analysis tools, there are many varying from code-based small programs for a specific analysis to comprehensive and state of the art commercial packages. ESA's Sentinel-1 Toolbox is one of the comprehensive and easy-to-use tools that are freely available for users.

Economic effects of SAR-based monitoring system on transportation agencies' ongoing pavement and infrastructure monitoring activities have briefly evaluated with a cost-benefit analysis to inform readers about the economic side of the technology and its components. Case study estimated the cost of establishing a SAR-based monitoring system in NCC, DE including necessary technical infrastructure, historical SAR dataset acquisition and monthly high-resolution SAR image acquisition. Comparing nine scenarios resulted valuable conclusions favoring the cost-effectiveness of SAR-based monitoring system with a benefit/cost ratio of 1.34 and five-year payback period.

4.2 CONCLUSIONS

This research project has investigated the possible use satellite remote sensing technology, specifically SAR, for pavement and infrastructure monitoring. Both pavement and infrastructure monitoring, and SAR concepts are presented in detail. Availability of SAR data sources and data analysis tools were investigated by giving priority to freely available resources. Evaluation of SAR-based monitoring presented with two case studies and cost-benefit analysis performed. The following can be concluded from the report:

- SAR-based monitoring, if applied on a regular basis and following a standard procedure, can result in valuable benefits for responsible agencies.
- SAR-based methods are highly effective for detection of surface deformations and determining deformation velocities with millimetric accuracy.
- Recent high-resolution SAR imagery has significant impact on the accuracy of the results and number of detected point in relatively small areas (such as less than 100 ft^2).
- SAR-based monitoring for pavement and infrastructure management found useful as a complementary tool rather than a replacement for current technologies and practices, specifically in the sense of state of good repair.
- One of the main advantages of satellite-based monitoring is the ability to cover very large areas with frequent revisit times to make it possible even monitoring daily and/or weekly changes.
- Regardless of the challenges, InSAR applications were found useful and promising for timely detection of problems and continuous monitoring of these problems by providing frequent (monthly or weekly) and continuous network level monitoring, specifically for pavement surface distress, infrastructure failures and geohazards. It is also expected that vehicle-based routine inspection trips may decrease and prioritized based on SAR-based network level monitoring, and better allocation of staff hours achieved.

- One of the great advantages of using satellite based monitoring is found that it is possible to evaluate any specific problem or site with historical data to better understand the deformation propagation in time.
- Results of transportation and infrastructure related studies found InSAR analysis useful for sinkhole detection, slow moving deteriorations, landslides, evaluation of rock slopes, and pavement surface deformation detections, which may directly affect the health and safety of transportation and infrastructure elements.
- SAR-based methods and InSAR has been widely and successfully used in some other disciplines that might indirectly affect the transportation related decision. Land development, hazard monitoring, coastal studies and see level rise scenarios, monitoring weather changes, etc. might have significant impact on transportation network.
- Although recent studies present SAR-based methods can effectively identify the location and sometimes severity of the problems, current practices cannot clearly identify the type of problems (for instance, distress type in pavement surface).
- Extensive implementation of SAR-based monitoring might yield comprehensive and more robust management programs leading to cost and energy savings.

4.3 RECOMMENDATIONS

Considering the limitations in economic resources, importance of effective and reliable decision support tools that support the monitoring and management of transportation infrastructure systems cannot be over-emphasized. Therefore, satellite-based network level monitoring has the opportunity to increase the efficiency of such monitoring efforts. Moreover, this approach will directly contribute to the US DOT strategic goals of “state of good repair” and “economic competitiveness”. However, since satellite remote sensing has been an emerging field in transportation and infrastructure management, it is particularly important to investigate the potential of technology for highest benefits.

Complexity of SAR image types and features require extra attention for evaluating the available and appropriate data sources for pavement and infrastructure monitoring. Besides the data selection, image processing should also be carried out carefully for accurate calculation of deformation and deformation velocities.

SAR-based monitoring and data analysis end products might also be very helpful and cost saving for many other departments and agencies in the region. Therefore, cooperation and collaboration within and between departments/agencies will reduce the total cost of monitoring and SAR data analysis efforts.

As emphasized previously, although current methods and techniques are very practical for determining the location and severity (at certain level) of problems, they do not yet differentiate problems among different types. For instance, it is hard to define the type of pavement surface distress with InSAR methods without further evaluation. However, this does not mean it is not possible, but it needs further research and investigation, specifically on pavement and infrastructure elements such as:

- Investigation of backscattering intensities of different pavement surface distress types
- Investigation of relationship between deterioration speed and deterioration types for pavement and infrastructure elements
- Investigating the contribution of possible other products such as optical satellite imagery for improving the detection of location, severity and type of problems
- Effect of current pavement and infrastructure database to improve the data accuracy and determination of type and severity of problems
- Evaluating these possibilities for different geological, traffic and weather conditions

5 REFERENCES

1. Simpson, A., G. Rada, B. Visintine, and J. Groeger. Evaluating Pavement Condition of the National Highway System. In *Transportation Research Record: Journal of Transportation Research Board*, Transportation Research Board of the National Academies, 2013, pp. 50-58.

2. Schnebele, E., Tanyu, B. F., Cervone, G.,Waters, N.,. Review of Remote Sensing Methodologies for Pavement Management and Assessment. *European Transport Research Review*, Vol. 7, No. 2, 2015.

3. The White House. *An Economic Analysis of Transportation Infrastructure Investment.* The White House, Washington D.C., 2014.

4. AASHTO. *AASHTO Guidelines for Pavement Management Systems.* American Association of State Highway and Transportation Officials, Washington, D.C., 1990.

5. Ferretti, A., A. Monti-Guarnieri, C. Prati, F. Rocca, and D. Massonet. *InSAR Principles-Guidelines for SAR Interferometry Processing and Interpretation.* ESA Publications, Noordwijk, Netherlands, 2007.

6. Ferretti, A., C. Prati, and F. Rocca. Permanent Scatterers in SAR Interferometry. *IEEE Transactions on Geoscience and Remote Sensing*, Vol. 39, No. 1, 2001, pp. 8-20.

7. Bianchini, S., F. Cigna, C. D. Ventisette, S. Moretti, and N. Casagli. Detecting and Monitoring Landslide Phenomena with TerraSAR-X Persistent Scatterers Data: The Gimigliano Case Study in Calabria Region (Italy). In *2012 IEEE International Geoscience and Remote Sensing Symposium (IGARSS)*, IEEE, 2012, pp. 982-985.

8. Cascini L., Peduto D., Arena L., Ferlisi S., Reale D., Verde S.,Fornaro G.,. Detection and Monitoring of Facilities Exposed to Subsidence Phenomena Via Past and Current Generation SAR Sensors. *Journal of Geophysics and Engineering*, Vol. 10, No. 6, 2013.

9. Bruckno, B., A. Vaccari, E. Hoppe, W. Niemann, and E. Campbell. Validation of Interferometric Synthetic Aperture Radar as a Tool for Identification of Geohazards and at-Risk Transportation Infrastructure. In *Highway Geology Symposium (HGS)*, DigitalCommons@University of Nebraska - Lincoln, 2013.

10. Hoppe, E., B. Bruckno, E. Campbell, S. Acton, A. Vaccari, M. Stuecheli, A. Bohane, G. Falorni, and J. Morgan. Transportation Infrastructure Monitoring using Satellite Remote Sensing. In *Transport Research Arena (TRA) 5th Conference: Transport Solutions from Research to Deployment*, Paris, 2014.

11. Hoppe, E. J., Y. Kweon, B. S. Bruckno, S. T. Acton, L. Bolton, A. Becker, and A. Vaccari. Historical Analysis of Tunnel Approach Displacements using Satellite Remote Sensing. In *Transportation Research Board 94th Annual Meeting*, 2015.

12. USDOT. *Beyond Traffic: Trend and Choices 2045.* U.S. Department of Transportation, Washington D.C., 2015.

13. Vaghefi K., Oats R.C., Harris D.K., Ahlborn T.M., Brooks C.N., Endsley K.A., Roussi C., Shuchman R., Burns J.W.,Dobson R.,. Evaluation of Commercially Available Remote Sensors for Highway Bridge Condition Assessment. *Journal of Bridge Engineering*, Vol. 17, No. SPECIAL ISSUE: Nondestructive Evaluation and Testing for Bridge Inspection and Evaluation, 2012, pp. 886-895.

14. Ouchi, K. Recent Trend and Advance of Synthetic Aperture Radar with Selected Topics. *Remote Sensing*, Vol. 5, No. 2, 2013, pp. 716-807.

15. Smadi, O. Pavement Management and Information Technology: Remote Sensing, GIS, and GPS. In *6th International Conference on Managing Pavements: The Lessons, the Challenges, the Way Ahead*, 2004.

16. Attoh-Okine, N., and O. Adarkwa. *Pavement Condition Surveys–Overview of Current Practices.* DCT 245, Delaware Center for Transportation, Newark, DE, 2013.

17. NCDOT. *Pavement Condition Survey Manual 2012.* North Carolina Department of Transportation, 2012.

18. McGhee, K. H. *Automated Pavement Distress Collection Techniques.* NCHRP Synthesis 334, Transportation Research Board of the National Academies, Washington D.C., 2004.

19. Miller, J. S., and W. Y. Bellinger. *Distress Identification Manual for the Long-Term Pavement Performance Program
*. FHWA-HRT-13-092. 2014, U.S. Department of Transportation Federal Highway Administration, 2014.

20. AASHTO. *Rough Roads Ahead: Fix them Now Or Pay for it Later.* RRA-1, American Association of State Highway and Transportation Officials and TRIP-a National Transportation Research Group, Washington D.C., 2009.

21. Galehouse, L., J. S. Moulthrop, and R. G. Hicks. Pavement Preservation Compendium II. May 1, 2015. https://www.fhwa.dot.gov/pavement/preservation/ppc0621.cfm, Accessed June 2, 2015.

22. Haider, S., K. Chatti, G. Baladi, and N. Sivaneswaran. Impact of Pavement Monitoring Frequency on Pavement Management System Decisions. In *Transportation Research Record: Journal of the Transportation Research Board*, Transportation Research Board of the National Academies, 2011, pp. 43-55.

23. Wang, K. C. Designs and Implementations of Automated Systems for Pavement Surface Distress Survey. *Journal of Infrastructure Systems*, Vol. 6, No. 1, 2000, pp. 24-32.

24. Joyce, K. E., Samsonov, S. V., Levick, S. R., Engelbrecht, J.,Belliss, S.,. Mapping and Monitoring Geological Hazards using Optical, LiDAR, and Synthetic Aperture RADAR Image Data. *Natural Hazards : Journal of the International Society for the Prevention and Mitigation of Natural Hazards*, Vol. 73, No. 2, 2014, pp. 137-163.

25. Higgins, C. UDOT FX. January 26, 2012. http://blog.udot.utah.gov/page/38/, Accessed June 10, 2015.

26. Wang, K. C. Elements of Automated Survey of Pavements and a 3D Methodology. *Journal of Modern Transportation*, Vol. 19, No. 1, 2011, pp. 51-57.

27. Maser, K. R. Condition Assessment of Transportation Infrastructure using Ground-Penetrating Radar. *Journal of Infrastructure Systems*, Vol. 2, No. 2, 1996, pp. 94-101.

28. Hong, Q., R. Wallace, T. M. Ahlborn, C. N. Brooks, E. P. Dennis, and M. Forster. Economic Evaluation of Commercial Remote Sensors for Bridge Health Monitoring. In *Transportation Research Board 92nd Annual Meeting*, 2013.

29. Morey, R. M. *Ground Penetrating Radar for Evaluating Subsurface Conditions for Transportation Facilities.* Synthesis of Highway Practice 255, Transportation Research Board National Research Council, Washington D.C., 1998.

30. Rott, H. Advances in Interferometric Synthetic Aperture Radar (InSAR) in Earth System Science. *Progress in Physical Geography*, Vol. 33, No. 6, 2009, pp. 769-791.

31. Bamler, R., and P. Hartl. Synthetic Aperture Radar Interferometry. *Inverse Problems*, Vol. 14, No. 4, 1998, pp. R1-R54.

32. Power, D., J. Youden, J. English, K. Russell, S. Croshaw, and R. Hanson. *INSAR Applications for Highway Transportation Projects.* FHWA-CFL/TD-06-002, U.S. Dept. of Transportation, Federal Highway Administration, Lakewood, CO, 2006.

33. Dousset, B. Synthetic Aperture Radar Imaging of Urban Surfaces: A Case Study. In *International Geoscience and Remote Sensing Symposium*, IEEE, 1995, pp. 2092 - 2096.

34. Tele-Rilevamento Europa (TRE). **SqueeSAR™**. http://treuropa.com/technique/squeesar/, Accessed June 14, 2015.

35. The SAR - Guidebook, Examples Based on SARscape. October 2007. https://www.exelisvis.com/portals/0/pdfs/envi/SAR_Guidebook.pdf, Accessed May 20, 2015.

36. Massonnet, D., M. Rossi, C. Carmona, F. Adragna, G. Peltzer, K. Feigl, and T. Rabaute. The Displacement Field of the Landers Earthquake Mapped by Radar Interferometry. *Nature*, Vol. 364, No. 6433, 1993, pp. 138-142.

37. Justice, C. O., L. Giglio, S. Korontzi, J. Owens, J. Morisette, D. Roy, J. Descloitres, S. Alleaume, F. Petitcolin, and Y. Kaufman. The MODIS Fire Products. *Remote Sensing of Environment*, Vol. 83, No. 1, 2002, pp. 244-262.

38. Maselli, F., S. Romanelli, L. Bottai, and G. Zipoli. Use of NOAA-AVHRR NDVI Images for the Estimation of Dynamic Fire Risk in Mediterranean Areas. *Remote Sensing of Environment*, Vol. 86, No. 2, 2003, pp. 187-197.

39. Hoque, R., D. Nakayama, H. Matsuyama, and J. Matsumoto. Flood Monitoring, Mapping and Assessing Capabilities using RADARSAT Remote Sensing, GIS and Ground Data for Bangladesh. *Natural Hazards*, Vol. 57, No. 2, 2011, pp. 525-548.

40. Zhang, Q., and K. C. Seto. Mapping Urbanization Dynamics at Regional and Global Scales using Multi-Temporal DMSP/OLS Nighttime Light Data. *Remote Sensing of Environment*, Vol. 115, No. 9, 2011, pp. 2320-2329.

41. Taubenböck, H., T. Esch, A. Felbier, M. Wiesner, A. Roth, and S. Dech. Monitoring Urbanization in Mega Cities from Space. *Remote Sensing of Environment*, Vol. 117, 2012, pp. 162-176.

42. Wang, L., C. Li, Q. Ying, X. Cheng, X. Wang, X. Li, L. Hu, L. Liang, L. Yu, and H. Huang. China's Urban Expansion from 1990 to 2010 Determined with Satellite Remote Sensing. *Chinese Science Bulletin*, Vol. 57, No. 22, 2012, pp. 2802-2812.

43. Saatchi, S. S., N. L. Harris, S. Brown, M. Lefsky, E. T. Mitchard, W. Salas, B. R. Zutta, W. Buermann, S. L. Lewis, S. Hagen, S. Petrova, L. White, M. Silman, and A. Morel. Benchmark Map of Forest Carbon Stocks in Tropical Regions Across Three Continents. *Proceedings of the National Academy of Sciences of the United States of America*, Vol. 108, No. 24, 2011, pp. 9899-9904.

44. Dubois, G., M. Clerici, J. Pekel, A. Brink, I. Palumbo, D. Gross, S. Peedell, D. Simonetti, and M. Punga. On the Contribution of Remote Sensing to DOPA, a Digital Observatory for Protected Areas. In *Proceedings of the 34th International Symposium on Remote Sensing of Environment*, 2011, pp. 10-15.

45. Ferretti, A., A. Fumagalli, F. Novali, A. Rucci, C. Prati, and F. Rocca. A New Algorithm for Processing Interferometric Data-Stacks: SqueeSAR. *IEEE Transactions on Geoscience and Remote Sensing*, Vol. 49, No. 9, 2011, pp. 3460-3470.

46. Morgan, J., G. Falorni, A. Bohane, and F. Novali. *Advanced InSAR Technology (SqueeSAR™) for Monitoring Movement of Landslides.* FHWA-CFL/TD-11-005, , 2011.

47. Berardino, P., G. Fornaro, R. Lanari, and E. Sansosti. A New Algorithm for Surface Deformation Monitoring Based on Small Baseline Differential SAR Interferograms. *IEEE Transactions on Geoscience and Remote Sensing*, Vol. 40, No. 11, 2002, pp. 2375-2383.

48. Ferretti, A., G. Savio, R. Barzaghi, A. Borghi, S. Musazzi, F. Novali, C. Prati, and F. Rocca. Submillimeter Accuracy of InSAR Time Series: Experimental Validation. *IEEE Transactions on Geoscience and Remote Sensing*, Vol. 45, No. 5, 2007, pp. 1142-1153.

49. Goel, K., and N. Adam. A Distributed Scatterer Interferometry Approach for Precision Monitoring of Known Surface Deformation Phenomena. *IEEE Transactions on Geoscience and Remote Sensing*, Vol. 52, No. 9, 2014, pp. 5454-5468.

50. Zebker, H. A., and Y. Lu. Phase Unwrapping Algorithms for Radar Interferometry: Residue-Cut, Least-Squares, and Synthesis Algorithms. *Journal of the Optical Society of America A*, Vol. 15, No. 3, 1998, pp. 586-598.

51. Suanpaga, W., and K. Yoshikazu. Riding Quality Model for Asphalt Pavement Monitoring using Phase Array Type L-Band Synthetic Aperture Radar (PALSAR). *Remote Sensing*, Vol. 2, No. 11, 2010, pp. 2531-2546.

52. Picchiani, M., and F. Del Frate. Learn EO! Lesson 8: Monitoring Urban Growth with SAR Time Series. www.learn-eo.org/lessons/l8, Accessed July 20, 2015.

53. Vavrik, W. R., L. D. Evans, J. A. Stefanski, and S. Sargand. *PCR Evaluation–Considering Transition from Manual to Semi-Automated Pavement Distress Collection and Analysis.* , Champaign, IL, 2013.

54. TerraSAR-X Services International Price List. September 2004. http://www2.geo-airbusds.com/files/pmedia/public/r463_9_itd-0508-cd-0001-tsx_international_pricelist_en_issue_6.00.pdf, Accessed July 27, 2015.

55. E-Geos Price List. April 1, 2015. http://www.e-geos.it/products/pdf/prices.pdf, Accessed July 28, 2015.

56. Chatti, K., and I. Zaabar. *Estimating the Effects of Pavement Condition on Vehicle Operating Costs.* NCHRP REPORT 720, Transportation Research Board, Washington D.C., 2012.

57. Kalluri, S., P. Gilruth, and R. Bergman. The Potential of Remote Sensing Data for Decision Makers at the State, Local and Tribal Level: Experiences from NASA's Synergy Program. *Environmental Science & Policy*, Vol. 6, No. 6, 2003, pp. 487-500.

58. Giuffre, W. L. *Evaluation of Highway Performance Measures for a Multi-State Corridor – A Pilot Study.* FHWA-HIF-10-015, , Cambridge, Massachusetts, 2010.

59. DELDOT. 2013 Highway Statistics - Delaware. 2013. https://www.deldot.gov/information/projects/hpms/2013/DVMT2013.pdf, Accessed June 06, 2015.

60. U.S DOT FHWA. Highway Performance Monitoring System (HPMS). November 7, 2014. https://www.fhwa.dot.gov/policyinformation/hpms/hpmsprimer.cfm, Accessed June 15, 2015.

61. Fine, A., P. Colton, B. Cotton, E. Futcher, S. Middleton, and C. Merrefield. *GIS in Transportation: Geospatial Tools for Data-Sharing, Case Studies of Select Transportation Agencies.* U.S. DOT, FHWA, Cambridge, MA, 2014.

62. Pavement Interactive. Roughness. August 16, 2007. http://www.pavementinteractive.org/article/roughness, Accessed June 17, 2015.